A Comparison Between STATCOMs Using PWM Voltage Control and Hysteresis Current Control (HCC)

Yongan Deng

A Thesis

In

The Department

of

Electrical and Computer Engineering

Presented in Partial Fulfillment of the Requirements
for the Degree of Master of Applied Science at
Concordia University
Montreal, Quebec, Canada

November 2007

Your file Votre référence
ISBN: 978-0-494-40879-7
Our file Notre référence
ISBN: 978-0-494-40879-7

ABSTRACT

A Comparison Between STATCOMs Using PWM Voltage Control and Hysteresis Current Control (HCC)

Yongan Deng

The Voltage Source Inverter (VSI) has now become the fundamental building block component in Flexible AC Transmission Systems (FACTS). Among the various applications of a VSI, the Static Synchronous Compensator (STATCOM) is the most popular one. It injects a set of three-phase balanced sinusoidal currents with controllable magnitude and phase angle, into the transmission line to regulate the transmission line voltage or to compensate for the reactive power. Under the condition that no external source/sink is available on the DC side, it should also absorb a small amount of active power from the transmission line to maintain the DC bus voltage constant and compensate for any real power losses within the VSI. In this process, the control method of the VSI is one of the key factors to influence the performance of the STATCOM. This thesis investigates the effect of two modulation schemes on the performance of a STATCOM. The first is the Pulse Width Modulation (PWM) voltage control and the second Hysteresis Current Control (HCC). The performance of the two schemes under steady-state and transient conditions are assessed by means of simulations using EMTP-RV. The results presented in the thesis justify the fact that PWM voltage control has become the de-facto modulation technique for STATCOM applications despite well known limitation of generation of low voltage harmonics with large magnitudes when operating at low switching frequencies.

ACKNOWLEDGMENTS

I would like to acknowledge the contribution of Prof. V. J. Sood as the supervisor to this research. Over the past years, I learned from him not only his broad and in-depth academic knowledge, but also his kindness and patience. Without his continuous guidance, supports and encouragement throughout the research, I could not have finished the MA.Sc study.

I would like to express my sincere gratitude to Prof. L. A. Lopes. As the co-supervisor of my program, Dr. Lopes always provide me valuable advice, especially the suggestion in the thesis writing stage. His serious academic spirit is always the model of my career.

I would also like to thank Eric Xu and Sasan Salem for their friendship. The discussion with them has brought a lot of inspiration to the research.

Last but never least; I would like to acknowledge the support from my family. Heartful thanks to my wife, Qin Shu, for her love, supporting and understanding no matter how difficult it was. Great thanks to my parents for their never-fading love.

TABLE OF CONTENTS

LIST OF FIGURES

LIST OF TABLES

LIST OF NOMENCLATURE

v_t	The instantaneous expression of the transmission line voltage
V_t	The magnitude of the transmission line voltage at the connection point of STATCOM
V_{td}, V_{tq}	The magnitude of the d-axis component of V_t
$V_{t\text{-}ref}$	The reference value of the transmission line voltage magnitude
V_{dc}	The DC bus voltage of the inverter
$V_{dc\text{-}ref}$	The reference value of the DC bus voltage
i_t	The instantaneous expression of the AC side output phase current of the inverter
I_t	The magnitude of the AC side output phase current
$i_{t\text{-}ref}$	The reference expression of i_t
i_{td}, i_{tq}	The d-axis and q-axis component of i_t
I_{td}, I_{tq}	The magnitude of the d-axis and q-axis component of i_t
$i_{td\text{-}ref}, i_{tq\text{-}ref}$	The d-axis and q-axis component of $i_{t\text{-}ref}$
$I_{td\text{-}ref}, I_{tq\text{-}ref}$	The magnitude of the d-axis and q-axis component of $i_{t\text{-}ref}$
v_s	The instantaneous expression of the equivalent source voltage for STATCOM
V_s	The magnitude of v_s
V_{sd}, V_{sq}	The magnitude of the d-axis and q-axis component of the source voltage
v_o	The AC side output voltage of the inverter
R_s, L_s	The equivalent source resistance and inductance
X_s	The equivalent source reactance
L_t, X_t	The coupling transformer inductance and reactance
R	The DC bus resistance representing the switching and other losses
C	The DC bus capacitance
P_{ac}, P_{dc}	The active power in AC side and DC side of STATCOM
Q_{ac}, Q_{dc}	The reactive power in AC side and DC side of STATCOM
φ	The phase angle between v_t and v_s
θ	The phase angle between v_t and i_t
α	The phase angle between v_t and v_o

$K_{0,}\ K_{\alpha}$	The transformation matrix of the synchronous rotating reference frame
$\Delta I,\ \Delta V$	The small disturbance in the current and voltage magnitude
D	The duty ratio of switch T_{A+}
v_{tri}	The triangular carrier wave of PWM
V_{tri}	The peak value of the triangular carrier wave of PWM
$v_{control}$	The control signal input of PWM
ω	The utility angle frequency
f_{sw}	The switching frequency of the inverter
f_{tri}	The frequency of the triangular carrier waveform of PWM
MI	The modulation index of PWM
m_f	The frequency modulation ratio of PWM
$K_{p1,}\ K_{i1}$	The **q-** loop PI block parameters of HCC STATCOM
$K_{p2,}\ K_{i2}$	The **d-** loop PI block parameters of HCC STATCOM
$K_{p3,}\ K_{i41}$	The **q-** loop PI block parameters of PWM STATCOM
$K_{p3,}\ K_{i4}$	The **d-** loop PI block parameters of PWM STATCOM
HBW	The hysteresis band width of HCC

1. INTRODUCTION

1.1 General Introduction

During the past two decades, the increase in electrical energy demand has presented higher requirements from the power industry. More power plants, substations, and transmission lines need to be constructed. However, the most commonly used devices in present power grid are the mechanically-controlled circuit breakers. The long switching periods and discrete operation make them difficult to handle the frequently changed loads smoothly and damp out the transient oscillations quickly. In order to compensate these drawbacks, large operational margins and redundancies are maintained to protect the system from dynamic variation and recover from faults. This not only increases the cost and lowers the efficiency, but also increases the complexity of the system and augments the difficulty of operation and control. Severe black-outs happened recently in power grids worldwide and these have revealed that conventional transmission systems are unable to manage the control requirements of the complicated interconnections and variable power flow.

Therefore, investment is necessary for the studies into the security and stability of the power grid, as well as the improved control schemes of the transmission system. Different approaches such as reactive power compensation and phase shifting have been applied to increase the stability and the security of the power systems. The demands of lower power losses, faster response to system parameter change, and higher stability of system have stimulated the development of the Flexible AC Transmission systems (FACTS) [1]. Based on the success of research in power electronics switching devices and advanced control technology, FACTS has become the technology of choice in

voltage control, reactive/active power flow control, transient and steady-state stabilization that improves the operation and functionality of existing power transmission and distribution system [2, 3]. The achievement of these studies enlarge the efficiency of the existing generator units, reduce the overall generation capacity and fuel consumption, and minimize the operation cost.

1.2 Basic principal of power compensation in transmission system.

Figure 1.1(a) shows the simplified model of a power transmission system. Two power grids are connected by a transmission line which is assumed lossless and represented by the reactance X_L. $V_1\angle\delta_1$ and $V_2\angle\delta_2$ represent the voltage vectors of the two power grid buses with angle $\delta = \delta_1 - \delta_2$ between the two. The corresponding phasor diagram is shown in Figure 1.1(b).

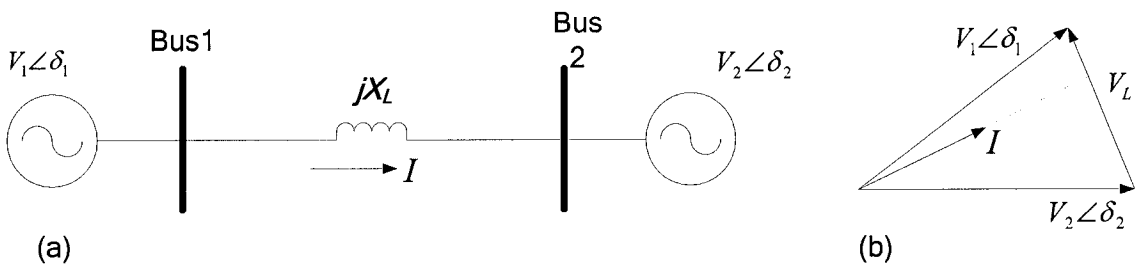

Figure 1. 1 Power transmission system: (a) simplified model; (b) phase diagram [5]

The magnitude of the current in the transmission line is given by:

$$I = \frac{V_L}{X_L} = \frac{|V_1\angle\delta_1 - V_2\angle\delta_2|}{X_L} \tag{1-1}$$

The active and reactive components of the current flow at bus 1 are given by:

$$I_{d1} = \frac{V_2 \sin\delta}{X_L}, \qquad I_{q1} = \frac{V_1 - V_2 \cos\delta}{X_L} \tag{1-2}$$

The active power and reactive power at bus 1 are given by:

$$P_1 = \frac{V_1 V_2 \sin\delta}{X_L}, \qquad Q_1 = \frac{V_1(V_1 - V_2 \cos\delta)}{X_L} \tag{1-3}$$

Similarly, the active and reactive components of the current flow at bus 2 can be given by:

$$I_{d2} = \frac{V_1 \sin\delta}{X_L}, \qquad I_{q2} = \frac{V_2 - V_1 \cos\delta}{X_L} \tag{1-4}$$

The active power and reactive power at bus 2 are given by:

$$P_2 = \frac{V_1 V_2 \sin\delta}{X_L}, \qquad Q_2 = \frac{V_2(V_2 - V_1 \cos\delta)}{X_L} \tag{1-5}$$

Equations (1-1) through (1-5) indicate that the active and reactive power/current flow can be regulated by controlling the voltages, phase angles and line impedance of the transmission system. From the power angle curve shown in Figure 1.1(b), the active power flow will reach the maximum when the phase angle δ is 90°. In practice, a large margin is kept in order to keep the system stable from the transient and dynamic oscillations [4].

Reactive power compensation is more related to the voltage magnitude regulation in the transmission system. From Figure 1.1(b), the change of voltage magnitude V_1 does not change the magnitude of V_L by much, but the current phase angle is correspondingly changed.

Generally, the compensation mode in transmission system can be divided into two main groups: shunt and series compensation.

1.2.1 Shunt compensation

Shunt compensation, especially shunt reactive compensation has been widely used in transmission system to regulate the voltage magnitude, improve the voltage quality, and enhance the system stability [5]. Shunt-connected reactors are used to reduce the line over-voltages by consuming the reactive power, while shunt-connected capacitors are used to maintain the voltage levels by compensating the reactive power to transmission line.

A simplified model of a transmission system with shunt compensation is shown in Figure 1.2(a). The voltage magnitudes of the two buses are assumed equal as V, and the phase angle between them is δ. The transmission line is assumed lossless and represented by the reactance X_L. At the midpoint of the transmission line, a controlled capacitor C is shunt-connected. The voltage magnitude at the connection point is maintained as V.

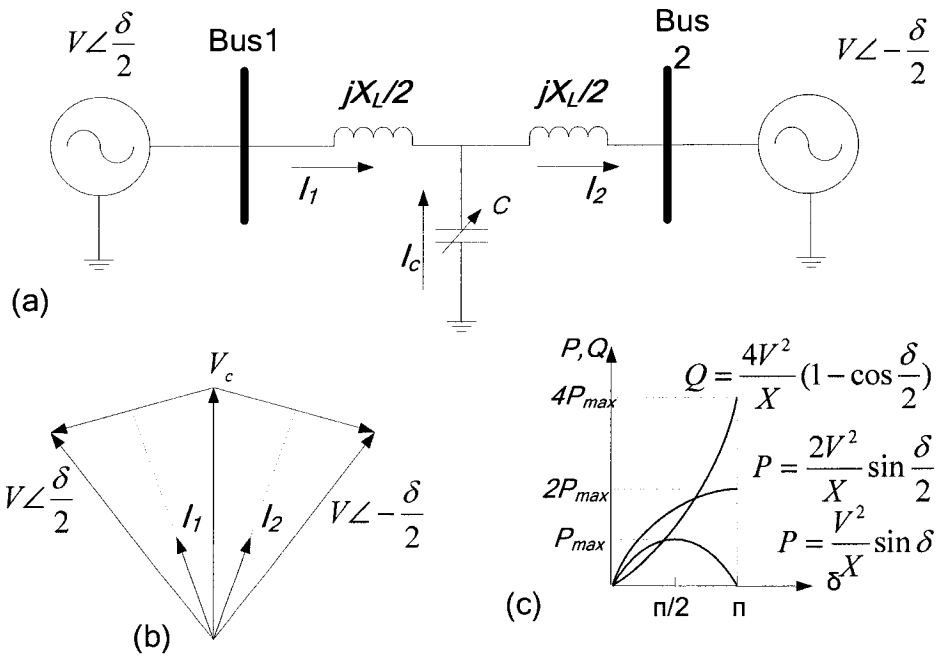

Figure 1. 2 Transmission system with shunt compensation: (a) simplified model; (b) phase diagram; (c) power-angle curve [2]

As discussed previously, the active powers at bus 1 and bus 2 are equal.

$$P_1 = P_2 = 2\frac{V^2}{X_L}\sin\frac{\delta}{2} \tag{1-6}$$

The injected reactive power by the capacitor is calculated as:

$$Q_c = 4\frac{V^2}{X_L}(1-\cos\frac{\delta}{2}) \tag{1-7}$$

From the power angle curve shown in Figure 1.2(c), the transmitted power is significantly increased, and the peak point shifts from δ=90° to δ=180°. The operation margin and the system stability are increased by the shunt compensation.

The voltage support function of the midpoint compensation can easily be extended to the voltage support at the end of the radial transmission, which will be proven by the system simplification analysis in a later section. The reactive power compensation at the end of the radial line is especially effective in enhancing voltage stability.

1.2.2 Series compensation

Series compensation aims to directly control the overall series line impedance of the transmission line. Tracking back to Equations (1-1) through (1-5), the AC power transmission is primarily limited by the series reactive impedance of the transmission line. A series-connected capacitor functions as a voltage injector. It can add a voltage in opposition to the transmission line voltage drop, therefore reducing the series line impedance.

A simplified model of a transmission system with series compensation is shown in Figure 1.3(a). The voltage magnitudes of the two buses are assumed equal as V, and the phase angle between them is δ. The transmission line is assumed lossless and represented by the

reactance X_L. A controlled capacitor is series-connected in the transmission line with voltage addition V_{inj}. The phase diagram is shown in Figure 1.3(b)

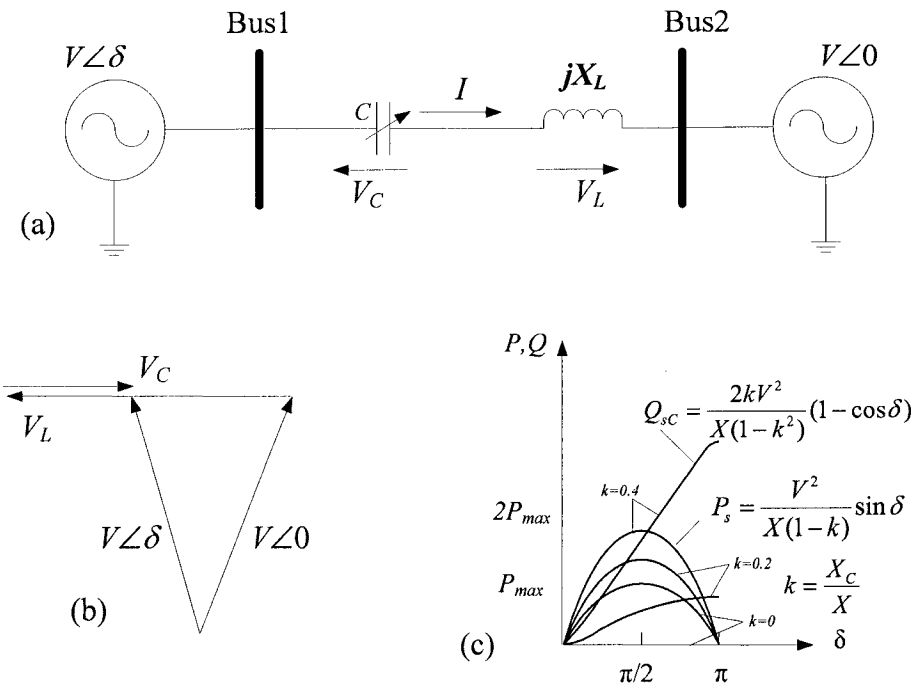

Figure 1. 3 Transmission system with series compensation: (a) simplified model; (b) phase diagram; (c) power-angle curve [2]

Defining the capacitance of C as a portion of the line reactance,

$$X_C = kX_L \tag{1-8}$$

The overall series inductance of the transmission line is,

$$X = X_L - X_C = (1-k)X_L \tag{1-9}$$

The active power transmitted is,

$$P = \frac{V^2}{(1-k)X_L}\sin\delta \tag{1-10}$$

The reactive power supplied by the capacitor is calculated as:

$$Q_c = 2\frac{V^2}{X_L}\frac{k}{(1-k)^2}(1-\cos\delta) \tag{1-11}$$

In Figure 1.3(c) shows the power angle curve from which it can be seen that the transmitted active power increases with ***k***.

1.3 Flexible AC Transmission System (FACTS)

The history of FACTS controllers can be traced back to 1970s when Hingorani presented the idea of power electronic applications in power system compensation. From then on, various researches were conducted on the application of high power semiconductor diodes and thyristors in transmission system. The shunt-connected Static VAR compensator (SVC) using solid-state switches and the series-connected controllers were proposed in AC transmission system application. In 1988, Hingorani defined the FACTS concept and described the wide prospects of the application in [6]. Nowadays, FACTS technology has shown strong potential. Many examples of FACTS devices and controllers are in operation

As presented in [7], FACTS and FACTS controllers are defined in IEEE Terms and Definitions as:

- ***Flexible AC Transmission System (FACTS)***: Alternating current transmission systems incorporating power electronic-based and other static controllers to enhance controllability and increase power transfer capability.
- ***FACTS Controller***: A power electronic-based system and other static equipment that provide control of one or more AC transmission system parameters.

As new technology for power transmission system, FACTS and FACTS controllers not only provide the same benefits as conventional compensators with mechanically-

controlled switches in steady state but also improve the dynamic and transient performance of the power system. The power electronics-based switches in the functional blocks of FACTS can usually be operated repeatedly and the switching time is a portion of a periodic cycle, which is much shorter than the conventional mechanical switches. The advance of semiconductors increases the switching frequency and voltage-ampere ratings of the solid switches and facilitates the applications. For example, the switching frequencies of Insulated Gate Bipolar Transistors (IGBTs) are from 3 kHz to 10 kHz which is several hundred times the utility frequency of power system (50~60Hz). Gate turn-off thyristors (GTOs) have a switching frequency lower than 1 kHz, but the voltage and current rating can reach 5-8 kV and 6 kA respectively [8].

FACTS controllers have many configurations. In general, they can be categorized into shunt-connected controllers, series-connected controllers and their combinations.

1.3.1 Shunt-connected controllers

FACTS controllers can be impedance type, based on thyristors without gate turn-off capability, which are called Static Var Compensator (SVC) for shunt-connected application. Another type of FACTS controllers is converter-based which is usually in the form of a Static Synchronous Compensator (STATCOM).

1.3.1.1 Static Var Compensator (SVC)

Static Var Compensator is "a shunt-connected static Var generator or absorber whose output is adjusted to exchange capacitive or inductive current so as to maintain or control specific parameters of the electrical power system (typically bus voltage)" [5].

SVC is based on thyristors without gate turn-off capability. The operating principal and characteristics of thyristors realize SVC variable reactive impedance. SVC includes two main components and their combination: (1) Thyristor-controlled and Thyristor-switched Reactor (TCR and TSR); and (2) Thyristor-switched capacitor (TSC). In Figure 1.4 shows the diagram of SVC.

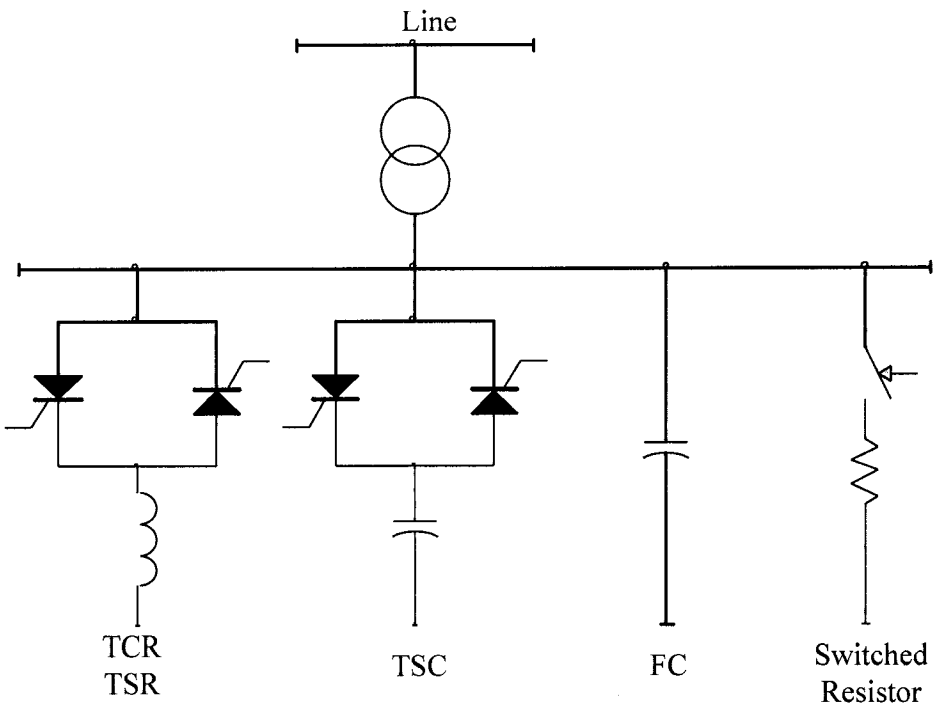

Figure 1. 4 Static VAR Compensators (SVC): TCR/TSR, TSC, FC and Mechanically Switched Resistor [2]

TCR and TSR are both composed of a shunt-connected reactor controlled by two parallel, reverse-connected thyristors. TCR is controlled with proper firing angle input to operate in a continuous manner, while TSR is controlled without firing angle control which results in a step change in reactance.

TSC shares similar composition and same operational mode as TSR, but the reactor is replaced by a capacitor. The reactance can only be either fully connected or fully disconnected zero due to the characteristic of capacitor.

With different combinations of TCR/TSR, TSC and fixed capacitors, a SVC can meet various requirements to absorb/supply reactive power from/to the transmission line.

1.3.1.2 Converter-based Compensator

Static Synchronous Compensator (STATCOM) is one of the key Converter-based Compensators which are usually based on the voltage source inverter (VSI) or current source inverter (CSI), as shown in Figure 1.5(a). Unlike SVC, STATCOM controls the output current independently of the AC system voltage, while the DC side voltage is automatically maintained to serve as a voltage source. Mostly, STATCOM is designed based on the VSI.

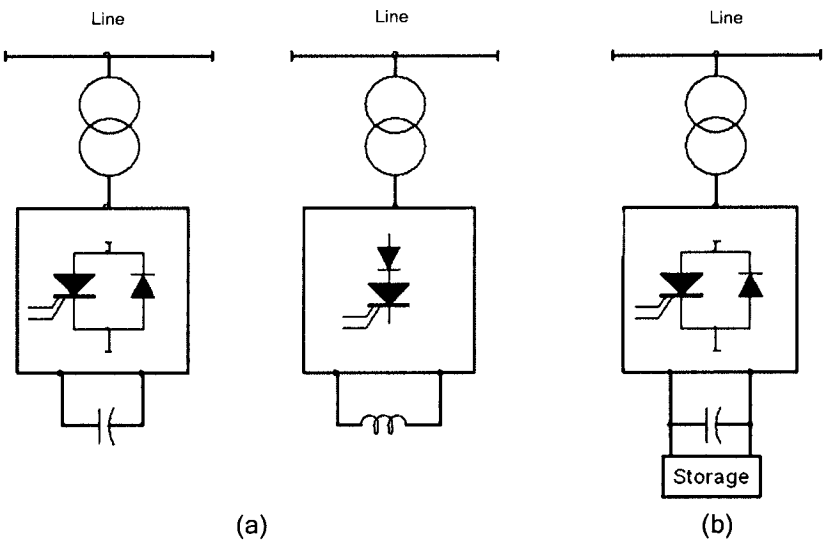

Figure 1. 5 STATCOM topologies: (a) STATCOM based on VSI and CSI (b) STATCOM with storage [5]

Compared with SVC, the topology of a STATCOM is more complicated. The switching device of a VSI is usually a gate turn-off device (GTO) paralleled by a reverse diode; this function endows the VSI advanced controllability. Various combinations of the switching devices and appropriate topology make it possible for a STATCOM to vary the AC output voltage in both magnitude and phase. Also, the combination of STATCOM with a different storage device or power source (as shown in Figure 1.5(b)) endows the STATCOM the ability to control the real power output.

STATCOM has much better dynamic performance than conventional reactive power compensators like SVC. The gate turn-off ability shortens the dynamic response time from several utility period cycles to a portion of a period cycle. STATCOM is also much faster in improving the transient response than a SVC. This advantage also brings higher reliability and larger operating range. Figure 1.6 shows the V-I characteristics of STATCOM and SVC [9].

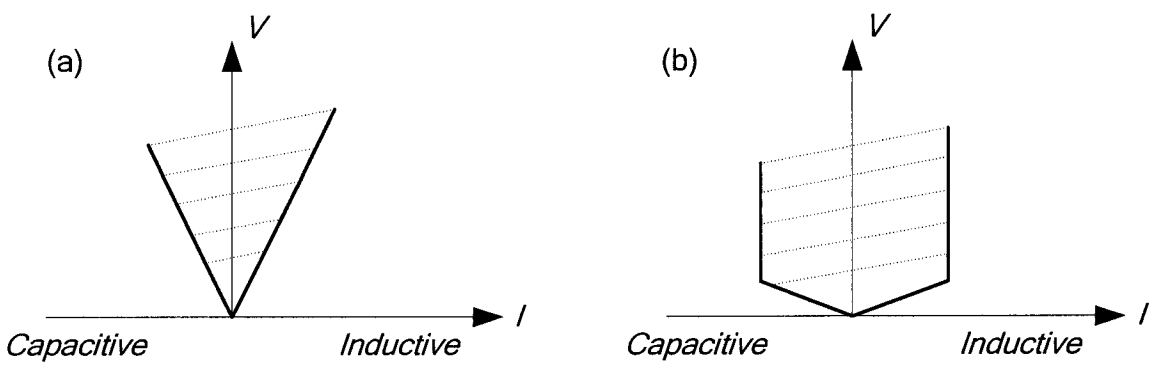

Figure 1. 6 V-I characteristics of SVC and STATCOM: (a) SVC; (b) STATCOM [24]

1.3.2 Series-connected controllers

As shunt-connected controllers, series-connected FACTS controllers can also be divided into either impedance type or converter type. The former includes Thyristor-Switched Series Capacitor (TSSC), Thyristor-Controlled Series Capacitor (TCSC), Thyristor-Switched Series Reactor, and Thyristor-Controlled Series Reactor. The latter, based on VSI, is usually in the form of a Static Synchronous Series Compensator (SSSC). The composition and operation of different types are similar to the operation of the shunt-connected peers.

Figure 1.7 shows the diagrams of various series-connected controllers.

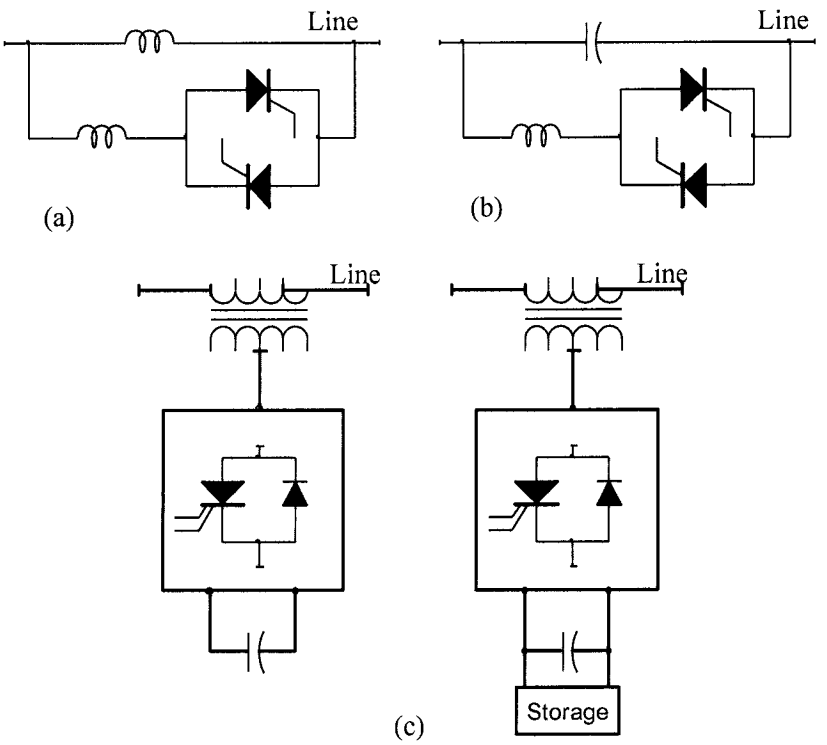

Figure 1. 7 Series-connected FACTS controllers: (a) TCSR and TSSR; (b) TSSC; (c) SSSC [5]

1.4 Static Synchronous Compensator (STATCOM)

As discussed in the previous section, STATCOM is a very popular FACTS controller application effective in transmission system voltage control. Since 1980 when the first STATCOM (rated at 20 Mvar) using force-commutated thyristor inverters was put into operation in Japan [10], many examples have been installed and the ratings have been increased considerably. In 1991, KEPCO and Mitsubish Motors installed a ±80MVar STATCOM at Inuyama Switching Station [11]. In 1996, TVA, EPRI and Westinghouse installed a ±100MVar STATCOM at Sullivan 500 kV Substation [12]. In 2001, EPRI and Siemens developed a ±200MVar STATCOM at Marcy 345kV substation [13]. It is expected that more STATCOMs will be installed due to the advances in technology and commercial success.

STATCOM could have many topologies, but in most practical applications it employs the DC to AC converter, which can also be called a Voltage Source Inverter (VSI) in 3-phase configuration as the primary block. The basic theory of VSI is to produce a set of controllable 3-phase output voltages/ currents at the fundamental frequency of the AC bus voltage from a DC input voltage source such as a charged capacitor or a DC energy supply device. By varying the magnitude and phase angle of the output voltage and current, the system can exchange active/reactive power between the DC and AC buses, and regulate the AC bus voltage.

The ability of a STATCOM to compensate the reactive power is directly influenced by the performance of the VSI, while the latter is determined by the switching technology and control strategy. Among the many ways in controlling VSI, pulse width modulation (PWM) voltage control and hysteresis current control (HCC) are very popular ones. In

PWM voltage control, STATCOM controls the output 3-phase voltage magnitude and phase angle with respect to the transmission line voltage, thus controlling the AC output current indirectly. The traditional way to obtain PWM is to compare a triangular carrier wave with a sine wave input which presents the same frequency and phase of the desired output voltage of the VSI, and the generated gating signals in turn create the desired AC output voltage. In this approach, STATCOM works as a solid state synchronous voltage source and has a fixed switching frequency [14]. However, the magnitude of the low order voltage harmonics that appear at the AC side are relatively high for the low switching frequencies used in high power applications, requiring the use of large and expensive low-pass filter to limit the magnitude of the current harmonics to acceptable levels.

An alternative technique to control the VSI is by using hysteresis current control. In this approach STATCOM controls the output 3-phase current waveform and VSI behaves as a synchronous current source [15, 16]. Unlike PWM, the HCC controls the current directly. The gating signals of the switches are generated by the comparison of the AC side actual output current and a reference signal so that the fundamental component of the former is identical to the latter. VSI using HCC is difficult to be described in mathematical equations, thus making it hard to design the controllers in a traditional way. The advantage of using HCC is when the tolerance band is set small, the magnitude of the harmonics is low, thus reducing the necessity of expensive low-pass filters. The disadvantage, however, is that the harmonic frequency across a wide band instead of fixed value. Furthermore, the low tolerance band results the variable switching frequency

which is usually high and might exceeds the rating of high power switches such as Insulated Gate Bipolar Transistors (IGBTs) and GTOs.

1.5 Literature Review

Since the focus of the thesis is on Static Synchronous Compensator (STATCOM), a brief literature review on this topic is presented below.

Paper [1] traces back the history and development of FACTS technology and emphasizes the power flow control function. Reference [2] gives a brief classification of the main FACTS controllers and describes their operating principles. It helps the reader know the definitions and terms of power electronics, and provide a basic understanding of different FACTS technologies. Reference [3] studies several American projects in which FACTS technology is put into practice and presents the benefits that are brought into power industry. Combined with [1], readers can have a general idea about the development trend of the FACTS technology and the power industry. Reference [4] introduces the developments of STATCOM MVA ratings and control technology. Many practical examples all over the world during the past twenty years are mentioned. Different power circuit topologies such as multi-level converters and multi-pulse converters and characters are introduced. The trend of STATCOM technology is predicted.

Paper [17] gives a very detailed discussion on the stationary and rotating synchronous reference frames in which 3-phase instantaneous vectors are transformed into **d-q** components. With the two reference frames, the control of VSI can be decoupled into **d-q** loops which facilitate the linearization of the system. This paper is widely applied by

further researches on the VSI based FACTS controllers. The rotating synchronous reference frame is utilized in this thesis for the mathematical analysis.

References [18] and [19] give a good insight on modeling 3-phase PWM converters. The research proposes a new technique to derive the linear model from nonlinear system therefore present a controller of good performance. However, the deduction of the mathematical expression is complicated and detail is not described. References [20] and [21] investigate the mathematical models using both stationery and rotating reference frame for 3-phase to **d-q** transformation The complex vectors are used to decouple the active and reactive control loops of the system. The paper provides a detailed procedure on controller design and focus on the effect of time constant and gains to the performance,. References [22] and [23] describe a new way to carry out the DC and AC analysis. By using synchronous rotating frame to decouple d-q control loops, the research also applies feedforward path to describe the interaction between the two loops. This method is utilized in the thesis for control analysis.

Paper [15] describes the operation of the VSI using HCC. It introduces the advantages of current control strategy, and several important features of the device. It reveals the possibility of STATCOM application using HCC. Although the paper tries to provide a model for control analysis, the nonlinear model makes the analysis hard to be realized. Reference [16] studies STATCOM using HCC for the first time. It describes in detail the switching function of HCC, and the simulation results of the studied case. A preliminary comparison of STATCOM using HCC and PWM voltage control is made. However, the control strategy of STATCOM using HCC is not analyzed. The comparison is not supported by details of control analysis and model description.

1.6 Objectives and Challenges

PWM control and HCC have their advantages and disadvantages respectively. Presently, most researches in STATCOM are based on PWM controlled VSI while STATCOM using HCC is rarely studied [14]. The reason why PWM voltage control is more popular and HCC is seldom employed deserves a more in-depth study. In this thesis, the modeling of a typical 6-pulse STATCOM using the two control strategies will be analyzed. The performances of STATCOM using two control strategies under different small disturbances are described with simulation results. The harmonic components in the output and the switching frequency of STATCOM switches are the two focuses of analysis. The advantages and drawbacks of the two control strategies are demonstrated by the detailed comparison.

1.7 Thesis Contribution and Outline

The major contribution of this thesis is included in four parts:

- Provide a preliminary mathematical model for current-controlled STATCOM, analyze the control loops, and design the controller.
- Implement the hysteresis current signal generator in EMTP-RV software
- Investigate the relationship between the switching frequency and the harmonic components of STATCOM in both control strategies
- Give detailed comparison between HCC and PWM voltage control in STATCOM application.

This Thesis is composed of six chapters and one appendix.

Chapter 2 gives a general introduction to the modulation techniques PWM and HCC. A HCC signal generator is designed.

Chapter 3 discusses the modeling and control analysis for a STATCOM using HCC. Circuit d-q transformation with synchronous rotating reference frame is emphasized in model derivation. A conventional PI control block is used to implement the controller. A sample power circuit is simulated in EMTP-RV software and its performance is discussed.

Chapter 4 discusses the modeling and control analysis for STATCOM using PWM voltage control in a similar manner presented in Chapter 3. The main controller is also implemented using a PI control block. The sample circuit used in Chapter 3 is employed again and performance discussed.

Chapter 5 compares the result of the two control methods. The relationship between the harmonic components and switching frequency is discussed. Several approaches to reduce the harmonics and switching frequencies are analyzed.

Chapter 6 gives the conclusion of the thesis work, and suggests the future directions for the research.

2. MODULATION TECHNIQUES

2.1 Introduction

Voltage Source Inverter (VSI) is the basic building block of a STATCOM. Although there are many configurations of VSI in various applications, the three phase six switch VSI is the most popular one. By inputting the pre-defined signals, the six switches are controlled on and off at designated intervals to convert the DC voltage into a 3-phase output voltage. Pulse Width Modulation (PWM) and Hysteresis Current Control (HCC) are very popular switching technologies of VSI. This chapter will provide a brief introduction to PWM and HCC technology. A one-leg switch mode converter will be taken as the example to explain the operation scheme of the two technologies. The switching signal generators are discussed also.

2.2 Pulse Width Modulation (PWM)

PWM is the most popular switching technology for VSI. By comparing the input signal with a fixed frequency triangular carrier wave to generate the firing pulses for the converter, the magnitude and phase of the fundamental component of the output voltage magnitude can be controlled by varying the magnitude and phase of the modulating signal. In this scheme the AC voltage contains fundamental and harmonic components located around the frequency multiples of the carrier frequency.

Figure 2.1 shows a one-leg switch mode converter with a DC voltage source input V_{dc}. The two switches T_{A+} and T_{A-} are controlled by the switching signal generator. The output voltage of the leg A to the ground point is v_{AO}. If each switch in the leg is operated

off when the other is on, the output voltage v_{AO} is determined by the status of the switches.

$$v_{AO} = \frac{V_{dc}}{2} \quad \text{(when } T_{A+} \text{ on)} \tag{2-1}$$

$$v_{AO} = -\frac{V_{dc}}{2} \quad \text{(when } T_{A-} \text{ on)} \tag{2-2}$$

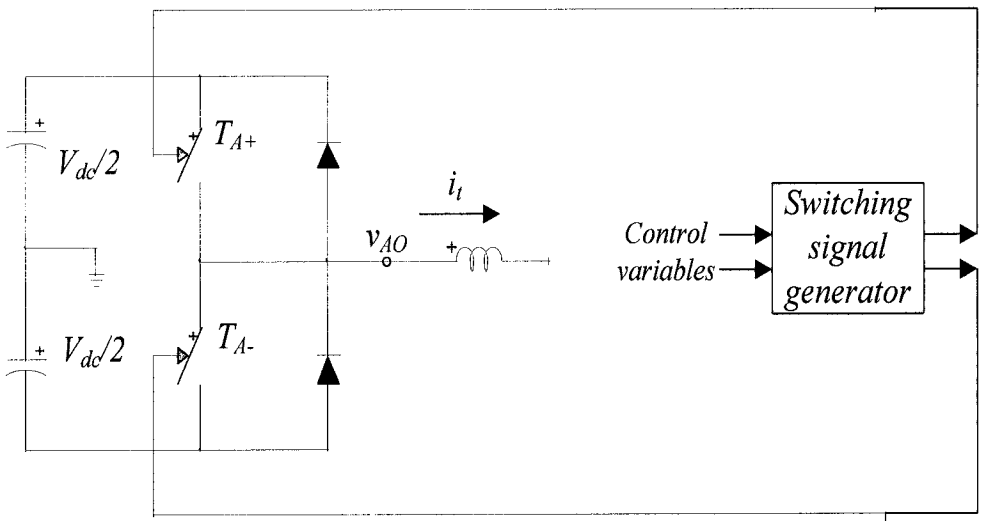

Figure 2. 1 One-leg switch mode converter

It can be shown that the average value of the output voltage V_{AO} in a switching period (T_{sw}) is given by

$$V_{AO} = (2D-1)\frac{V_{dc}}{2} \tag{2-3}$$

where, D is the duty ratio of switch T_{A+} and is defined as

$$D = \frac{t_{on}}{T} \tag{2-4}$$

In PWM switching technology, the control signal $v_{control}$ is compared with a triangular carrier wave v_{tri}, as shown in Figure 2.2. When $v_{control} > v_{tri}$, T_{A+} is turned on. When $v_{control} < v_{tri}$, T_{A-} is turned on. Since V_{tri} and V_{dc} are both fixed value, the duty ratio D is determined by the ratio of $v_{control}$ and the peak value of the triangular carrier V_{tri}, therefore,

$$V_{AO} = (2D-1)\frac{V_{dc}}{2} = \frac{v_{control}}{V_{tri}}\frac{V_{dc}}{2} = \frac{V_{dc}}{2V_{tri}}v_{control} \tag{2-5}$$

The average output voltage V_o changes linearly with the control signal $v_{control}$. The converter behaves as a gain factor or as a linear amplifier.

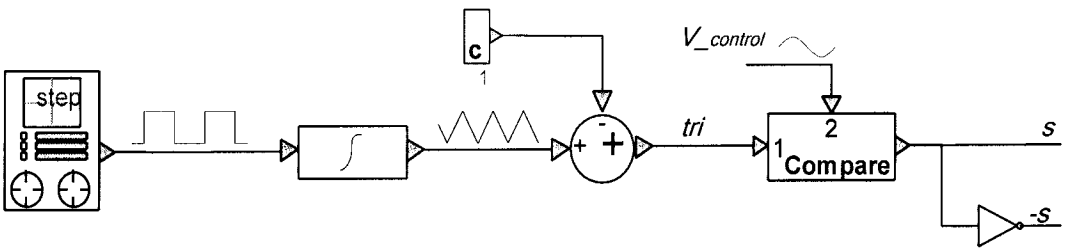

Figure 2. 2 PWM signal generator structure implemented in EMTP-RV

When the control signal is a sinusoidal wave instead of a dc value, the output voltage of the leg v_{AO} is a series of pulses of different width. Because the carrier frequency f_{tri} is much higher than the frequency of the control signal f_1, the control signal in a switching period T_{tri} could be viewed approximately constant, and Eq.2-5 could be applied here. Consequently, the pulse width varies linearly with the ratio of the control signal $v_{control}$ to the peak value of the triangular carrier V_{tri}, as Figure 2.3 shows. And the square wave could be decomposed into a fundamental component at frequency f_1 and harmonic

components. In Fourier analysis we notice that the harmonic components are focused close to the multiple of f_1. If we define the modulation index MI as:

$$MI = \frac{V_{control}}{V_{tri}} \tag{2-6}$$

where $V_{control}$ is the peak value of the control signal;

And the frequency modulation ratio m_f as:

$$m_f = \frac{f_{tri}}{f_1} \tag{2-7}$$

where f_{tri} is the carrier frequency, equal to the switching frequency of switches f_{sw}.

The peak value of the fundamental component of v_{AO} is calculated as:

$$V_{Ao-1} = \frac{V_{control}}{V_{tri}} \frac{V_{dc}}{2} = MI \frac{V_{dc}}{2} \tag{2-8}$$

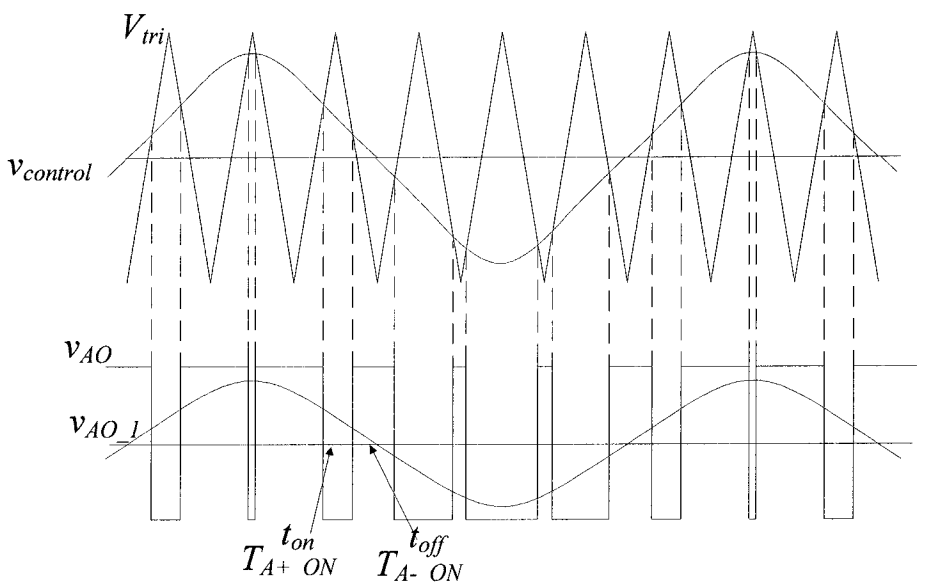

Figure 2. 3 Sinusoidal Pulse Width Modulation (SPWM)

2.3 Hystersis current control (HCC)

Hysteresis current control (HCC) is another popular switching technology of VSI. Unlike PWM, HCC controls the current variable instead of a voltage variable. In this technology, the output AC phase current of the VSI is compared with the input reference sinusoidal current. With the help of a pre-defined tolerance band, the output AC phase current is limited into the tolerance band and approximately viewed same as the reference current if the harmonic components are neglected. Therefore, by controlling the magnitude and phase angle of the reference current, VSI can output a set of 3-phase sinusoidal currents to exchange reactive power between STATCOM and transmission system [26].

In order to demonstrate the control scheme of HCC, the one-leg switch mode converter in Figure 2.1 is taken as an example, and the HCC switching signal generator structure is shown in Figure 2.4.

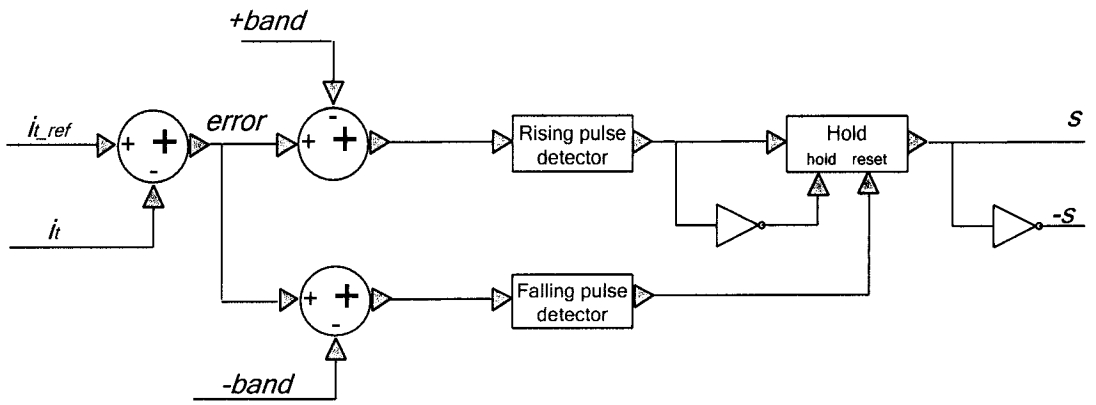

Figure 2. 4 HCC signal generator implemented in EMTP-RV

The actual output phase current i_t is compared with the tolerance band around the reference current i_{t_ref}. Once i_t goes beyond the upper tolerance band, the upper switch T_{A+} is turned off, and the lower switch T_{A-} is turned on. Since V_{dc} is higher than the

magnitude of the phase voltage V_t, the opposite potential on the inductance will force the output phase current i_t to decrease. The opposite operation will take place when i_t goes below the lower tolerance band. Therefore, the actual output phase current i_t is kept inside the tolerance band and along with the reference current i_{t_ref} as shown in Figure 2.5. Similar technique can be applied to a 3-phase VSI.

From Figure 2.5, we can see that the narrower the tolerance band, the higher the switching frequency, the more sinusoidal the actual output phase current i_t, and the less the harmonic components in i_t. In other words, smaller is the magnitude of the current ripple on the fundamental component. If the tolerance band is narrow enough that the harmonic components are negligible, the VSI is working as a unit gain factor with small transportation lag so that the fundamental component of the AC side actual output current i_t is very close to the input reference current i_{t_ref}. But the switching frequency of VSI will be very high.

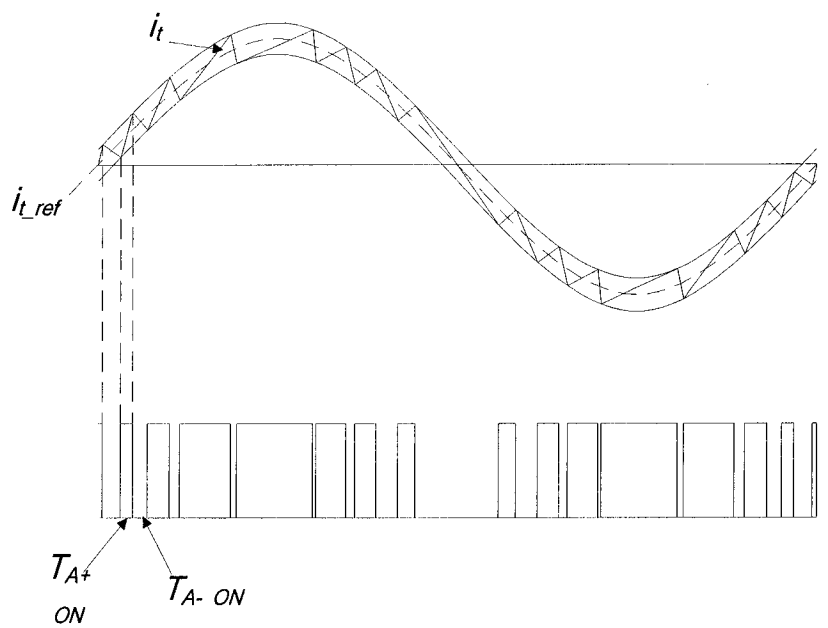

Figure 2. 5 Hysteresis Current Control (HCC)

2.4 Summary

This chapter has introduced the operational scheme of PWM switching technology and HCC technology. The signal generators of the two technologies are implemented in EMTP-RV package.

PWM technology operates the VSI at a fixed frequency and outputs the voltage with low order harmonics with high magnitude when the switching frequency is relatively low, to meet the limitations of high power semiconductor switches. This characteristic makes a low-pass filter a necessity for the STATCOM using PWM VSI. In HCC technology, the magnitude of the harmonic components can be made smaller by using a narrow tolerance band. However, this approach results in pulses with variable frequencies and a relatively high average switching frequency. This problem can be overcome by increasing the size of the inductor that connects the VSC to an ac bus, which is equivalent to including a low pass filter in the system. In a later chapter, the application of the VSI using the two switching technologies as STATCOM will be discussed, and the effects will be compared to each other.

3. MODEL AND ANALYSIS OF STATCOM USING HCC

3.1 Introduction

In an AC transmission system, power transmission and the system stability is largely related to the transmission line voltage. As the system is under constantly changing status, fast reactive power compensation over a wide range is increasingly required to keep a relatively stable transmission line voltage. STATCOM is such a device that can resemble a rotating synchronous compensator. By controlling the magnitude and phase angle of the output 3-phase voltages and currents, STATCOM generates a set of inductive or capacitive current to exchange the reactive power with the transmission system and regulate the voltage.

A STATCOM using HCC directly controls the AC side actual output current to exchange the power with transmission line. When the AC side output current flowing to the connection point leads to the transmission line voltage, the STATCOM injects reactive power and the transmission line voltage is boosted. When the AC side output current flowing to the connection point lags to the transmission line voltage, the STATCOM absorbs reactive power, and the transmission line voltage is reduced [18]. This characteristic also applies to the active power exchange.

In this chapter, a STATCOM using three-phase VSI is modeled. The control strategy using HCC will be analyzed in the synchronous rotating reference frame. The reactive power compensation control loop and active power absorption control loop are discussed. The controller based on PI control will be designed accordingly. Finally, a power circuit of the STATCOM model will be simulated in EMTP-RV package to verify the performance of the designed controller.

3.2 Power Circuit Configuration

A STATCOM is connected to the transmission line through a coupling transformer. In order to provide the voltage support, the connection point is usually at the middle of the transmission line. The VSI employs six self-commutated semiconductor switches with a diode reverse-paralleled to each switch. The coupling transformer primary windings are star-connected and the secondary windings are connected in parallel with each phase of the transmission line.

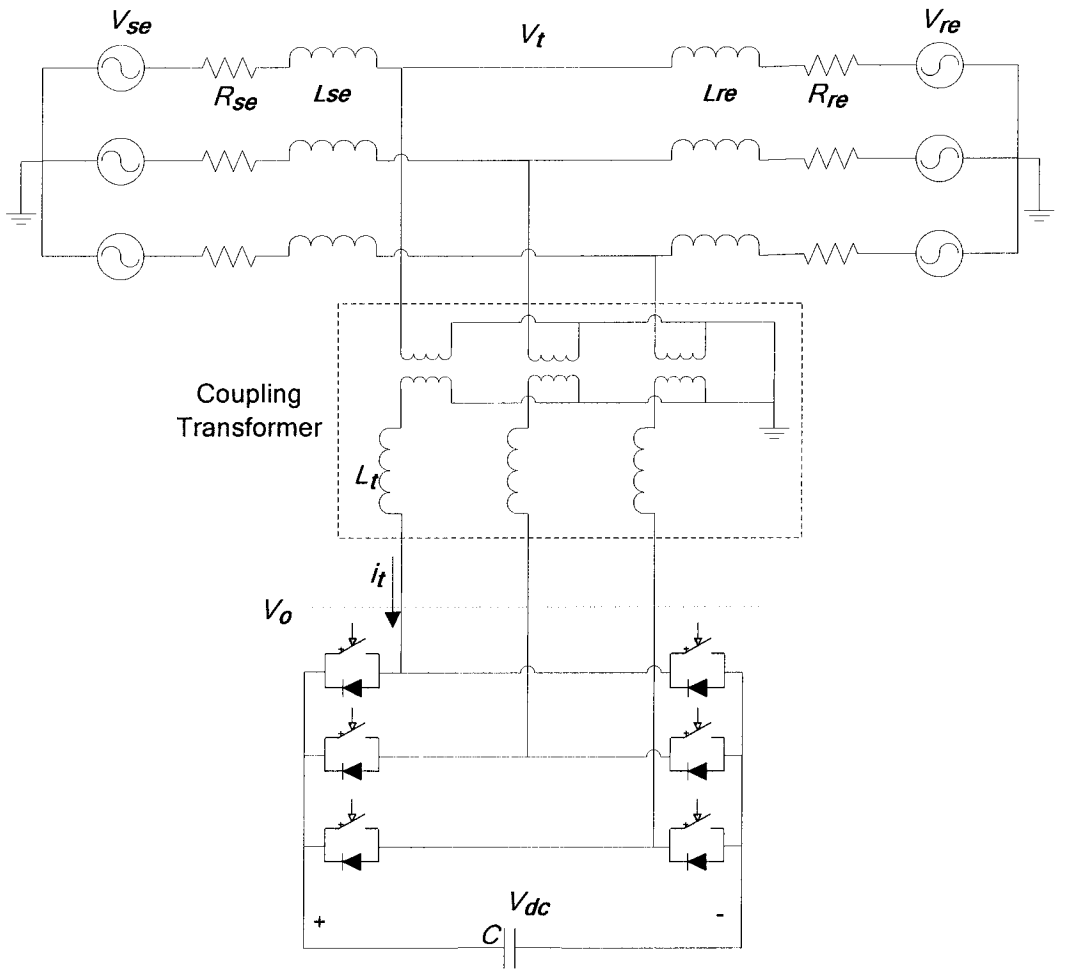

Figure 3. 1 3-phase diagram of STATCOM

A detailed 3-phase diagram of the STATCOM using a typical three phase VSI is given in Figure 3.1, where

v_{se} and v_{re}: voltages at the sending-end and receiving-end of the transmission line.

R_l and X_l: transmission line resistance and reactance respectively.

δ: the phase angle between v_{se} and v_{re}.

L_t: the internal leakage inductance of the coupling transformer.

v_o: output voltage of VSI.

i_t: the output phase current injected into the transmission line.

V_{dc}: the voltage across the DC-link of VSI.

3.3 System Simplification

In the practical application, the transmission system to which the STATCOM is connected is under constantly varying status. The load variation, action of protection relays and system operation make the system parameters always changing. It is very difficult to take into consideration the very complex system when modeling STATCOM. However, when seen from the STATCOM, the complicated power system could all be represented as equivalent Thevenin voltage source v_s with the equivalent Thevenin resistance and reactance R_s and X_s. All the changes in system parameters can be simply viewed as changes in data of v_s, R_s and X_s [28].

To further simplify the circuit, some assumptions are introduced as follows:

(1) All switches and diodes used in the converter are ideal,

(2) Power system is 3-phase balanced,

(3) Coupling transformer is represented by the inductive element L_t,

(4) Switching loss of the converter is represented as a parallel connected resistance $\boldsymbol{R}$ on the DC side.

The simplified 3-phase version of the STATCOM circuit is shown in Figure 3.2.

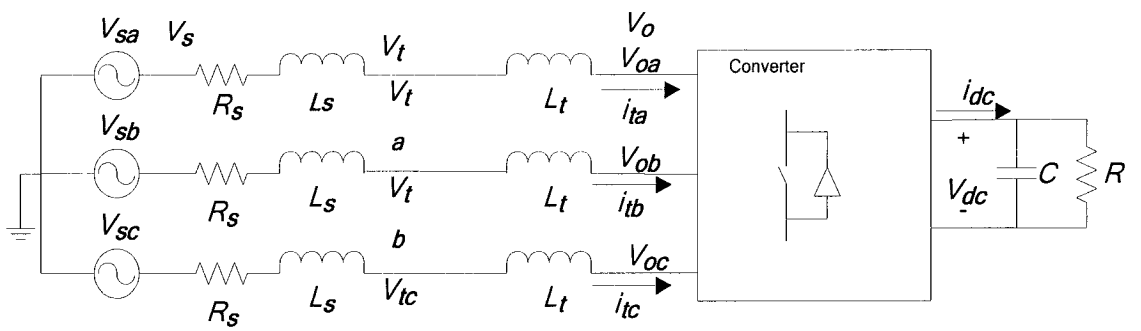

Figure 3. 2 Simplified 3-phase STATCOM circuit

The AC side output phase currents of STATCOM are denoted by $[\boldsymbol{i_t}]=[\boldsymbol{i_{ta}}, \boldsymbol{i_{tb}}, \boldsymbol{i_{tc}}]^T$, the AC side output voltages of the converter are denoted by $[\boldsymbol{v_o}]=[\boldsymbol{v_{oa}}, \boldsymbol{v_{ob}}, \boldsymbol{v_{oc}}]^T$, and the AC bus voltages at the connection point are denoted by $[\boldsymbol{v_t}]=[\boldsymbol{v_{ta}}, \boldsymbol{v_{tb}}, \boldsymbol{v_{tc}}]^T$. The equivalent Thevenin impedance is denoted by $\boldsymbol{R_s}$ and $\boldsymbol{\omega L_s}$, and Thevenin source voltage is denoted by $\boldsymbol{v_s}$, $[\boldsymbol{v_s}]=[\boldsymbol{v_{sa}}, \boldsymbol{v_{sb}}, \boldsymbol{v_{sc}}]^T$.

From the simplified circuit in Figure 3.2, the regulated voltage at AC bus $\boldsymbol{v_t}$ is dependant on the reactive power compensation of VSI which is directly controlled by the AC side actual output current $\boldsymbol{i_t}$ or indirectly by the VSI output voltage $\boldsymbol{v_o}$. The loop equation for the simplified equivalent circuit can be written as:

$$v_{sa,b,c} = v_{ta,b,c} + R_s i_{ta,b,c} + L_s \frac{di_{ta,b,c}}{dt} \tag{3-1}$$

The power balance equation for the DC-AC sides of VSI can be written as:

$$P_{ac} = P_{dc} \tag{3-2}$$

3.4 Control Analysis

3.4.1 Synchronous Rotating Reference Frame

Analysis of the system in Figure 3.2 is done by using **d-q** coordinates. The equivalent Thevenin voltage v_s can not be measured but AC bus voltages at the connection point v_t can. Therefore v_t is employed to build a rotating reference frame in which the loop equations are decomposed into **d-** and **q-** components. The rotating d axis is superimposed to v_{ta} as shown in Figure 3.3, and v_t is defined as:

$$[v_t] = \begin{bmatrix} v_{ta} \\ v_{tb} \\ v_{tc} \end{bmatrix} = V_t \begin{bmatrix} \sin\theta \\ \sin(\theta - \frac{2\pi}{3}) \\ \sin(\theta + \frac{2\pi}{3}) \end{bmatrix} \tag{3-3}$$

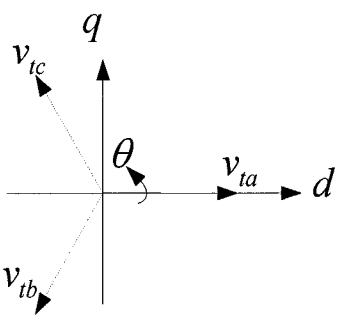

Figure 3. 3 **d-q** transformation of rotating reference frame

Where $\theta = \omega t$ is the rotating phase angle of v_t.

The transformation matrix K_θ of synchronous rotating reference frame is defined as:

$$K_\theta = \frac{2}{3} \begin{bmatrix} \sin\theta & \sin(\theta - \frac{2\pi}{3}) & \sin(\theta + \frac{2\pi}{3}) \\ \cos\theta & \cos(\theta - \frac{2\pi}{3}) & \cos(\theta + \frac{2\pi}{3}) \\ \frac{1}{\sqrt{2}} & \frac{1}{\sqrt{2}} & \frac{1}{\sqrt{2}} \end{bmatrix} \tag{3-4}$$

The inverse transformation matrix is $\boldsymbol{K_\theta^{-1}}$,

$$K_\theta^{-1} = \begin{bmatrix} \sin\theta & \cos\theta & \frac{1}{\sqrt{2}} \\ \sin(\theta - \frac{2\pi}{3}) & \cos(\theta - \frac{2\pi}{3}) & \frac{1}{\sqrt{2}} \\ \sin(\theta + \frac{2\pi}{3}) & \cos(\theta + \frac{2\pi}{3}) & \frac{1}{\sqrt{2}} \end{bmatrix} \tag{3-5}$$

The voltage and current variables can be decomposed into **d-** and **q-** components by the transformation matrix $\boldsymbol{K_\theta}$:

$$\begin{bmatrix} V_{sd} \\ V_{sq} \\ 0 \end{bmatrix} = K \begin{bmatrix} v_{sa} \\ v_{sb} \\ v_{sc} \end{bmatrix}, \begin{bmatrix} V_{td} \\ V_{tq} \\ 0 \end{bmatrix} = K \begin{bmatrix} v_{ta} \\ v_{tb} \\ v_{tc} \end{bmatrix}, \begin{bmatrix} I_{td} \\ I_{tq} \\ 0 \end{bmatrix} = K \begin{bmatrix} i_{ta} \\ i_{tb} \\ i_{tc} \end{bmatrix} \tag{3-6}$$

It is easy to get:

$$V_{td} = V_t,\ V_{tq} = 0 \tag{3-7}$$

The phase diagram of voltage and current variables analyzed in **d-q** rotating reference frame is shown as Figure 3.4[17].

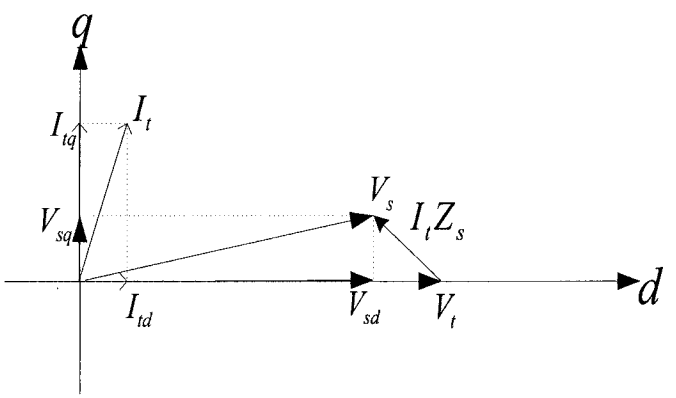

Figure 3. 4 d-q analysis of STATCOM variables in synchronous rotating reference frame.

With the transformation matrix K_θ, i_t is decomposed into two components, I_{td} and I_{tq}, which are in quadrature with each other and both synchronous with the AC bus voltage v_t. Therefore, I_{td} and I_{tq} are responsible for the active power absorption and reactive power compensation respectively.

$$P_{ac} = \frac{3}{2}(V_{td}I_{td} + V_{tq}I_{tq}) = \frac{3}{2}V_tI_{td} \tag{3-8}$$

$$Q_{ac} = \frac{3}{2}(V_{td}I_{tq} - V_{tq}I_{td}) = \frac{3}{2}V_tI_{tq} \tag{3-9}$$

Then the analysis of the system is decomposed into two control loops: (1) reactive power compensation control loop (simply called **q-** loop) which is largely responsible for the AC bus voltage regulation, and (2) the active power absorption control loop (simply called **d-** loop) which accounts for the DC bus voltage stabilization.

3.4.2 Reactive power compensation control loop

Using Synchronous Rotating Reference Frame, loop equation Eq. (3-1) can be rewritten as:

$$V_{sd} - V_t = R_sI_{td} + L_s\frac{dI_{td}}{dt} - \omega L_sI_{tq} \tag{3-10}$$

Using Laplace transformation, we get:

$$R_sI_{td} + sL_sI_{td} - \omega L_sI_{tq} = V_{sd} - V_t \tag{3-11}$$

Considering that the active power loss of the VSI is usually much less than the reactive power compensation, the magnitude of the **d-** component output phase current I_{td} is much less than the magnitude of the **q-** component output phase current I_{tq}. In order to simplify

the analysis, the influence of I_{td} over the **q-** control loop is ignored. Eq. (3-11) can be rewritten as:

$$V_t - V_{sd} = \omega L_s I_{tq} \tag{3-11}$$

Then Eq. (3-11) is the mathematical expression of the **q-** control loop of the STATCOM model.

3.4.3 Active power absorption control loop

The power balance equation Eq. (3-2) gives the relationship between the active power delivered by the AC source and absorbed by the DC side of STATCOM. The active power loss P_{loss} includes the switching loss, VSI and transformer conduction losses. In order to simplify the analysis and maintain accuracy, the portion of active power loss is counted to DC side parallel connected resistance R without loss of accuracy.

The active power of the VSI on the DC side is:

$$P_{dc} = \frac{V_{dc}^{\ 2}}{R} + V_{dc} C \frac{dV_{dc}}{dt} \tag{3-12}$$

Combining Eqs. (3-2), (3-8) and (3-12), we can get:

$$\frac{3}{2} V_t I_{td} = \frac{V_{dc}^2}{R} + V_{dc} C \frac{dV_{dc}}{dt} \tag{3-13}$$

To analyze the small signal disturbance response, V_t is assumed as regulated stable.

Using ΔI_{td} and ΔV_{dc} to represent the small disturbances, Eq. (3-13) is rewritten as:

$$\frac{3}{2} V_t \left(I_{td} + \Delta I_{td}\right) = \frac{\left(V_{dc} + \Delta V_{dc}\right)^2}{R} + \left(V_{dc} + \Delta V_{dc}\right) C \frac{d\left(V_{dc} + \Delta V_{dc}\right)}{dt} \tag{3-14}$$

Ignoring the DC steady state values and second order signals,

$$\frac{3}{2}V_t\Delta I_{td} = \frac{2V_{dc}\Delta V_{dc}}{R} + V_{dc}C\frac{d\Delta V_{dc}}{dt} \tag{3-15}$$

After using Laplace transformation, Eq. (3-15) is transformed into:

$$\frac{\Delta V_{dc}(s)}{\Delta I_{td}(s)} = \frac{3V_t/2}{2V_{dc}/R + sCV_{dc}} \tag{3-16}$$

Hence, Eq. (3-16) represents the small signal response of DC side voltage V_{dc} to the **d-** component of the output phase current i_{td}

3.5 Controller Design

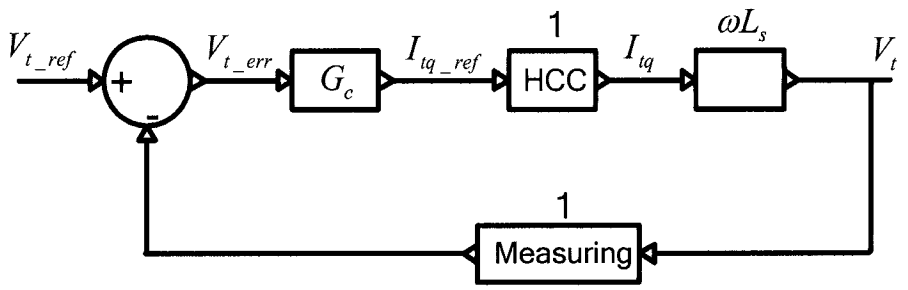

Figure 3. 5 The equivalent **q-** control loop block diagram

With the help of synchronous rotating reference frame, STATCOM is decomposed into two mathematical models, i.e. Eq. (3-11) and Eq. (3-16), which represent the transmission line voltage control and the DC bus voltage regulation respectively. From Eq. (3-11), we notice that in steady state, or under small signal disturbances, the magnitude of transmission line voltage V_t shows a linear relationship to the magnitude of the **q-** component output phase current I_{tq}. Figure 3.5 shows the control structure of the **q-** control loop using PI controller based on STATCOM model Eq. (3-11).

Ignoring the transportation lag of the voltage measurement block, the transmission line voltage magnitude V_t is monitored, and compared with the reference voltage V_{t_ref}. The error is inputted to a PI controller to generate the magnitude of the **q-** component reference current I_{tq_ref}. In the control strategy of HCC, the actual output phase current i_t is controlled to track the reference current i_{t_ref}. Although i_t presents harmonics, but the fundamental component is in phase and has same magnitude with i_{t_ref}. Therefore, the overall function block of HCC can be similarly operated as a unit gain factor. The magnitude of the **q-** component of output phase current I_{tq} is therefore obtained.

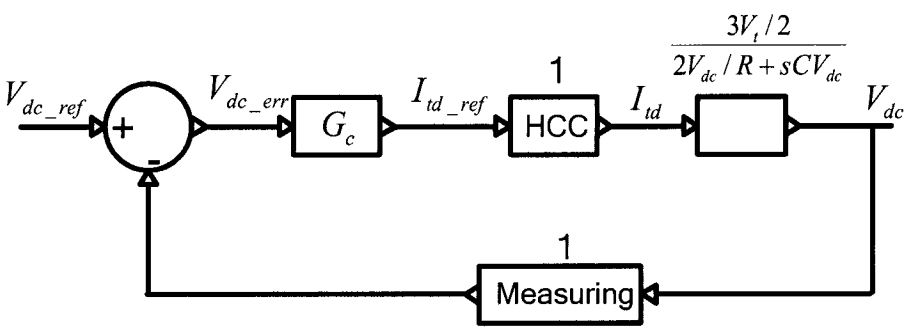

Figure 3. 6 The equivalent **d-** control loop block diagram

In an identical manner to the **q-** control loop, the control structure of **d-** control loop is obtained based on Eq. (3-16), and the equivalent **d-** control loop block diagram is shown as Figure 3.6. The magnitude of the **d-** component of output phase current I_{td} is therefore obtained.

With the above discussion, the overall control structure The parameters of **d-** and **q-** Loop Regulators are calculated in Appendix C. of STATCOM using HCC is as shown as Figure 3.7. Important components are discussed below:

(1) Measure Block. The DC side voltage V_{dc} and the transmission line voltage v_t are monitored with Measure Block. 3-phase voltage v_t is fed to **abc to dq** block to calculate the magnitude V_t. Phase-locked loop (PLL) block is used to maintain the synchronization to the transmission line voltage v_t.

(2) **q-** Loop Regulator. V_t is compared with the required value V_{t_ref}. The error is sent to the PI block to generate the magnitude of the **q-** component reference current I_{tq_ref}.

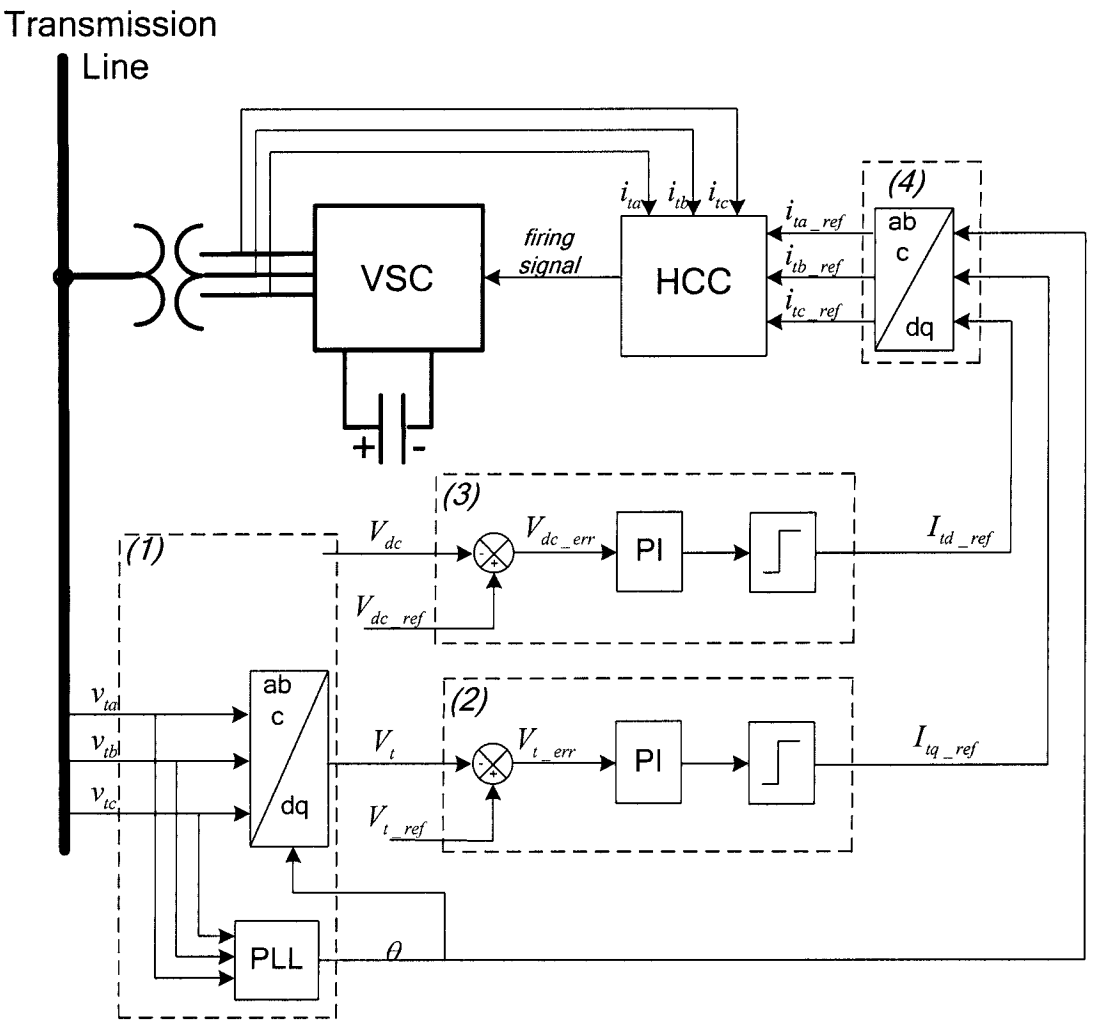

Figure 3. 7 Overall control structure of STATCOM using HCC

(3) **d-** Loop Regulator. V_{dc} compared with the required value V_{dc_ref}. The error is sent to the PI controller to generate the magnitude of the **d-** component reference current I_{td_ref}.

(4) Reference Current Generator. The synchronization of reference output phase current i_{t_ref} to the transmission line voltage v_t is maintained by feeding the unit magnitude waveform to **dq to abc** block. With reference to Eqs. (3-6), I_{td_ref} and I_{tq_ref} are calculated to get the overall reference output phase current i_{t_ref}. This reference current is sent to HCC switching signal generator to generate the firing signals which control STATCOM switches to output the actual phase current i_t.

3.6 Simulation Results

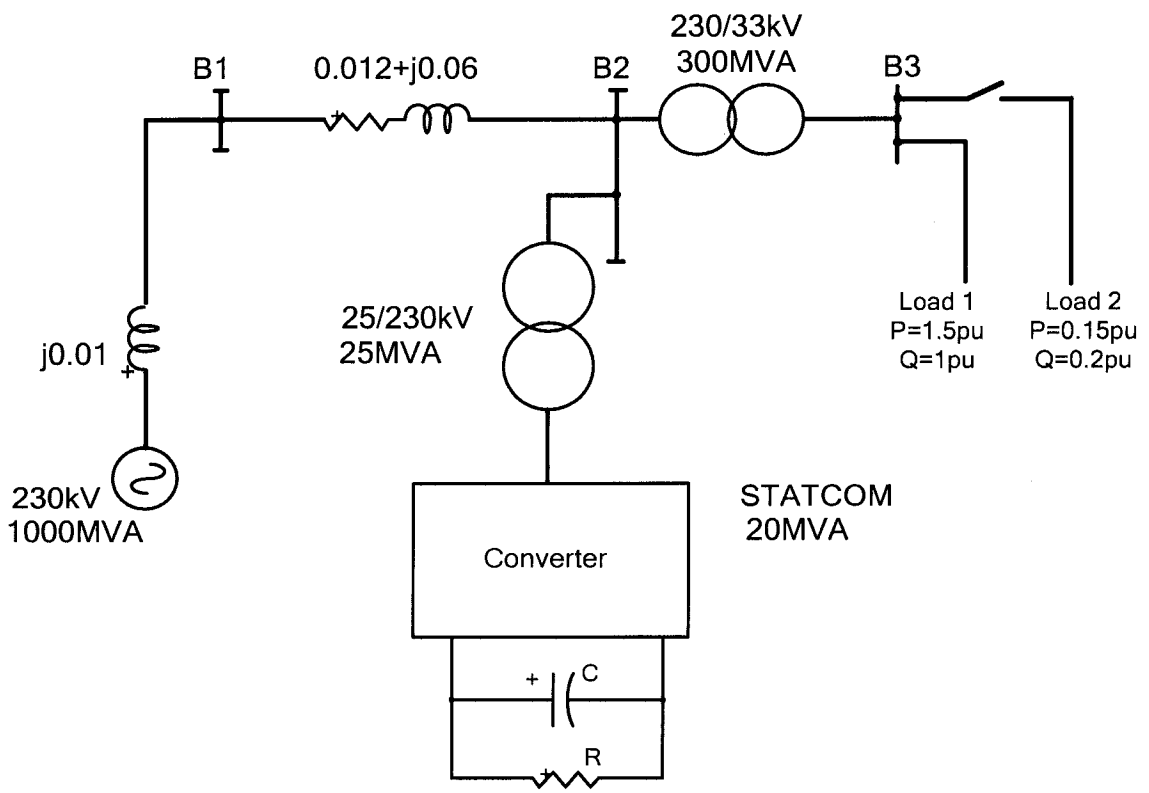

Figure 3. 8 Single line diagram of STATCOM model using HCC

In order to verify the performance of the controller, a STATCOM model (Figure 3.8) is simulated in EMTP-RV package.

A transmission line is connected from the grid to the power transformer which supplies load 1 connected to bus B3. In order to maintain the voltage at the end of transmission line in the range from 95% to 105% of the rated value, a STATCOM is connected to bus B2 through a coupling transformer. The system parameters are listed in Table 3.1. (MVA_{base}=100, kV_{base}=230). The parameters of **d-** and **q-** Loop Regulators are calculated in Appendix C.

Table 3. 1 System parameters of power circuit

Components	**Power**	**Voltage (kV)**	**R (pu)**	**X (pu)**
Grid	1000MVA	230		0.02
Transmission line		230	0.012	0.06
Power transformer	300MVA	230/33		0.01
Load 1	1.5+j1 pu	33		
Load 2	0.15+j0.2 pu	33		
Coupling transformer	25MVar	25/230		0.08
STATCOM	20MVar	25		
STATCOM DC side			27kΩ	0.2mF

3.6.1 Steady state performance

This simulation is to verify the steady state performance of the controller. A detailed analysis of the harmonic components is presented in Chapter 5. The STATCOM device shown in Figure 3.8 is connected into transmission system at 0.2s. Figure 3.9 (a) shows the voltage regulation effect of STATCOM. Before the introduction of STATCOM, the transmission line voltage magnitude V_t is about 0.83 pu which is

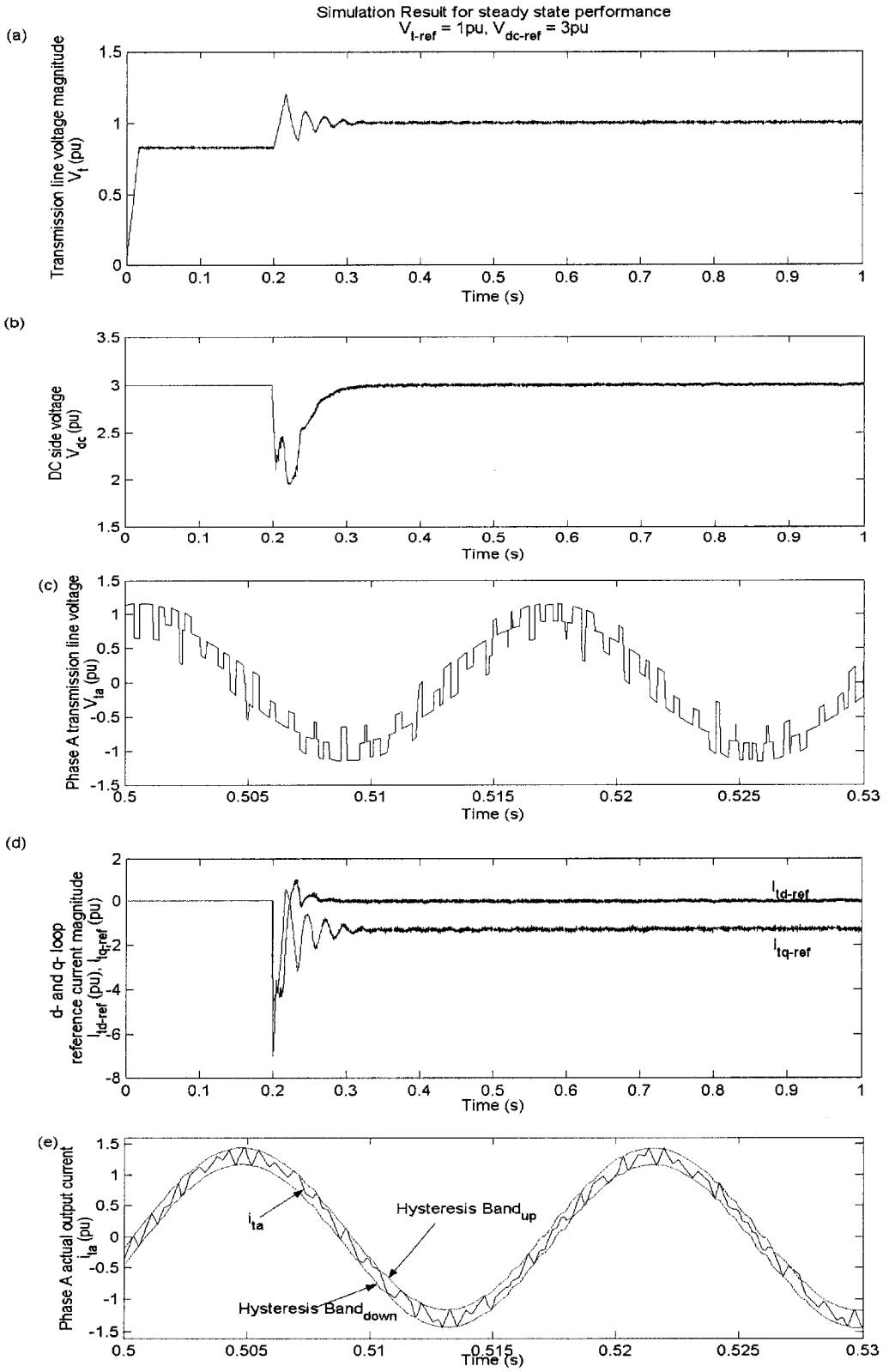

Figure 3. 9 Simulation result for steady state performance of HCC STATCOM

below the limit of the transmission requirement. With the compensation of STATCOM, the magnitude of fundamental component V_t is maintained at 1 pu after a start up oscillation lasting about 0.12s. In order to keep the actual output phase current i_t at a certain slope, the DC side voltage V_{dc} is maintained at 75kV.

Figure 3.9 (b) shows the waveform of DC side voltage V_{dc}. At the moment of connection, V_{dc} has dropped greatly. It takes the startup oscillation period lasting about 0.12s for V_{dc} to regain steady state at 3 pu.

Figure 3.9 (c) shows the steady state waveform of instantaneous phase A voltage v_{ta} at transmission line bus B2. A close look at the waveform shows v_{ta} is composed of a series of pulses with different widths. The maximum value of v_{ta} has reached 1.15 pu. This means a large amount of harmonics are contained in the transmission line voltage.

Figure 3.9 (d) shows the magnitude of the **d-** and the **q-** components output phase current I_{td} and I_{tq}. After the startup oscillation lasting 0.12s, I_{td} reaches steady state at 0.004 pu and I_{tq} reaches steady state at -1.3 pu. The positive value indicates active power is flowing from transmission line to VSI, while negative value indicates reactive current is injected from VSI to transmission line.

Figure 3.9 (e) shows the steady state waveform of the actual output phase A current i_{ta}. A close look at the waveform indicates that i_{ta} is composed of a series of irregular saw tooth which is limited in the hysteresis band of i_{t_ref}. In this test, the hysteresis bandwidth is set as ± 0.135 pu. This waveform proves the validity of the HCC signal generator designed in Section 2.3.

3.6.2 Dynamic response to system perturbation

After verifying the performance of STATCOM using HCC in steady state, the model is subjected to different dynamic tests to check the operation under small signal perturbations. The transient tests include (a) reference value change in **d-** and **q-** control loops, and (b) step change of load.

3.6.2.1 Impact of variation in reference transmission line voltage magnitude

This test of variation in the reference magnitude of the transmission line voltage V_{t_ref} is to monitor the response of the **q-** control loop. In the test, the DC voltage V_{dc} is maintained at 3 pu, and V_{t_ref} is changed from 1 pu to 0.7 pu at 0.4s, and recovered at 0.7s. During this test, the operation mode of STATCOM is changed from capacitive to inductive, and the performance of controller will be verified.

Figure 3.10 (a) shows the waveform of transmission line voltage magnitude V_t. V_t reaches new steady state level when the reference symbol V_{t_ref} changes at 0.4s and 0.7s. This proves the step response stability of **q-** control loop. The **q-** loop has an overshoot of 7.3%, rising time of 30ms, and settling time of 60ms.

Figure 3.10 (b) shows the influence of **q-** control loop over **d-** control loop. The step change of V_{t_ref} results in a fluctuation of 4.5% at DC voltage V_{dc}. But the fluctuation is damped out quickly and V_{dc} regains 3 pu in only 50ms.

Figure 3.10 (c) shows the output of the **d-** and **q-** control loops in the simulation. When V_{t_ref} changes from 1 to 0.7 pu, I_{td_ref} changes from 0.004 to 0.0057 pu, and I_{tq_ref} increases from -1.3 to 1 pu. The increase of d- component output phase current is to counteract the drop of the transmission line voltage, and STATCOM absorbs more active current to maintain the DC side voltage stable. The change of q- component output phase

current indicates that the operation mode of STATCOM changes from capacitive to inductive and reactive power flow changes from supplying to absorbing.

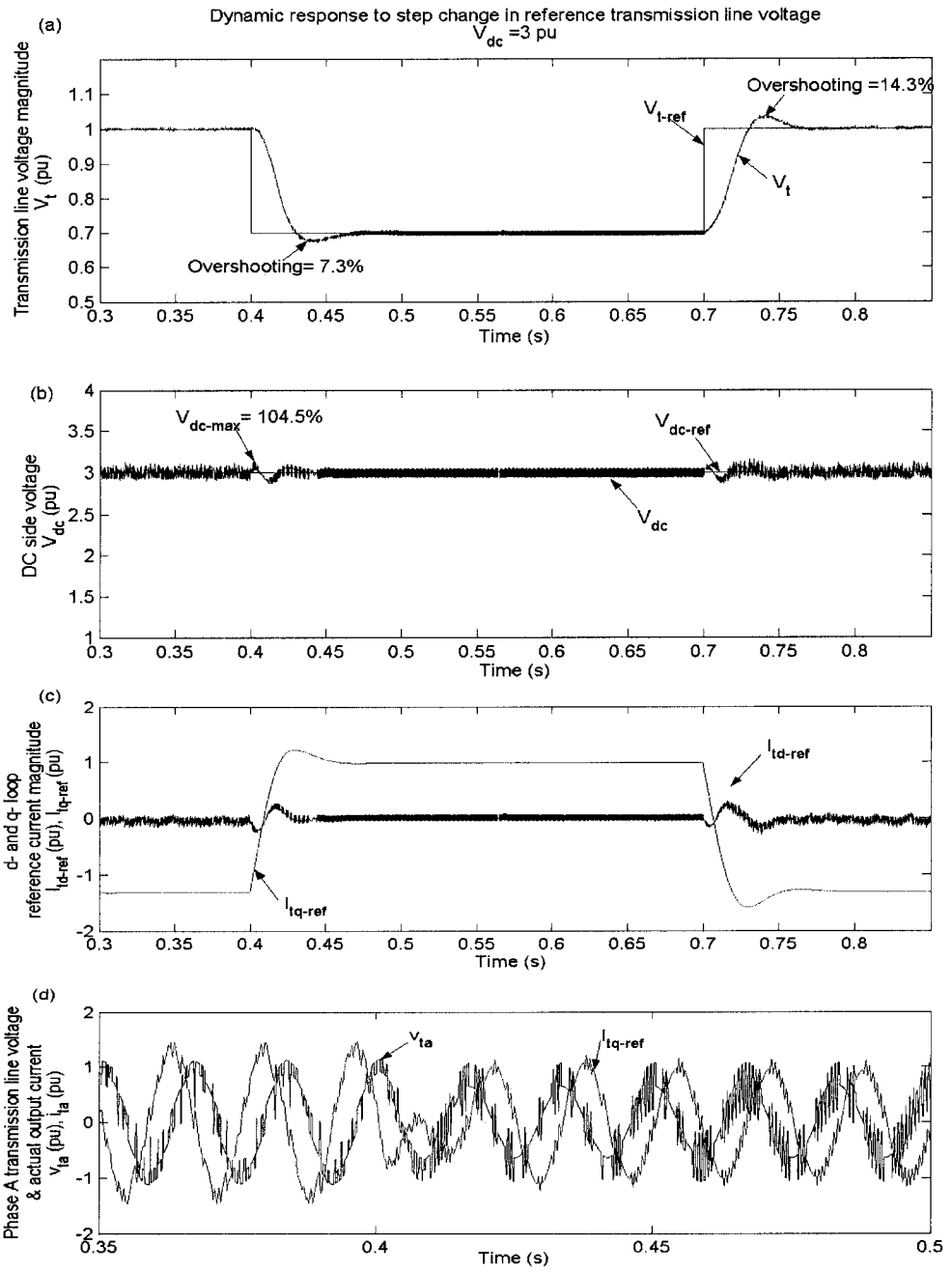

Figure 3. 10 Step responses to variation in reference transmission line voltage magnitude of HCC STATCOM

Figure 3.10 (d) illustrates the instantaneous waveform of phase A transmission line voltage v_{ta} and actual output phase current i_{ta} before and after the step change at 0.4s. It is clear that after the change at 0.4s, both of the voltage and current reach steady state in only three cycles, and i_{ta} changes from leading to lagging to v_{ta}. The harmonic components in v_{ta} are increased after the magnitude is decreased.

3.6.2.2 Impact of variation in reference DC side voltage

This test of variation in the reference DC side voltage V_{dc_ref} is to monitor the dynamic response of the **d-** control loop. In the test, the transmission line voltage magnitude V_t is maintained at 1 pu, and V_{dc_ref} is changed from 3 pu to 2.6 pu at 0.4s, and recover at 0.7s. In this simulation, the outputs of **d-** and **q-** control loops are monitored and the performance of controller will be checked.

In Figure 3.11 (a) shows the waveform of DC side voltage V_{dc}. V_{dc} reaches new steady state level with an overshoot of 9.5% when the reference symbol V_{dc_ref} changes at 0.4s, and regains steady state level with an overshoot of 7.3% when the reference symbol V_{dc_ref} recovers at 0.7s. This proves the stability and fast step response of the **q-** control loop. The **q-** loop has a rising time of about 18 ms, and settling time of 30ms.

Figure 3.11 (b) shows the influence of **d-** control loop over **q-** control loop. The step change in V_{dc_ref} results in a fluctuation of only 1.7% at transmission line voltage magnitude V_t. But the fluctuation is damped quickly and V_t regains 1 pu in only 30ms. Figure 3.11 (c) shows the output of the **d-** and **q-** control loops in the simulation. When V_{dc_ref} changes from 3 to 2.6 pu, I_{td_ref} changes from 0.004 to 0.003 pu, and I_{tq_ref} keeps at

-1.3 pu. This figure indicates that **d-** control loop has very little influence over **q-** control loop.

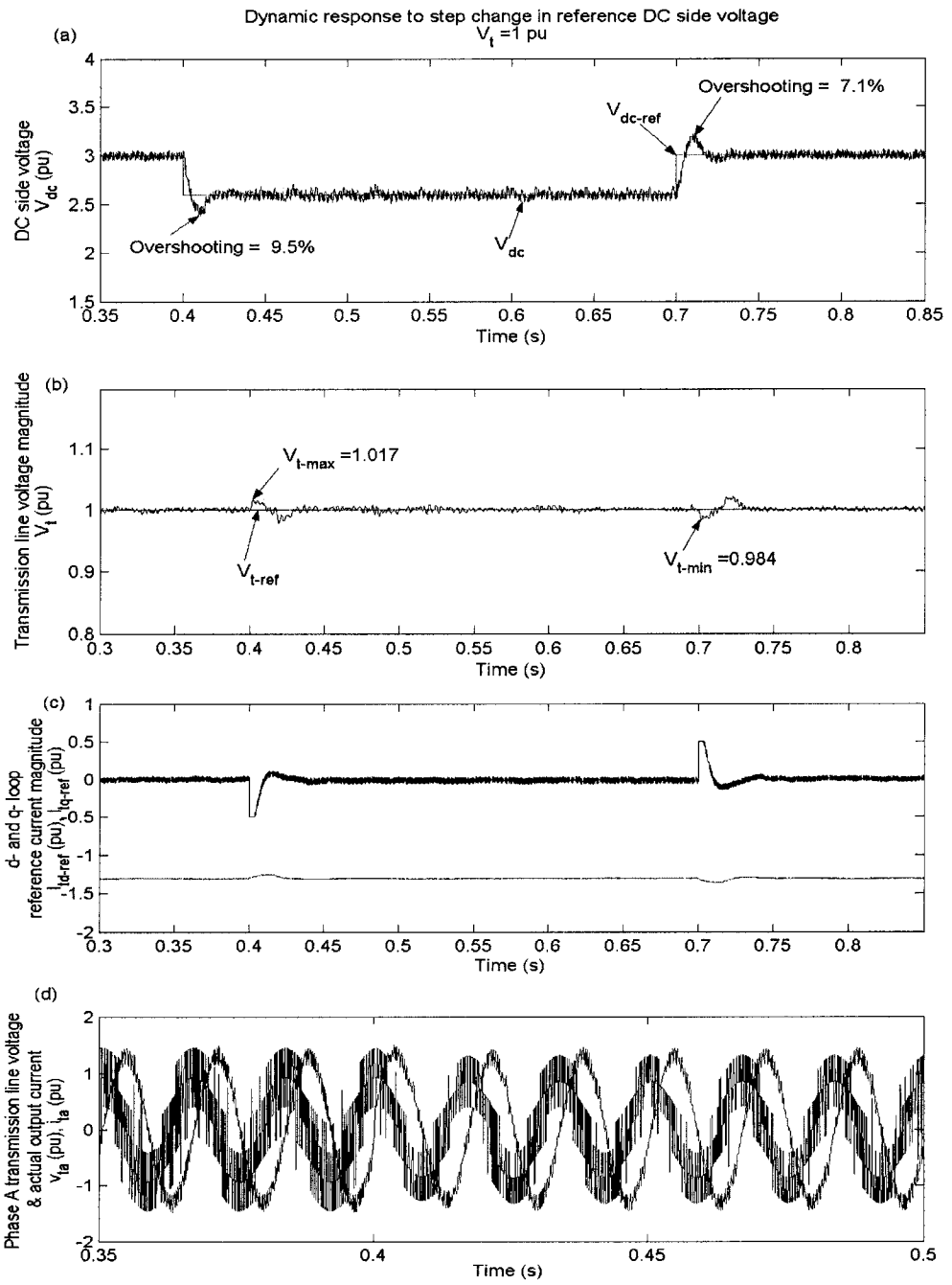

Figure 3. 11 Step responses to variation in reference DC side voltage of HCC STATCOM

Figure 3.11 (d) illustrates the instantaneous waveform of phase A transmission line voltage v_{ta} and actual output phase current i_{ta} before and after the step change at 0.4s. The magnitudes of the two waveforms are not influenced by the variation in DC side voltage, but the harmonic components are slightly reduced in both signals.

3.6.2.3 Impact of variation in load

This test of variation in the load is to monitor the dynamic response of the controller to the system parameter change. As discussed in section 3.3, the power grid impedance and transmission line impedance have the same effect over the system as the load since they will finally be represented by equivalent impedance $R_s + j\omega L_s$. In this simulation, load 2 will be parallel connected to bus B3 at 0.4s and disconnected at 0.7s. Load 2 will increase active load by 10%, reactive load by 20%. The voltage and current variables will be monitored to verify the stability of the controller.

Figures 3.12 (a) and (b) show the waveform of transmission line voltage magnitude V_t and DC side voltage V_{dc} respectively. Both of V_t and V_{dc} keeps steady state level after a short time oscillation when the load changes at 0.4s and recovers at 0.7s. The simulation result proves the dynamic responses of the two control loops under small scale disturbances are quick and stable. In 60ms, the **q-** control loop regains the steady state with an overshoot of 3.8%, while **d-** control loop needs 45ms to reach steady state with an overshoot of 2.2%.

Figure 3.12 (c) shows the output of the **d-** and **q-** control loops in the simulation. When the load changes at 0.4s, I_{td_ref} keeps 0.004 after the short time oscillation, and I_{tq_ref}

changes from -1.3 to -2.35 pu. This means the injected reactive power from STATCOM to transmission line is increased to supply the increase in load 2 .

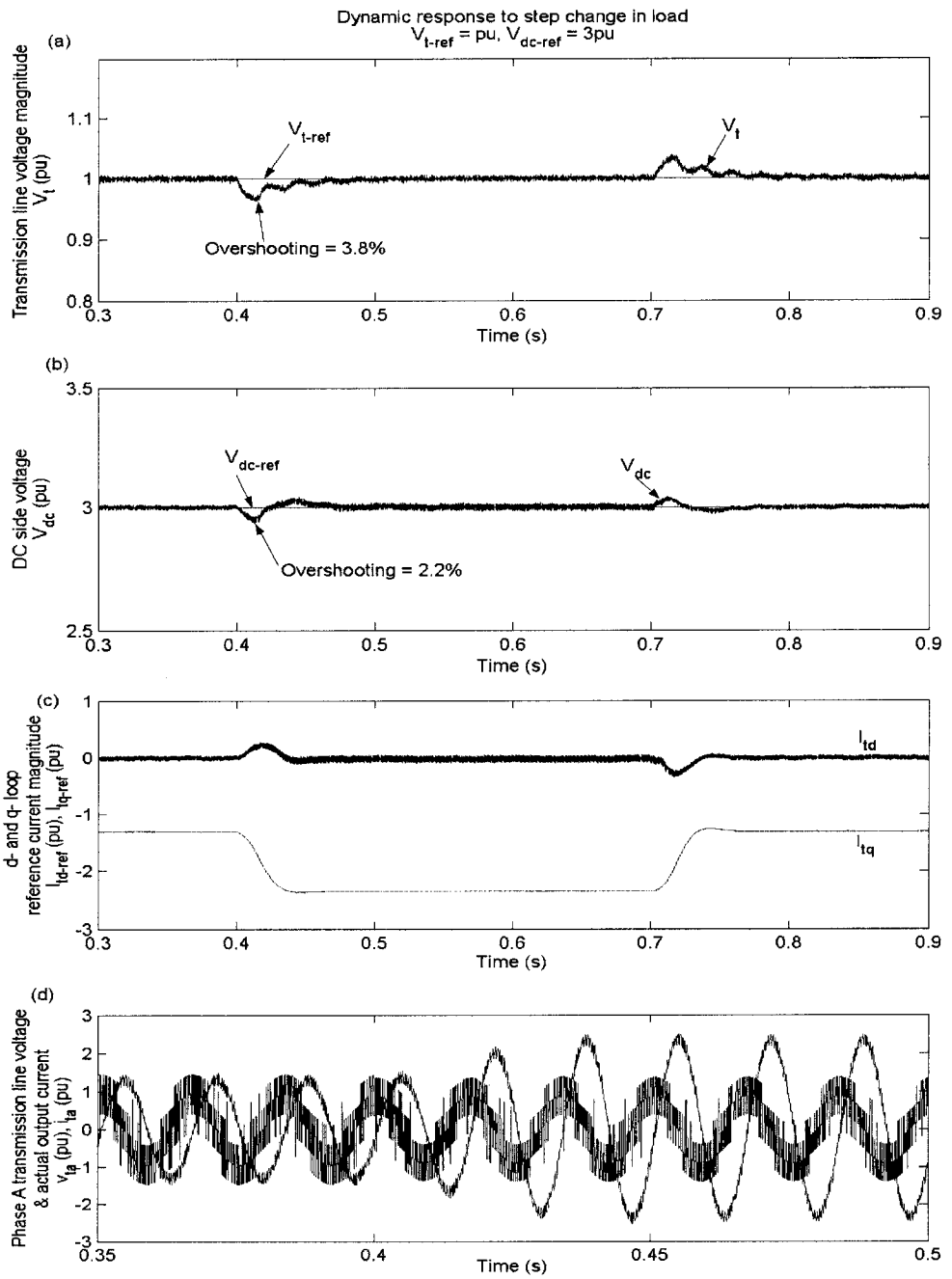

Figure 3. 12 Step responses to variation in load of HCC STATCOM

Figure 3.12 (d) illustrates the instantaneous waveform of phase A transmission line voltage v_{ta} and actual output phase current i_{ta} before and after the step change at 0.4s. The voltage and current symbols reaches new steady state in three cycles after the load 2 is introduced at 0.4s. It is clear that after the change at 0.4s, both of the voltage and current signals reach steady state in only three cycles, and the harmonic components in v_{ta} are slightly reduced after the AC side reactance is increased.

3.7 Summary

In this chapter, the mathematical model of STATCOM using HCC is deduced. The control strategy is analyzed in synchronous rotating reference frame. The reactive power compensation control loop and active power absorption control loop are analyzed respectively. PI type controllers are used in the control loops.

The designed controller is subjected to the small signal disturbance. The impact of variation in the reference signals demonstrates the fast response of the controller, and the impact of variation in the system parameter verifies the stability. The performance of the controller proves the mathematical model and the analysis of the control loops.

Although the two control loops are responsible for the active power absorption and reactive power compensation respectively in the analysis, they do interact with each other in practice. The simulation results indicate that the transient oscillation resulted from the interaction is very small and is damped in less than three cycles. So, the approximations made in deriving the equivalent models are justifiable.

Several other characteristics of STATCOM using HCC will be introduced in chapter 5 for further discussion.

4. MODEL AND ANALYSIS OF STATCOM USING PWM

4.1 Introduction

PWM switching technology is very common in controlling the VSI. Unlike HCC, PWM technology controls the output voltage instead of current variables. When the actual output phase voltage v_o is bigger than the AC bus voltage v_t, STATCOM injects reactive power to the transmission system; When v_o is smaller than v_t, STATCOM absorbs reactive power from the transmission system. By controlling the magnitude of the actual output phase voltage v_o, the STATCOM can be controlled in capacitive mode or inductive mode.

In this chapter, the power circuit of modeled STATCOM is same as the one discussed in the last chapter, but the control strategy is analyzed for PWM VSI in the synchronous rotating reference frame. The control loops are also decomposed into reactive power compensation control loop and active power absorption control loop and the controller is also designed based on PI control. Finally, the power circuit introduced in last chapter will be simulated in EMPT-RV package again to verify the performance of the designed controller for PWM VSI.

4.2 Control Analysis

The output voltage of VSI is a series of pulses with predefined magnitude and variable pulse width. By controlling the magnitude and pulse width, the fundamental component of the output voltage is controlled. Therefore, the reactive power is compensated and the transmission line voltage is regulated.

In order to facilitate the comparison to the STATCOM using HCC, a STATCOM using PWM VSI which is connected to a similar power circuit (Figure 3.1) is taken as the example. Therefore, the simplified 3-phase circuit of STATCOM shown in Figure 3.2 can be used for the analysis of the PWM VSI [22, 23]. The relationship between the transmission line voltage v_t and the actual output phase voltage v_o is described as:

$$\begin{cases} v_{ta} = v_{oa} + L_t \dfrac{di_{ta}}{dt} \\ v_{tb} = v_{ob} + +L_t \dfrac{di_{tb}}{dt} \\ v_{tc} = v_{oc} + +L_t \dfrac{di_{tc}}{dt} \end{cases} \tag{4-1}$$

4.2.1 Synchronous Rotating Reference Frame

Ideally, STATCOM exchange reactive power with transmission line and v_o is in phase with v_t. However, in practical operation, the switching losses of STATCOM and other active power consumption make the active power absorption from transmission line necessary. As described in the simplified circuit in Figure 3.2, the DC side parallel connected resistor R represents the switching loss and other active power losses in the STATCOM. In order to compensate the active power consumption which may cause the DC side voltage to decrease, a small phase displacement angle α is imposed between v_o and v_t. Ignoring the harmonics in v_o, the actual output phase voltage v_o can be described as:

$$\begin{cases} v_{oa} = V_o \sin(\theta - \alpha) \\ v_{ob} = V_o \sin(\theta - \alpha - \dfrac{2\pi}{3}) \\ v_{oc} = V_o \sin(\theta - \alpha + \dfrac{2\pi}{3}) \end{cases} \tag{4-2}$$

Turn the synchronous rotating reference frame in Section 3.4.1 an angle α clockwise, the new synchronous rotating reference frame for VSI STATCOM is shown in Figure 4.1, and the transformation matrix K_α is:

$$K_\alpha = \frac{2}{3}\begin{bmatrix} \sin(\theta-\alpha) & \sin(\theta-\alpha-\frac{2\pi}{3}) & \sin(\theta-\alpha+\frac{2\pi}{3}) \\ \cos(\theta-\alpha) & \cos(\theta-\alpha-\frac{2\pi}{3}) & \cos(\theta-\alpha+\frac{2\pi}{3}) \\ \frac{1}{\sqrt{2}} & \frac{1}{\sqrt{2}} & \frac{1}{\sqrt{2}} \end{bmatrix} \tag{4-3}$$

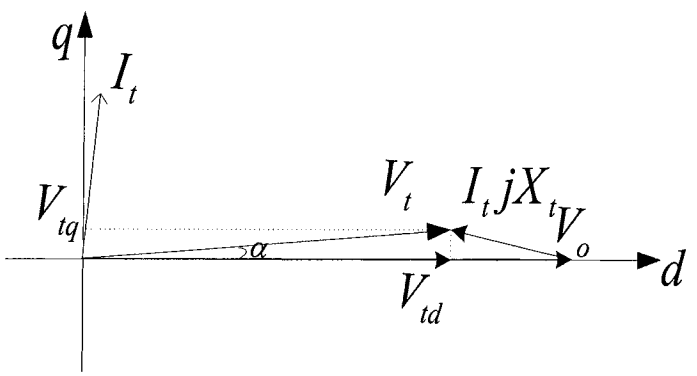

Figure 4. 1 Synchronous rotating reference frame with transformation matrix K_α

Hence, the transmission line voltage v_t is decomposed into **d-** and **q-** components:

$$\begin{bmatrix} V_{td} \\ V_{tq} \\ 0 \end{bmatrix} = K_\alpha \begin{bmatrix} v_{ta} \\ v_{tb} \\ v_{tc} \end{bmatrix} = V_t \begin{bmatrix} \cos\alpha \\ \sin\alpha \\ 0 \end{bmatrix} \tag{4-4}$$

Since the active power loss is very small compared to the reactive power compensation, and the equivalent resistance of the coupling transformer is very small compared to the leakage reactance, angle α is very small. If α varies in a small range (i.e. from +5° to -5°), we can assume:

$$\sin\alpha \approx \alpha, \cos\alpha \approx 1 \tag{4-5}$$

The actual output phase voltage v_o is decomposed into:

$$\begin{matrix} V_{od} \\ V_{oq} \end{matrix} = \begin{bmatrix} V_o \\ 0 \end{bmatrix} = \begin{bmatrix} \frac{V_{dc}}{2} MI \\ 0 \end{bmatrix} \tag{4-6}$$

Where ***MI*** is the modulation index of VSI.

With the transformation matrix $\boldsymbol{K_\alpha}$, Eq. (4-1) can be rewritten as:

$$\begin{cases} V_{td} - V_{od} = L_t \dfrac{dI_{td}}{dt} - \omega L_t I_{tq} \\ V_{tq} - V_{oq} = L_t \dfrac{dI_{tq}}{dt} + \omega L_t I_{td} \end{cases} \tag{4-7}$$

Considering that the active power loss of the STATCOM is represented by the DC side parallel connected resistance $\boldsymbol{R}$, the active power exchange between the DC side and AC side of VSI can be rewritten as:

$$P_{ac} = \frac{3}{2}(V_{od} I_{td} + V_{oq} I_{tq}) = \frac{3}{2} MI * V_{dc} I_{td} \tag{4-8}$$

Combine Eq. (3-2), (3-8) and (4-8)

$$\frac{3}{2} MI * I_{td} = \frac{V_{dc}}{R} + C\frac{dV_{dc}}{dt} \tag{4-9}$$

4.2.2 Mathematical Model Deduction

To analyze the small signal disturbance response, ΔMI is defined as the perturbation of the modulation index, and ΔI and ΔV are the current and voltage magnitude variations under the perturbation. Ignoring the second order terms and discarding the DC components, the state equation of the small signal equivalent system can be given as:

$$\frac{d}{dt}\begin{bmatrix}\Delta I_{tq}\\ \Delta I_{td}\\ \Delta V_{dc}\end{bmatrix}=\begin{bmatrix}0 & -\omega & 0\\ \omega & 0 & -\frac{MI}{2L_t}\\ 0 & \frac{3MI}{2C} & -\frac{1}{RC}\end{bmatrix}\begin{bmatrix}\Delta I_{tq}\\ \Delta I_{td}\\ \Delta V_{dc}\end{bmatrix}+\begin{bmatrix}\frac{V_t}{L}\Delta\alpha\\ -\frac{V_{dc}}{2L}\Delta MI\\ 0\end{bmatrix} \tag{4-10}$$

Applying Laplace transformation, the final state equation is given by:

$$\begin{bmatrix}sL_t & \omega L_t & 0\\ -\omega L_t & sL_t & \frac{MI}{2}\\ 0 & -\frac{3R}{2}MI & 1+sRC\end{bmatrix}\begin{bmatrix}\Delta I_{tq}(s)\\ \Delta I_{td}(s)\\ \Delta V_{dc}(s)\end{bmatrix}=\begin{bmatrix}V_t\Delta\alpha(s)\\ -\frac{V_{dc}}{2}\Delta MI(s)\\ 0\end{bmatrix} \tag{4-11}$$

Eq. (4-11) can be rewritten as:

$$\begin{bmatrix}\Delta I_{tq}(s)\\ \Delta I_{td}(s)\\ \Delta V_{dc}(s)\end{bmatrix}=\frac{1}{A(s)}\begin{bmatrix}sL_t(1+sRC)+\frac{3R}{4}MI^2 & \omega L_t(1+sRC) & \frac{\omega L_t}{2}MI\\ \omega L_t(1+sRC) & sL_t(1+sRC) & -\frac{sL_t}{2}MI\\ \frac{3\omega L_t R}{2}MI & \frac{3sL_tR}{2}MI & (s^2+\omega^2)L_t^2\end{bmatrix}\begin{bmatrix}V_t\Delta\alpha(s)\\ -\frac{V_{dc}}{2}\Delta MI(s)\\ 0\end{bmatrix} \tag{4-12}$$

Among which,

$$A(s)=s^3L_t{}^2RC+s^2L_t{}^2+s(\frac{3}{4}MI^2RL_t+\omega^2L_t{}^2RC)+\omega^2L_t{}^2 \tag{4-13}$$

To achieve a fast dynamic response without using an independent DC voltage source, it is required that the DC side voltage V_{dc} should be kept constant by controlling the phase angle α while simultaneously compensating the load reactive power by controlling the modulation index ***MI***. From Eq. (4-12), ΔV_{dc} is given by:

$$\Delta V_{dc}(s)=\frac{1}{A(s)}\left[\frac{3\omega L_tRV_tMI}{2}\Delta\alpha(s)-\frac{3sL_tRV_{dc}MI}{4}\Delta MI(s)\right] \tag{4-14}$$

In order to keep the DC side variation as small as possible, which means $\Delta V_{dc} = 0$, the right side of Eq. (4-14) must be zero. Therefore,

$$\Delta\alpha(s) = \frac{sV_{dc}}{2\omega V_t}\Delta MI(s) \tag{4-15}$$

From Eq. (4-12) through (4-15), the block diagram of the active power absorption control loop is described in Figure 4.2:

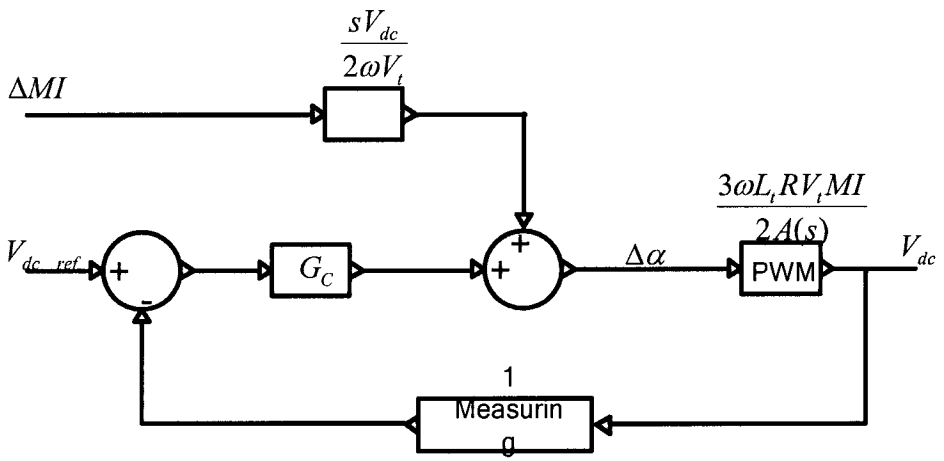

Figure 4. 2 Equivalent **d-** control loop block diagram

Considering the fact that the active power absorption is much smaller than the reactive power exchange in maintaining the transmission line voltage, the magnitude of the active component of actual phase current I_{td} is much smaller than the magnitude of the reactive component I_{tq}, and the phase angle displacement α is varied in a very small range. It is reasonable to ignore the impact of I_{td} on the control of transmission line voltage Vt.

The transfer function of the small signal equivalent circuit can be described as:

$$\frac{\Delta V_t(s)}{\Delta I_{tq}(s)} = sL_t \tag{4-16}$$

From Eq. (4-12), we have:

$$\frac{\Delta I_{tq}(s)}{\Delta MI(s)} = -\frac{\omega L_t (1+sRC) V_{dc}}{2A(s)} \tag{4-17}$$

Placing Eq. (4-17) into Eq. (4-16) gives,

$$\frac{\Delta V_t(s)}{\Delta MI(s)} = -\frac{s\omega L_t^2 (1+sRC) V_{dc}}{2A(s)} \tag{4-18}$$

From Eq. (4-18), the block diagram of the reactive power compensation control loop is described in Figure 4.3:

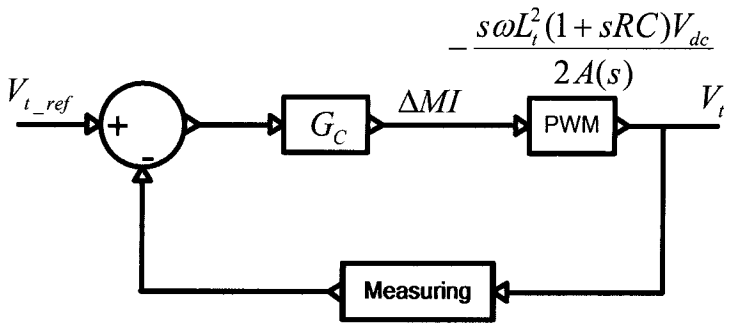

Figure 4. 3 Equivalent **q-** control loop block diagram

4.3 Control Loops

With the above discussion, the control system of the STATCOM circuit is decomposed into two loops: the active power absorption control loop to maintain the DC side voltage V_{dc}, simply called **d-** control loop; and the reactive power compensation control loop to regulate the transmission line voltage V_t, simply called **q-** control loop. The interaction of the two control loops with each other is simplified to facilitate the analysis of the circuit. The parameters of **d-** and **q-** Loop controllers are calculated in Appendix D.

4.3.1 Reactive Power Compensation Control Loop

Figure 4.4 describes the structure of the **q-** loop controller. With reference to Eqs. (4-4) and (4-5), the magnitude of the transmission line voltage V_t is calculated by the **abc** to **dq** block, and compared with the pre-defined reference value V_{t_ref}. The error signal is fed to the PI block to generate the small signal oscillation of the modulation index. This oscillation is limited to suppress the variation in the output. The final modulation index ***MI*** after introducing the bias value is 0.8.

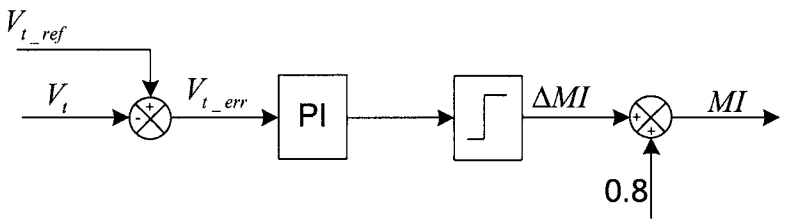

Figure 4. 4 Structure of **q-** loop controller

4.3.2 Active Power Absorption Control Loop

Figure 4.5 describes the structure of the **d-** loop controller. The DC side voltage V_{dc} is measured and compared with the reference voltage side voltage V_{dc_ref}, and the error signal is fed to PI block to generate the phase displacement α. A limit of $\pm 5^{\circ}$ is used to limit the variation of active power and keep the control loop stable.

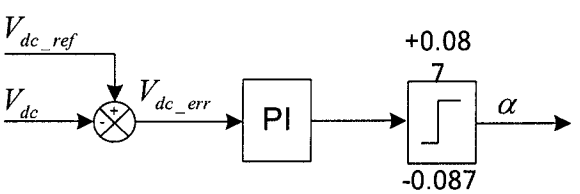

Figure 4. 5 Structure of **d-** loop controller

4.3.3 Overall controller for PWM VSI

The overall control structure of STATCOM using PWM is shown in Figure 4.6.

Important components are demonstrated as follows,

(1) Measure Block. The DC side voltage V_{dc} and the transmission line voltage v_t are monitored with Measure Block. 3-phase voltage v_t is fed to **abc to dq** block to calculate the magnitude V_t. The unit magnitude waveform $\sin \omega t$ is achieved to maintain the synchronization to v_t.

(2) **q-** Loop Regulator as described in Section 4.3.1

(3) **d-** Loop Regulator as described in Section 4.3.2

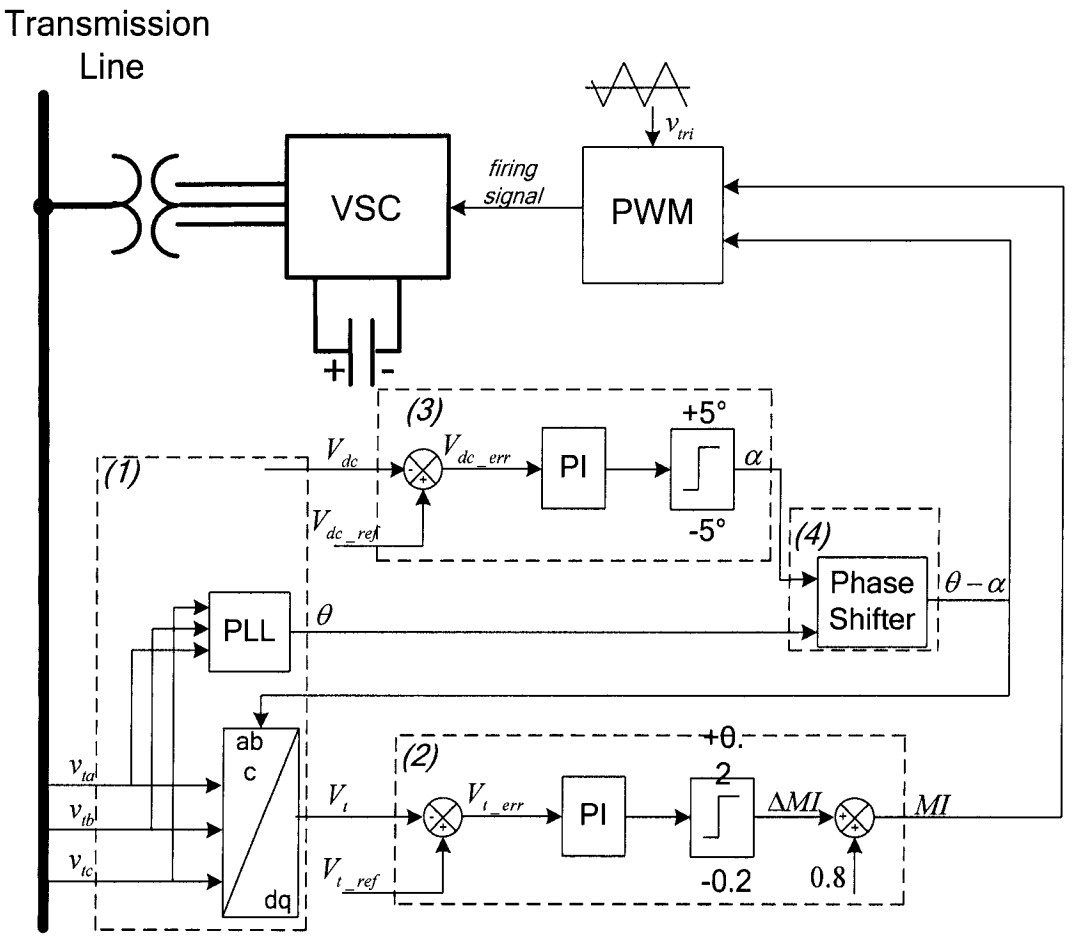

Figure 4. 6 Overall Control Structure of STATCOM using PWM

(4) Phase Shifter Block. α and the unit waveform $\sin \omega t$ are fed to a phase shifter to generate the unit magnitude control signal which is synchronous and locked to transmission line voltage v_t. This control signal is fed to PWM block together with modulation index ***MI*** to generate the firing signals which control the STATCOM switches to generate the required actual output phase voltage v_o.

4.4 Simulation Result

The performance of STATCOM depends to a large extent on the control system utilized. In order to validate the operation of the controller, STATCOM using PWM controller will be connected to the power circuit described in Figure 3.8 to testify the dynamic response and stability. In order to eliminate the low order harmonics, the frequency modulation ratio m_f is set as 15 and the frequency of triangular carrier signal is 900Hz. The parameters of **d-** and **q-** Loop Regulators are calculated in Appendix D

4.4.1 Steady state performance

This simulation is done to verify the steady state performance of the controller. Figure 4.7 (a) shows the voltage regulation effect of STATCOM. Without reactive power compensation, the transmission line voltage magnitude V_t is about 0.83 pu which is below the limit of the transmission requirement. With the compensation of STATCOM introduced at 0.2s, the magnitude of fundamental component V_t is maintained at 1 pu after a start up oscillation lasting about 0.5s, the DC side voltage V_{dc} is maintained at 75kV.

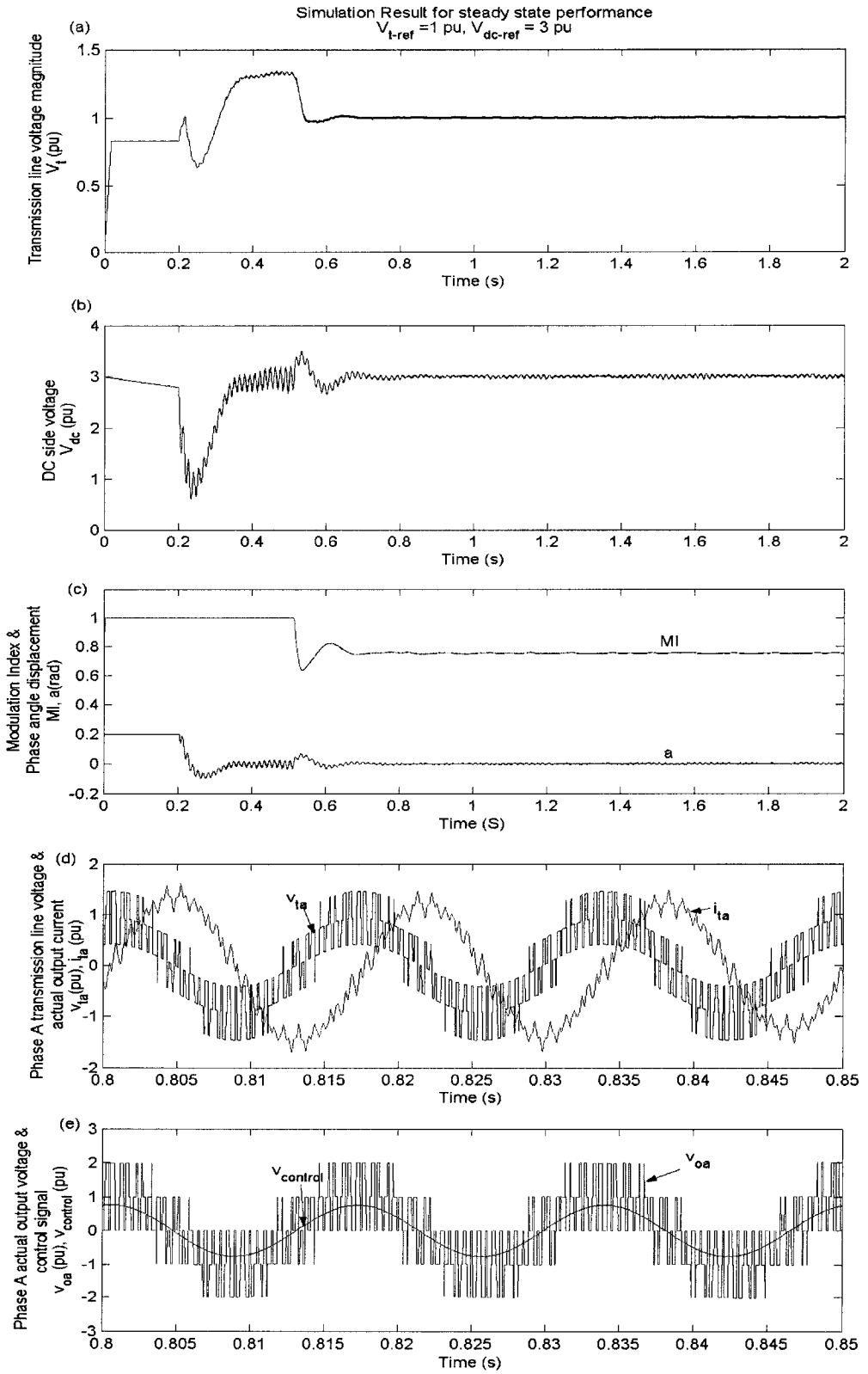

Figure 4. 7 Simulation result for steady state performance of PWM STATCOM

Figure 4.7 (b) shows the waveform of DC side voltage V_{dc}. After the startup oscillation period lasting about 0.5s, V_{dc} reaches steady state at 3 pu. In steady state, the highest and lowest voltages are 3.051 pu and 2.947 pu respectively, which means that the voltage ripple is only $\pm 1.77\%$ of V_{dc}.

Figure 4.7 (c) shows the waveform of the phase angle displacement α and the modulation index ***MI***. They are also the output of the d- and q- control loop respectively. During the startup oscillation period, ***MI*** is limited lower than 1 pu. The application of the limit minimizes the oscillations of the power. In steady state, ***MI*** reaches 0.753 while α reaches 0.0015 rad.

Figure 4.7 (d) shows the steady state waveform of the actual output phase A current and e instantaneous phase A voltage at transmission line v_{ta}. The waveform of i_{ta} lags v_{ta} about 1/4 cycle which means STATCOM is working in capacitive mode and compensating reactive power. The waveform of i_{ta} and v_{ta} also indicates the existence of harmonic components in the output.

Figure 4.7 (e) shows the steady state waveform of control signal $v_{control}$ and AC side output voltage v_{oa}. The waveform of v_{oa} is in phase with $v_{control}$ which proves the switching technology of PWM.

4.4.2 Dynamic response to system perturbation

After verifying the performance of the STATCOM using PWM in steady state, the model is subjected to different dynamic tests to check the operation under small signal perturbations. The transient tests include (a) reference value changes in **d-** and **q-** control loops, and (b) step change in load.

4.4.2.1 Impact of variation in reference transmission line voltage magnitude

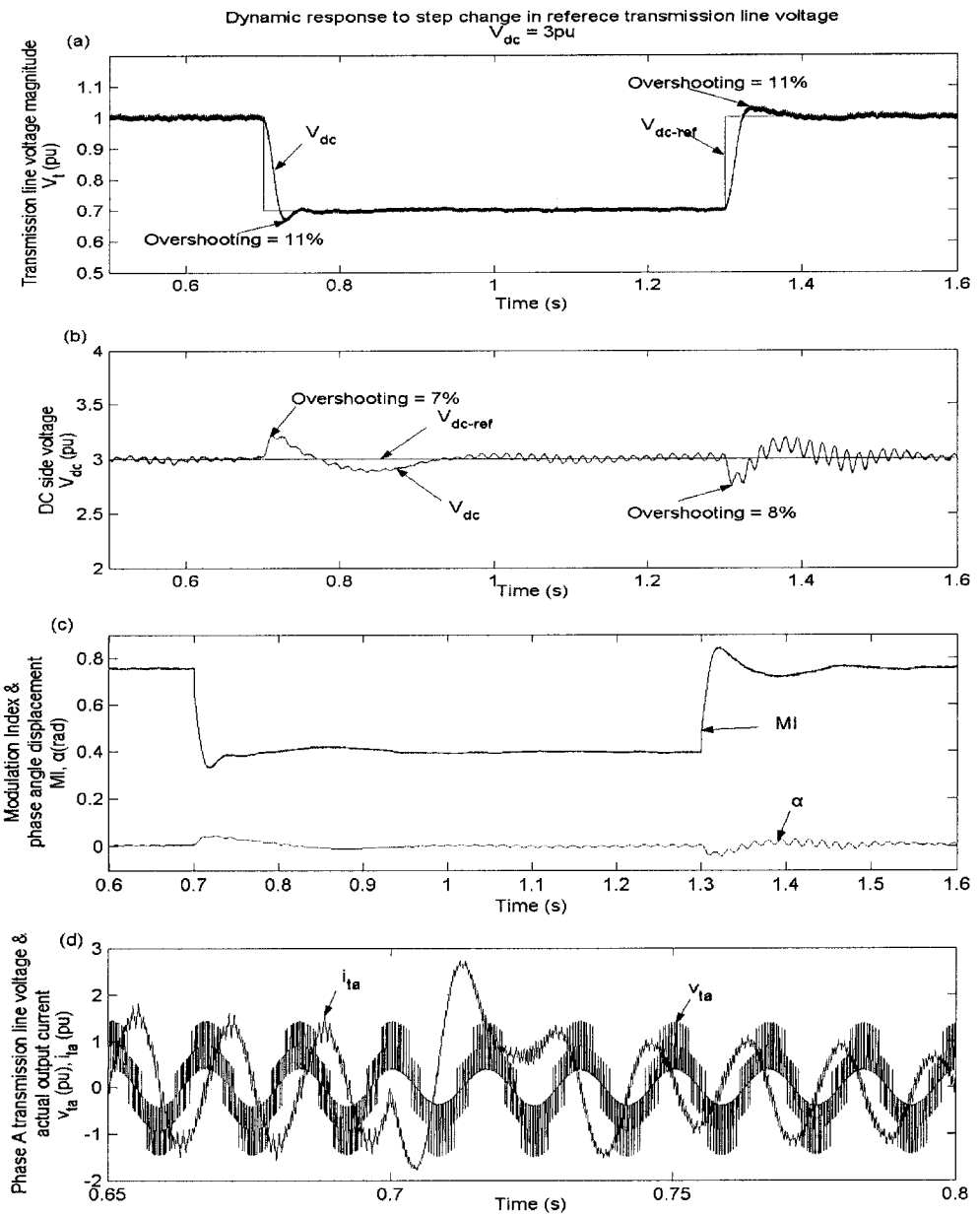

Figure 4. 8 Step responses to variation in reference transmission line voltage magnitude of PWM STATCOM

This test of variation in the reference magnitude of the transmission line voltage V_{t_ref} is to monitor the response of the **q**- control loop. In the test, the DC voltage V_{dc} is

maintained at 3 per unit, and V_{t_ref} is changed from 1 per unit to 0.7 per unit at 0.7s, and recovered at 1.3s. During this change, the operation mode of STATCOM will be changed from capacitive to inductive, and the performance of controller will be testified.

Figure 4.8(a) shows the waveform of the transmission line voltage magnitude V_t. V_t tracks back with the reference value after the perturbation. This proves the step response stability of **q-** control loop. The **q-** loop has overshooting of 11%, rising time of 30ms, and settling time of 80ms.

Figure 4.8(b) shows the waveform of the transmission line voltage magnitude V_{dc}. V_{dc} also tracks back the reference value in 150ms after the perturbation, but the oscillation caused by the step change in V_t reaches 7% at 0.7s, and 8% at 1.3 s.

Figure 4.8 (c) shows the output of the **d-** and **q-** control loops in the simulation. When V_{t_ref} changes from 1 to 0.7 per unit, ***MI*** changes from 0.757 to 0.396, and α changes from 0.003 to -0.002 rad. The drop of α indicates the operation mode of STATCOM changes from capacitive to inductive and reactive power flow changes from supplying to absorbing.

Figure 4.8 (d) shows the instantaneous waveform of phase A transmission line voltage v_{ta} and actual output phase current i_{ta} before and after the step change at 0.7s. It is clear that after the change at 0.7s, both of the voltage and current curves reach steady state in about five cycles, and i_{ta} changes from leading to lagging to v_{ta}.

4.4.2.2 Impact of variation in reference DC side voltage

This test of variation in the reference DC side voltage V_{dc_ref} is to monitor the dynamic response of the **d-** control loop. In the test, the transmission line voltage magnitude V_t is

maintained at 1 pu, and V_{dc_ref} is changed from 3 pu to 2.6 pu at 0.7s, and recovered at 1.3s. In this simulation, the outputs of **d-** and **q-** control loops are monitored and the performance of controller will be verified.

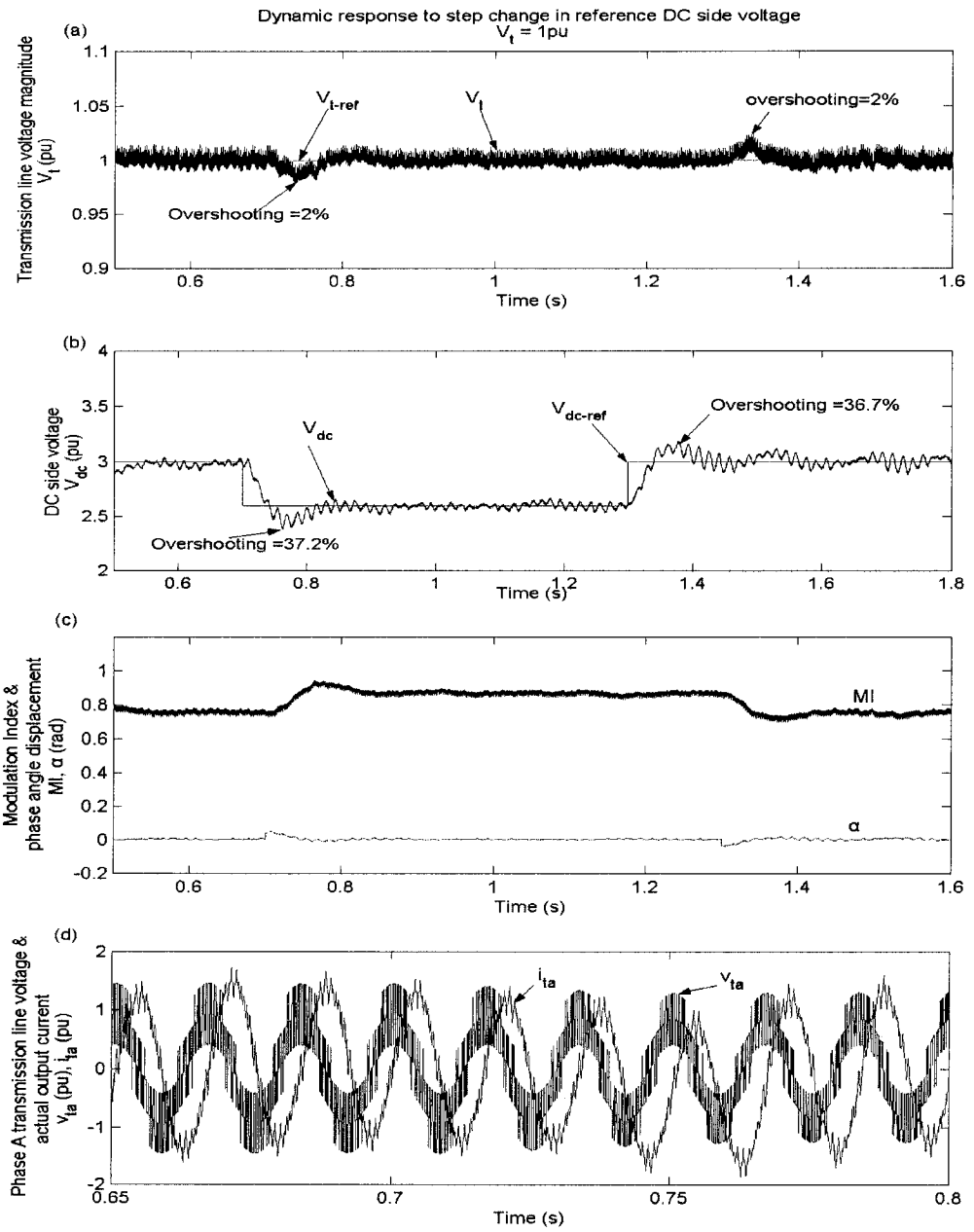

Figure 4. 9 Step responses to variation in reference DC side voltage of PWM STATCOM

Figure 4.9 (a) shows the waveform of the transmission line voltage magnitude V_t which also illustrates the influence of **d-** control loop over the **q-** control loop. The step change of V_{dc_ref} results in a fluctuation of only 2% at transmission line voltage magnitude V_t. But the fluctuation is damped quickly and V_t regains 1 pu in about 150ms.

Figure 4.9 (b) shows the waveform of DC side voltage V_{dc}. V_{dc} reaches new steady state level with overshoot of 37.2% when the reference symbol V_{dc_ref} changes at 0.7s, and regains steady state level with overshoot of 36.7% when the reference symbol V_{dc_ref} recovers at 1.3s. This test demonstrates the stability of the **q-** control loop. The **q-** loop has rising time of about 50 ms, and a settling time of 150ms.

Figure 4.9 (c) shows the output of the **d-** and **q-** control loops in the simulation. When V_{dc_ref} changes from 3 to 2.6 pu, ***MI*** changes from 0.757 to 0.893, and α changes from 0.003 to 0.002 rad. The drop of α indicates that less active power is absorbed so that DC side voltage is dropped. ***MI*** increases to keep the magnitude of the AC side output voltage therefore the transmission line voltage magnitude.

Figure 4.9 (d) illustrates the instantaneous waveform of phase A transmission line voltage v_{ta} and actual output phase current i_{ta} before and after the step change at 0.7s. Unlike the simulation of variation in V_{t_ref}, variation in V_{dc_ref} does not have much impact to the phase difference between v_{ta} and i_{ta}. This is because α is very small and the operation mode of STATCOM is not changed.

4.4.2.3 Impact of variation in load

This test of variation in the load is to monitor the dynamic response of the controller to a system parameter change. As discussed in section 3.3, the power grid impedance and

transmission line impedance have the same effect over the system as the load since they will finally be represented by equivalent impedance $R_s + j\omega L_s$. In this simulation, load 2 will be connected in parallel to bus B3 at 0.7s and disconnected at 1.3s. The voltage and current signals s will be monitored to verify the stability of the controller.

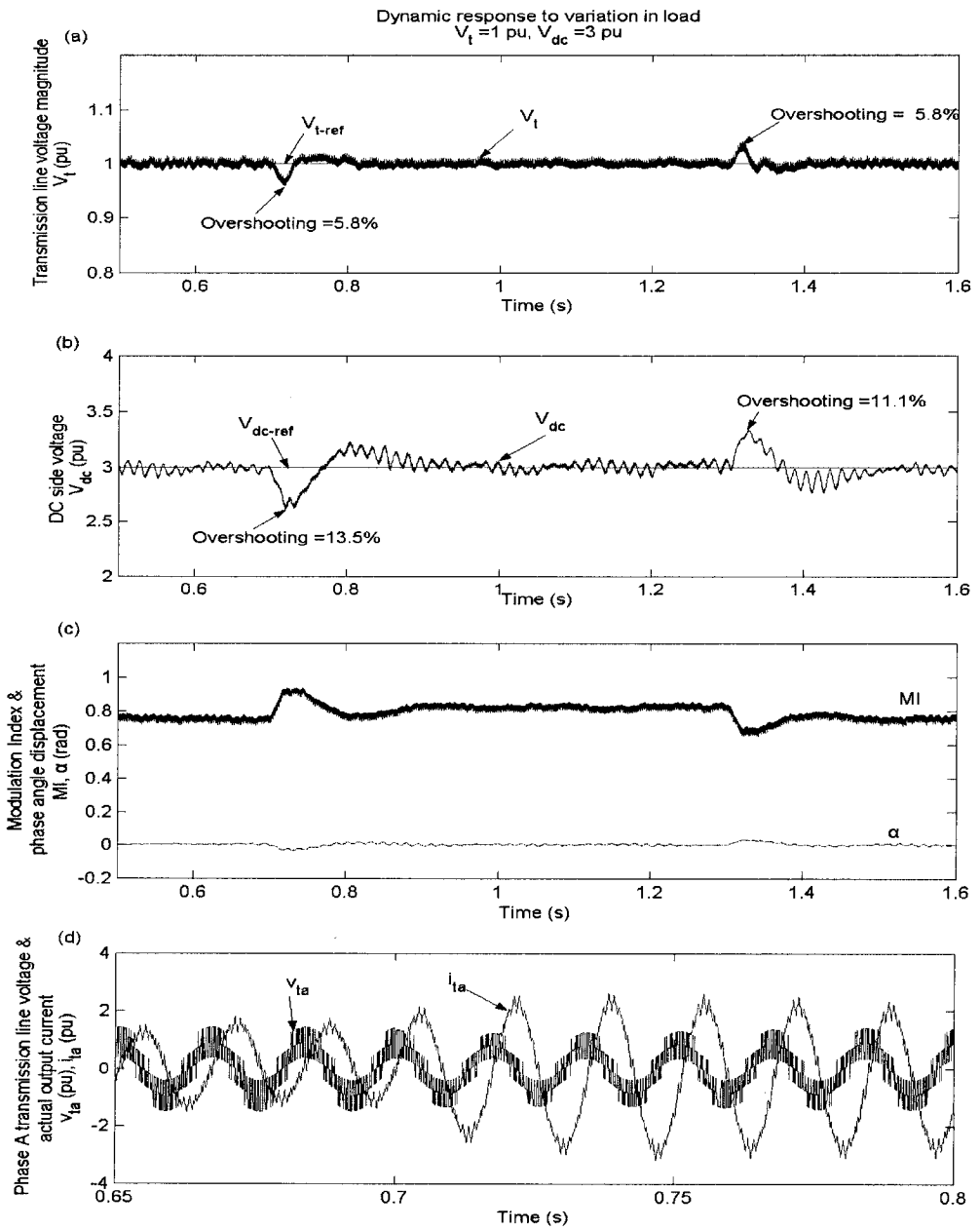

Figure 4. 10 Step responses to variation in load of PWM STATCOM

Figure 4.10 (a) and (b) shows the waveforms of transmission line voltage magnitude V_t and DC side voltage V_{dc} respectively. Both V_t and V_{dc} keep steady state levels after a short time oscillation when the load changes at 0.7s and recovers at 1.3s. The simulation result proves the dynamic responses of the two control loops under small disturbance are quick and stable. During 110ms, the V_t regains the steady state with overshoot of 5.8%, while V_{dc} spends 180ms to reach steady state with overshoot of 13.5%. It is clear that the V_{dc} is more influenced by the increased load.

Figure 4.10 (c) shows the output of the **d-** and **q-** control loops in the simulation. When the load2 is introduced at 0.7s, ***MI*** changes from 0.757 to 0.83, and α keeps 0.003 rad. The absorbed active power is kept unchanged and reactive power request from transmission line is increased. Therefore ***MI*** has to be increased to enhance the AC side output voltage and compensate more reactive power.

Figure 4.10 (d) illustrates the instantaneous waveform of phase A transmission line voltage v_{ta} and actual output phase current before and after the step change at 0.7s. The voltage and current symbols reach new steady state values in three cycles after the load 2 is introduced at 0.7s. The waveform of v_{ta} does not have much change while magnitude of i_{ta} is largely increased This means the injected reactive power from STATCOM to transmission line is increased to supply the increase in load 2.

Figure 4.10 (d) illustrates the instantaneous waveform of phase A transmission line voltage v_{ta} and actual output phase current i_{ta} before and after the step change at 0.7s. The voltage and current symbols reaches new steady state in three cycles after the load 2 introduced at 0.7s. The waveform of v_{ta} does not have much change while I_{ta} has increased a lot.

4.5 Summary

In this chapter, the mathematical model of a STATCOM using PWM is deduced. The control strategy is analyzed in the synchronous rotating reference frame. The reactive power compensation control loop and active power absorption control loop are decoupled and analyzed respectively. PI type controllers are used in the control loops.

The designed controller is subjected to small signal disturbances. The impact of variation in the reference signals demonstrates the response of the controller, and the impact of variation in the system parameter verifies the stability. The performance of the controller proves the mathematical model and the analysis of the control loops.

Several other characteristics of STATCOM using PWM will be introduced in chapter 5 for further discussion.

5. PERFORMANCE COMPARISON AND ANALYSIS

5.1 Introduction

PWM voltage control and HCC are the two popular control strategies for VSI. Most applications of STATCOM are based on PWM voltage control. Some applications using HCC also exist, but this method is not popular for high power transmission. In previous chapters, these two control strategies have been utilized and the stability under small signal disturbances was verified by simulation. It is necessary to make a more detailed discussion to determine why PWM voltage control is more preferred for STATCOM applications.

In this chapter, the performance of STATCOMs using these two control strategies will be analyzed. The comparison of data acquired in previous chapters indicates the advantages and drawbacks of the two control strategies applied to STATCOM. The reason that most STATCOM is controlled in PWM voltage control will be demonstrated by the comparison. The discussion will be focused on three areas: the controller performance, the switching frequency choice and the harmonic components which are very important to the STATCOM.

5.2 Performance Comparison

5.2.1 Controller Performance Comparison

Compared with PWM voltage control, HCC directly controls the output phase current of STATCOM injected into the transmission system, thus controlling the injected reactive power. Therefore, this control strategy not only makes the controller hardware simpler,

but also improves the speed response of the control. In Table 5.1 shows the comparison of the response time of a STATCOM using the two control strategies.

Table 5. 1 Comparison of Response Time

	Settling Time (ms)	
	HCC	PWM voltage control
Transmission line voltage magnitude step response	60	80
DC side voltage step response	30	150
Load variation response	60	110

As shown in the comparison, under start up oscillation and other small signal disturbance, the settling time of STATCOM using HCC is much shorter than the settling time of STATCOM using PWM voltage control. A conclusion can be made that HCC has faster control speed than PWM voltage control.

Table 5. 2 Comparison of Response Overshooting

	Overshooting	
	HCC	PWM voltage control
Transmission line voltage magnitude step response	7.3%	11%
DC side voltage step response	9.5%	37%
Load variation response	3.8%	5.8%

Overshoot in control response is an important factor to evaluate the performance of controller. As shown in Table 5.2, the overshoot of HCC controllers responding to the small signal disturbance is always smaller than that of PWM voltage controlled.

5.2.2 Switching frequency comparison

One advantage of power electronics-based switches to the traditional mechanically controlled switches is the high switching frequency. The very short switching period makes FACTS devices operate faster. However, the switching frequency is limited by the switching speed of the semiconductor. For example, the switching frequencies of IGBT are from 3 kHz to 10 kHz, and the GTO are up to 900 Hz.

Switching losses of STATCOM are also dependant on the switching frequency. When the switching devices are turned on, the forward current rises before the forward voltage drops to zero; when the switching devices are turned off, the forward voltage rises before the forward current drops to zero. At the moment when the forward voltage and current both exist, the power loss occurs in the device. When the switching time, forward voltage and current is fixed in a switching cycle, the higher the switching frequency, the higher the switching losses. The high switching losses not only reduce the efficiency of STATCOM, but also bring heavy burden to the cooling facilities.

For STATCOM using PWM voltage control, the switching frequency is fixed and determined by the triangular carrier signal. As described in Chapter 2, the switching frequency is equal to the predefined frequency of the carrier wave. This characteristic makes the switching frequency control of PWM STATCOM very easy.

Figure 5.1 shows the relationship of switching signal, control signal and triangular carrier signal of the STATCOM using PWM voltage control before and after the step change in V_t which is described in Section 3.6.2.1. In steady state before and after the disturbance at 0.7s, for each turn-on and turn-off cycle of the switching signal square-wave, the switching time is constant and equal to 11ms and switching frequency f_{sw} is equal to

900Hz. During the transient period, the switching time period does not change with the change of the control signal. This also applies other small signal disturbance.

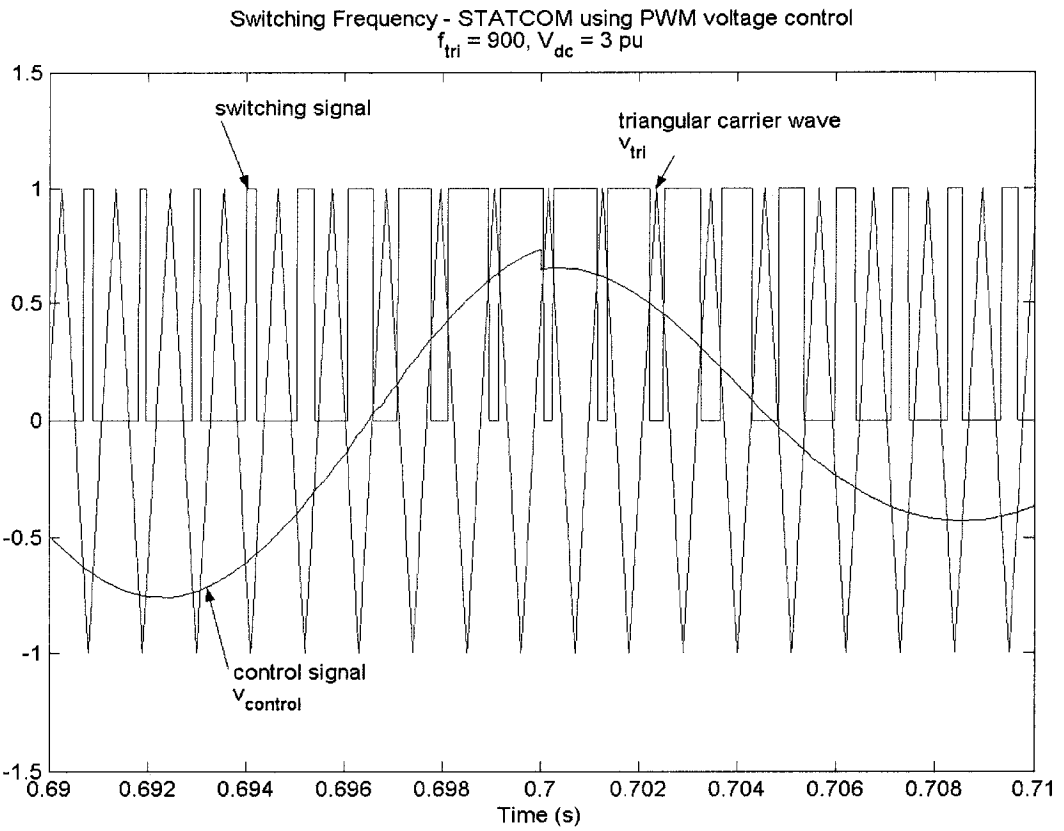

Figure 5. 1 Relationship of switching signal, control signal and triangular carrier signal of PWM STATCOM

For STATCOM using HCC, the switching frequency f_{sw} is continuously changing and difficult to control. As discussed in Chapter 2, the switching frequency of HCC is determined by the joint effect of the hysteresis band and the actual output phase current. Because the latter is dependant on multiple parameters such as DC and AC side voltages and impedance of the coupling transformer, it is hard to get a function to derive a the switching frequency for HCC STATCOM.

Figure 5.2 shows the relationship of the switching signal, actual output phase current and the hysteresis band when STATCOM is operated in steady state, which is described in Section 3.6.1. Although the average value is around 1 kHz, the instantaneous switching frequency f_{sw} is varying continuously. The shortest switching time can even reach 370μs.

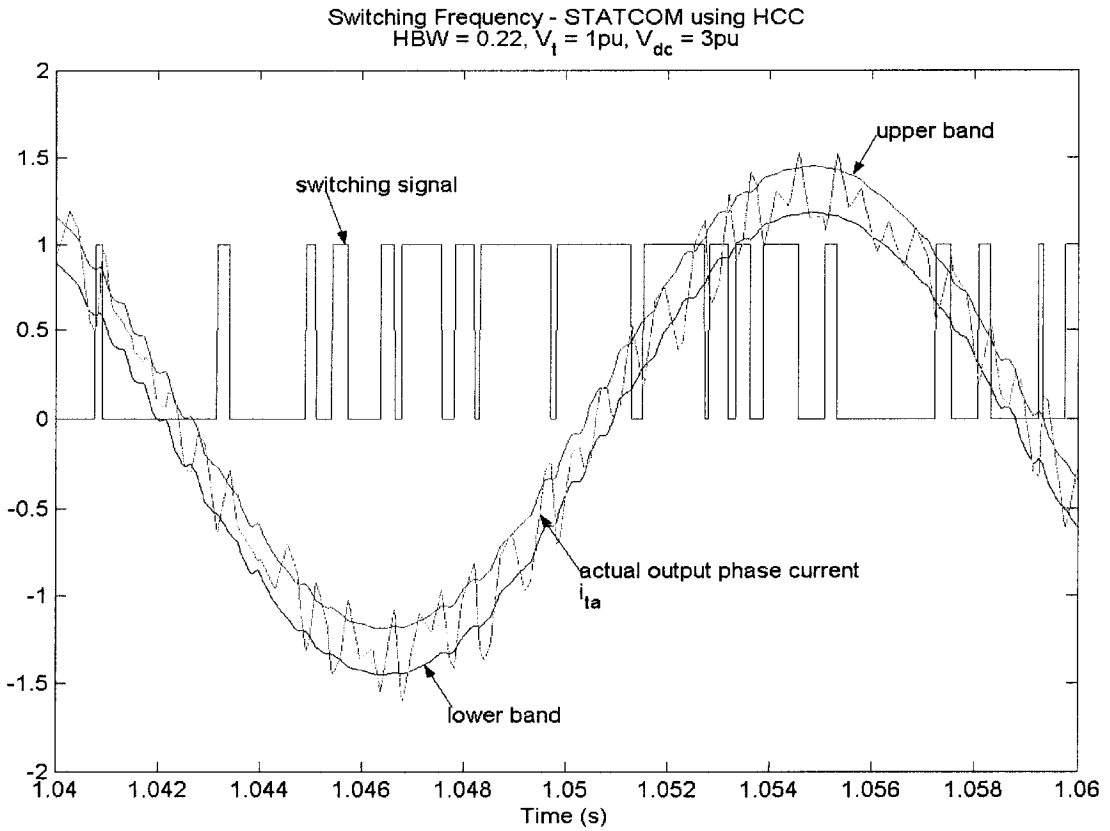

Figure 5. 2 Relationship of switching signal, phase A actual output current and hysteresis band of HCC STATCOM

5.2.3 Harmonics comparison

When the transmission system is operated at utility frequency (usually 50Hz or 60Hz), harmonic components exist in the voltage and current variables. The level of harmonic components is an important gauge to evaluate the performance of STATCOM.

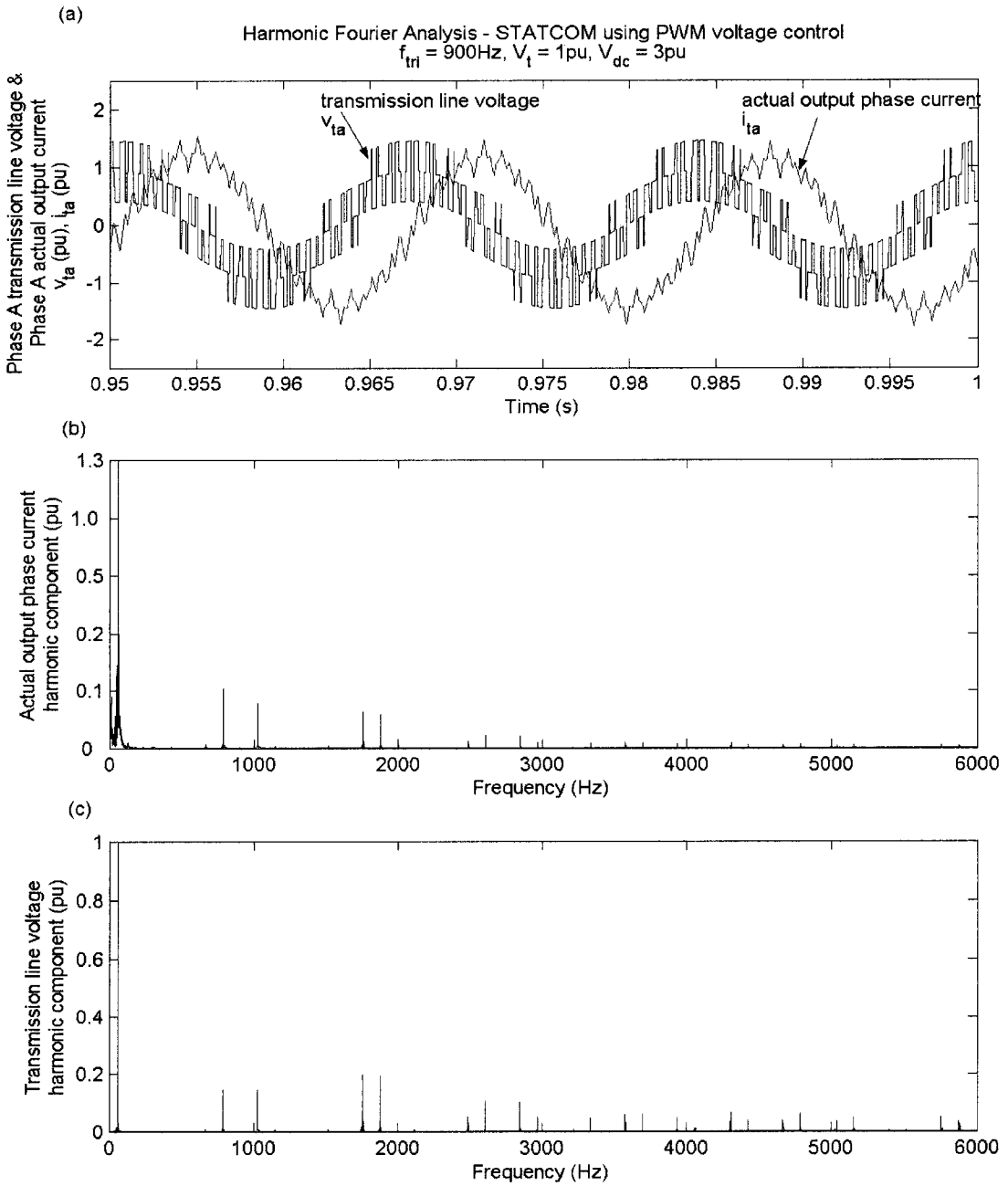

Figure 5. 3 Harmonic analysis for STATCOM using PWM voltage control

For STATCOM using PWM voltage control, the output voltage and current are rich in harmonic components. In Figure 5.3 shows the harmonic analysis of STATCOM using PWM voltage control operated in steady state when switching frequency is 900Hz, which

is described in Section 4.4.1. As can be seen from harmonic spectrum in Figure 5.3(b) and (c), the harmonic components are symmetrically distributed around m_f and the multiples. The total harmonic distortion in actual output phase current is 2.3%, in the transmission line voltage is 18.4%.

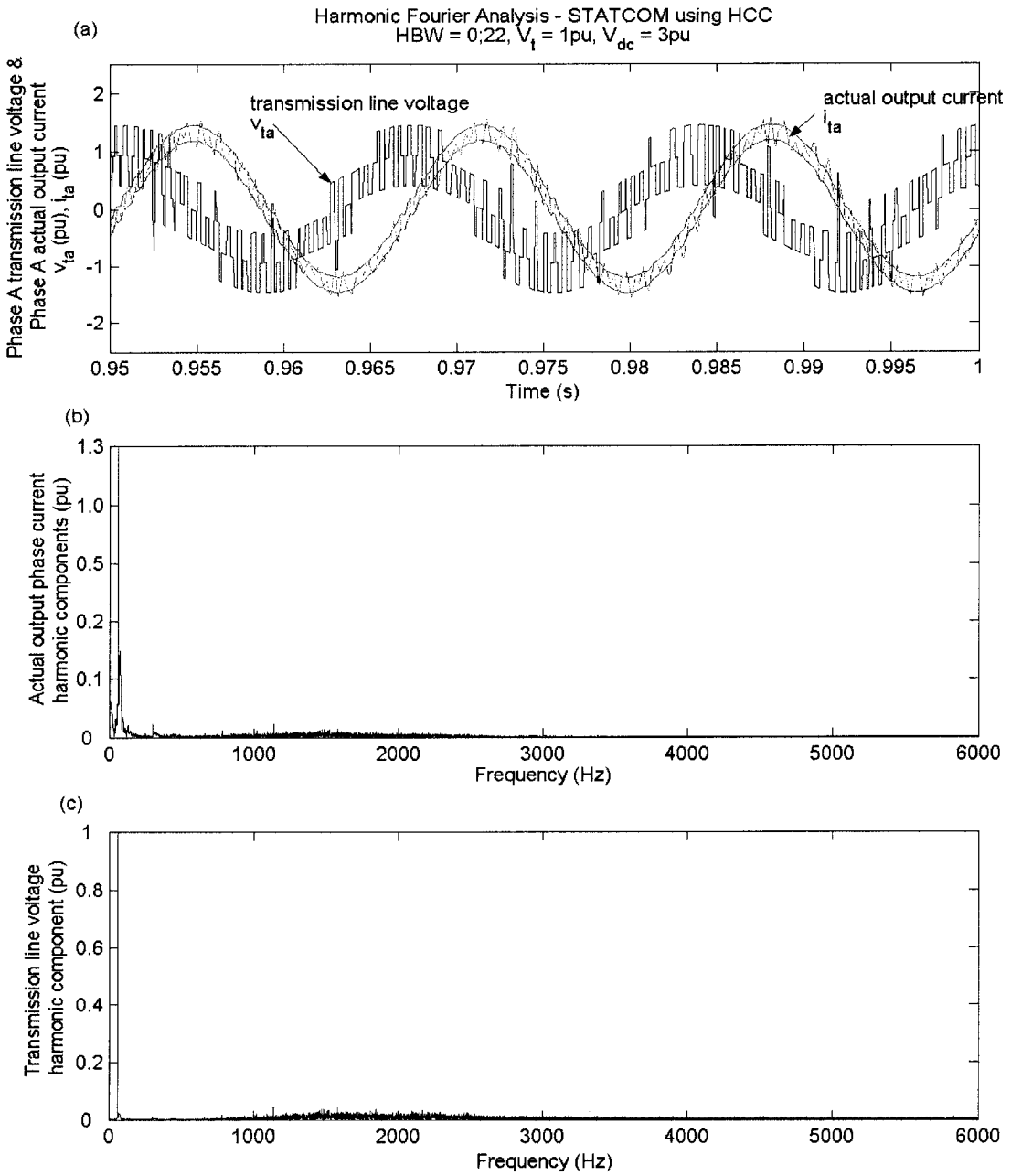

Figure 5. 4 Harmonic analysis for STATCOM using HCC when HBW=0.22

For STATCOM using HCC, there are also harmonic components in the AC side output current. Figure 5.4 shows the harmonic analysis of STATCOM using HCC operated in steady state when the average switching frequency is about 1kHz, which is described in Section 3.6.1. As can be seen from Fourier harmonic analysis in Figure 5.4(b) and (c), the harmonic components are not focused at any specified frequency but are mainly distributed in a band from around 1000 Hz to 3000 Hz. The magnitudes are also very low compared to PWM STATCOM harmonics and are less than 1% of the fundamental components.

5.3 Switching frequency control and harmonics suppression

5.3.1 Relationship of switching frequency to harmonics for PWM STATCOM

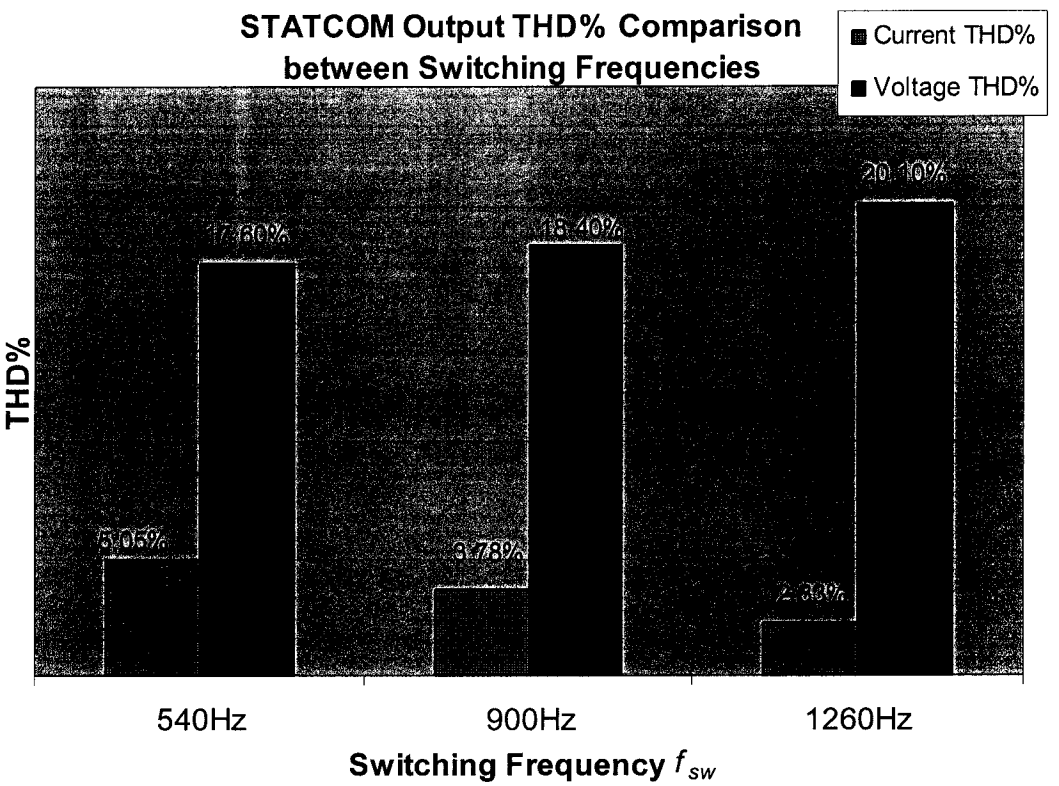

Figure 5. 5 STATCOM output THD% comparisons between switching frequencies

For STATCOM using PWM voltage control, the switching frequency f_{sw} is constant and set as the triangular carrier waveform. But the change of f_{sw} has some influence over the harmonic components in the output voltage and current. When the frequency modulation ratio m_f is increased and the switching frequency f_{sw} is higher, the center frequency and the multiples around which the harmonic components are distributed will be moved forward along the frequency axis in the harmonic spectrum figure. In Figure 5.5 shows the comparison of the total harmonic distortion (THD%) of the actual output phase current i_t and the transmission line voltage v_t when STATCOM is operated in different switching frequency. With the increase of f_{sw}, the THD% in i_t is slightly decreased and THD% in v_t is slightly increased. This is because the inductance L_t increases while resistance keeps stable with the switching frequency.

5.3.2 Effect of high-pass filter to PWM STATCOM

High-pass filter is an effective application to suppress the harmonic components in the output especially for PWM due to its fixed frequency. The capacitors of the filter are also responsible for compensating part of the reactive power.

In Figure 5.6 shows the effect of high-pass filters applied to the STATCOM described in Section 4.4. Since the highest harmonic components in v_t are at 13^{th} and 17^{th} order as shown in Figure 5.3(b), the filter frequencies are designed as 780 Hz. The filters are connected to the transmission line at 0.7s. Parameters of filters are calculated in Appendix A.

Figure 5.6(a) indicates that the harmonic components in i_t and v_t are greatly reduced and waveform qualities are improved by the filter. Although there is a sudden increase at the

voltage and current value due to the introduction of reactive power from filter capacitor, STATCOM adjusts the compensation and keeps the transmission line voltage magnitude to 1 pu in about 5 cycles. The Fourier harmonic analysis in Figure 5.6(b) and (c) shows the harmonic components at 13^{th}, 15^{th} and higher frequencies are minimized to be neglectable.

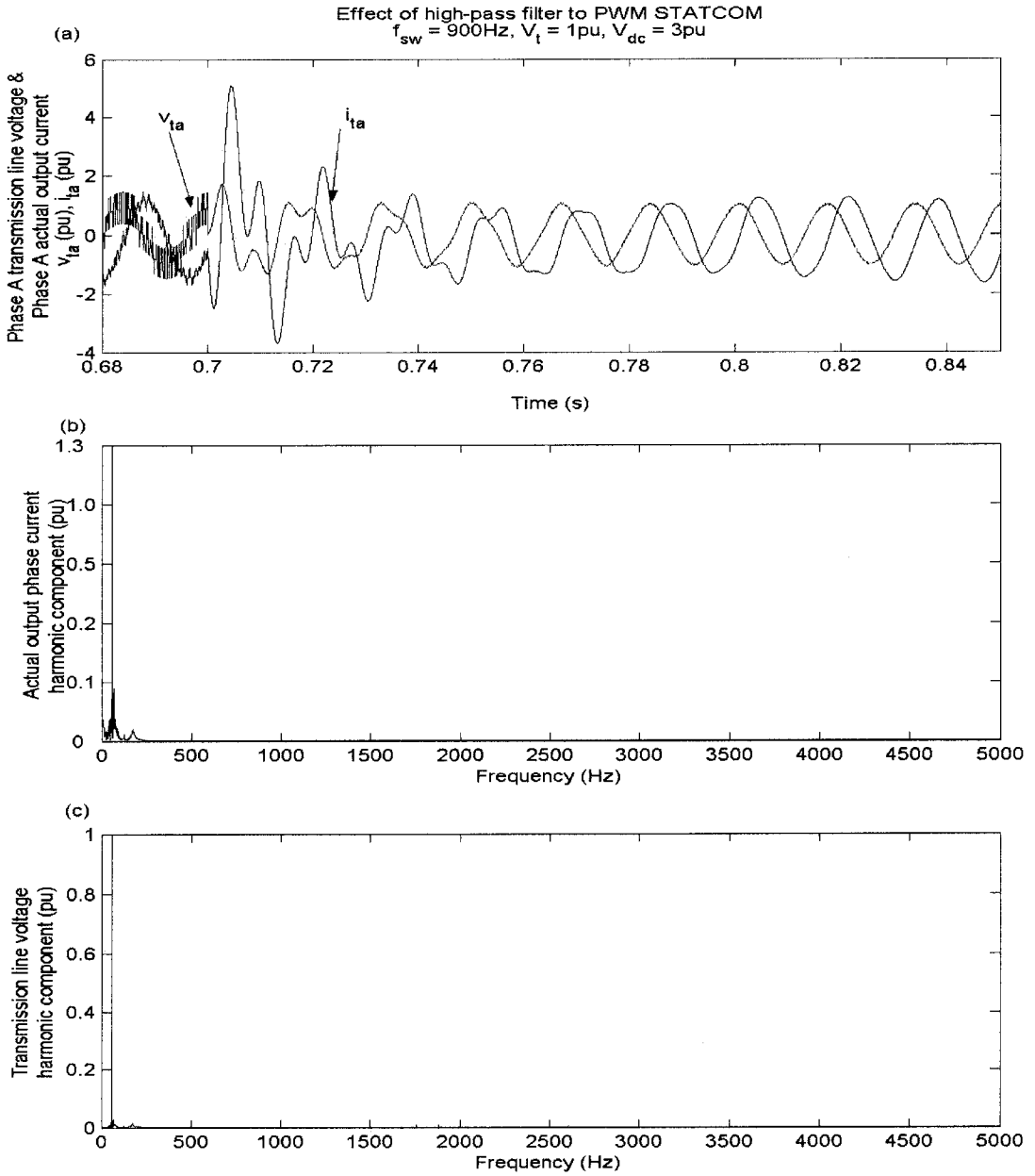

Figure 5. 6 Effects of high-pass filter to STATCOM using PWM voltage control

5.3.3 Influence of coupling transformer reactance over PWM STATCOM

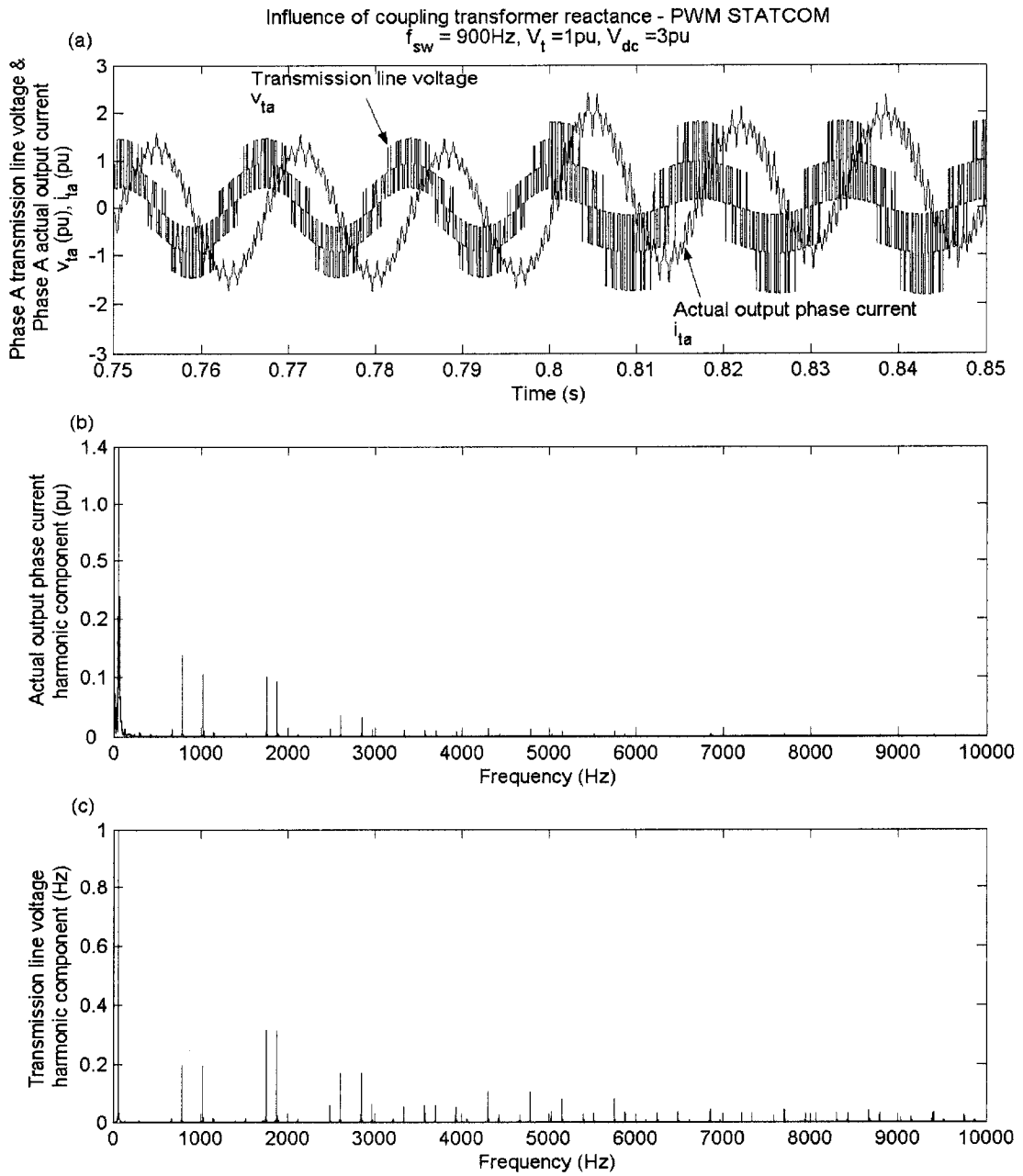

Figure 5. 7 Influence of coupling transformer reactance over PWM STATCOM output

The series-connected coupling transformer reactance is another factor to attenuate the harmonic components. Increasing the series-connected reactance L_t can effectively

reduce the harmonic components in the output voltage and current, while the reduction of L_t has the opposite effect. Figure 5.7(a) shows the changes of output voltage and current when L_t is reduced from 0.1 pu to 0.025 pu at 0.8s. The waveforms of v_t and i_t are both distorted after L_t is reduced. Comparing Figure 5.7 with Figure 5.3, the harmonic components in v_t and i_t are both increased noticeably. THD% of v_t has reached 61% while THD% of i_t has reached 16.4%.

5.3.4 Influence of hysteresis band over HCC STATCOM

Hysteresis bandwidth (HBW) is a very important parameter to HCC especially for harmonic suppression. Narrowing HBW can effectively reduce the harmonic components in the actual output phase current i_t, therefore improve the quality of the transmission line voltage. In Figure 5.8(a) shows the output of STATCOM described in Section 3.6.1 when HBW is changed from 0.22 to 0.1. The harmonic spectrum in Figure 5.8(b) indicates that the harmonic components in the actual output phase current i_t are eliminated. The harmonic spectrum in Figure 5.8 (c) indicates that the harmonic components in transmission line voltage v_t are moved forward along with the frequency axis. The low-order harmonic components are reduced.

However, the narrowing of HBW also results in the rise of the switching frequency. Figure 5.8(d) indicates that the average switching frequency rises to 1600 Hz, and the shortest switching time reaches 270μs. This is an obvious disadvantage to high power semiconductor devices like GTO switches.

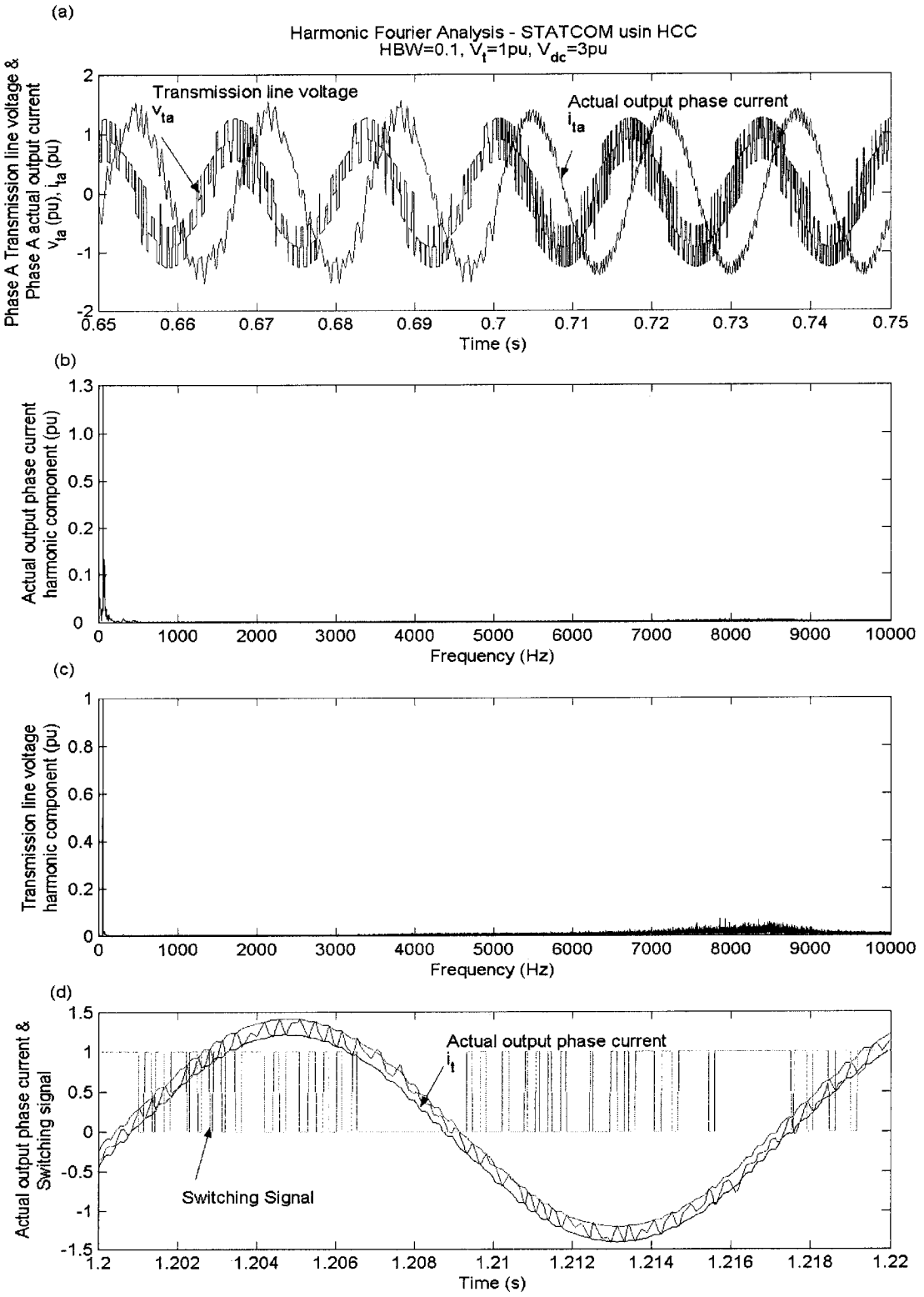

Figure 5. 8 Harmonic analysis for STATCOM using HCC when HBW=0.1

5.3.5 Influence of high-pass filter over HCC STATCOM

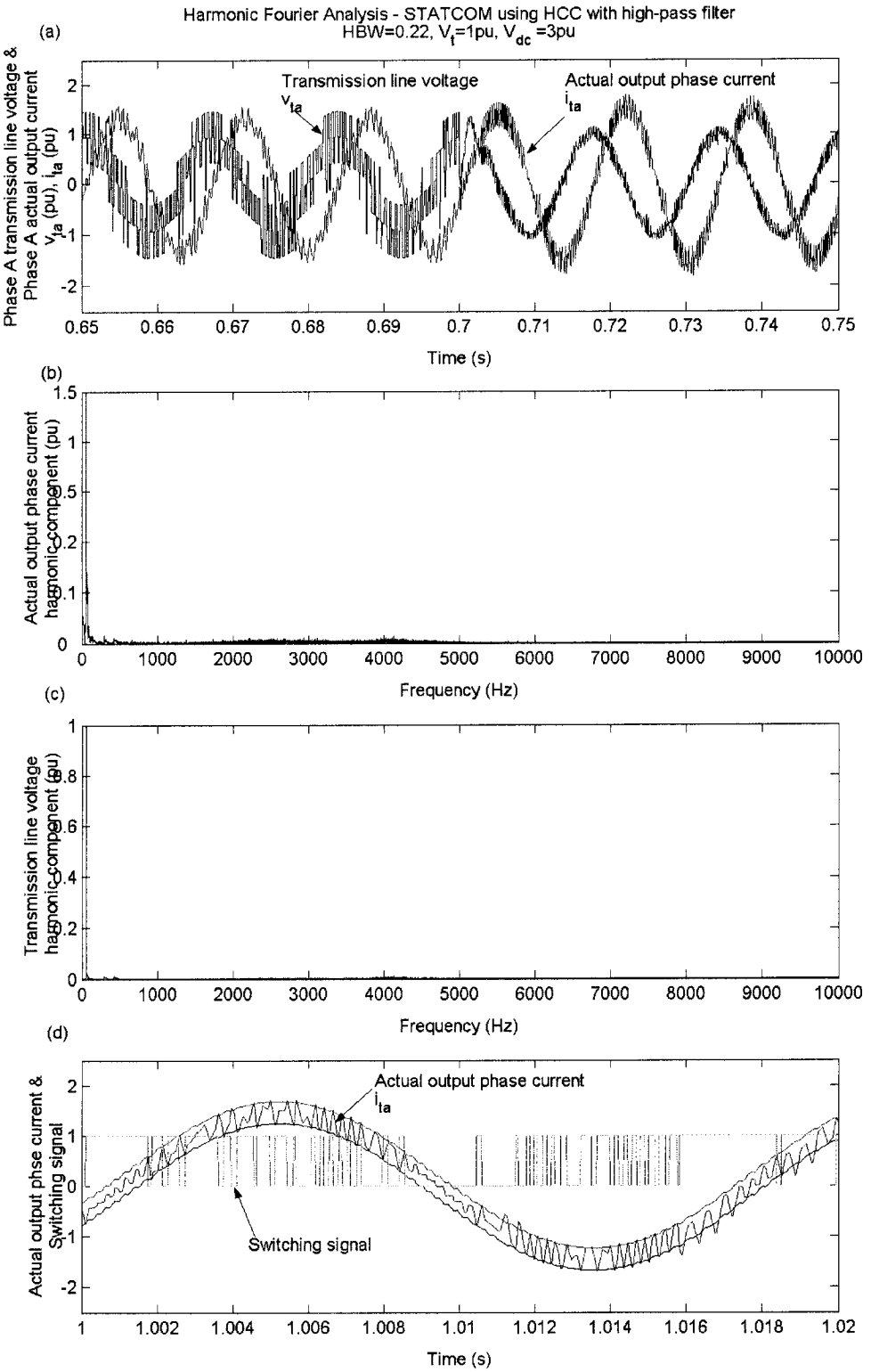

Figure 5. 9 Effect of high-pass filter to HCC STATCOM

Another step to eliminate the harmonics is the use of passive filters. Figure 5.4(b) and (c) indicates that the harmonic components are mainly distributed in a band from 1000 Hz to 3000 Hz. A high-pass filter is effective in eliminating harmonics with such characteristic. In Figure 5.9(a) shows the improvement of the transmission line voltage waveform when a high-pass filter is connected to the transmission line at 0.7s. Parameters of the high-pass filter are calculated in Appendix B.

As indicated by harmonic spectrum shown in Figure 5.9(c), the harmonic components are reduced to a low level. The magnitude of fundamental component of i_t has decreased to 1.17pu because the high-pass filter contributes part of reactive power to transmission line.

However, the high-pass filter also results in the rise of the switching frequency because the high-pass filter reduces the series impedance therefore increases the slope of i_t and the times i_t hit the band over each cycle. Figure 5.9(b) shows the switching signal when STATCOM recovers steady state after the high-pass filter is connected. The average value of f_{sw} has reached 1750 Hz and the shortest switching time reaches 210μs.

5.3.6 Influence of coupling transformer reactance over HCC STATCOM

As described in Eq. (3-16) and (3-21), control equations do not involve the coupling transformer reactance L_t and the transmission line voltage regulation is independent of L_t. However, L_t is effective in suppressing the harmonic components while not increase the switching frequency. In Figure 5.10(a) shows that when L_t is reduced to be 0.025 pu, the waveform of v_t is seriously distorted but i_t not. The harmonic spectrum in Figure 5.10(c) shows that the harmonic component magnitudes of v_t have increased. Figure 5.10(b)

indicates that the harmonic components of i_t move forward along the frequency axis while the fundamental component magnitude is kept as 1.3pu. This proves that HCC STATCOM is working as a reactive current source. The comparison between 5.10(d) and 5.2 indicates that the average switching frequency is increased from 900 Hz to about 1800Hz. This is because lower L_t increases the slope of i_t and the times it hits the hysteresis band.

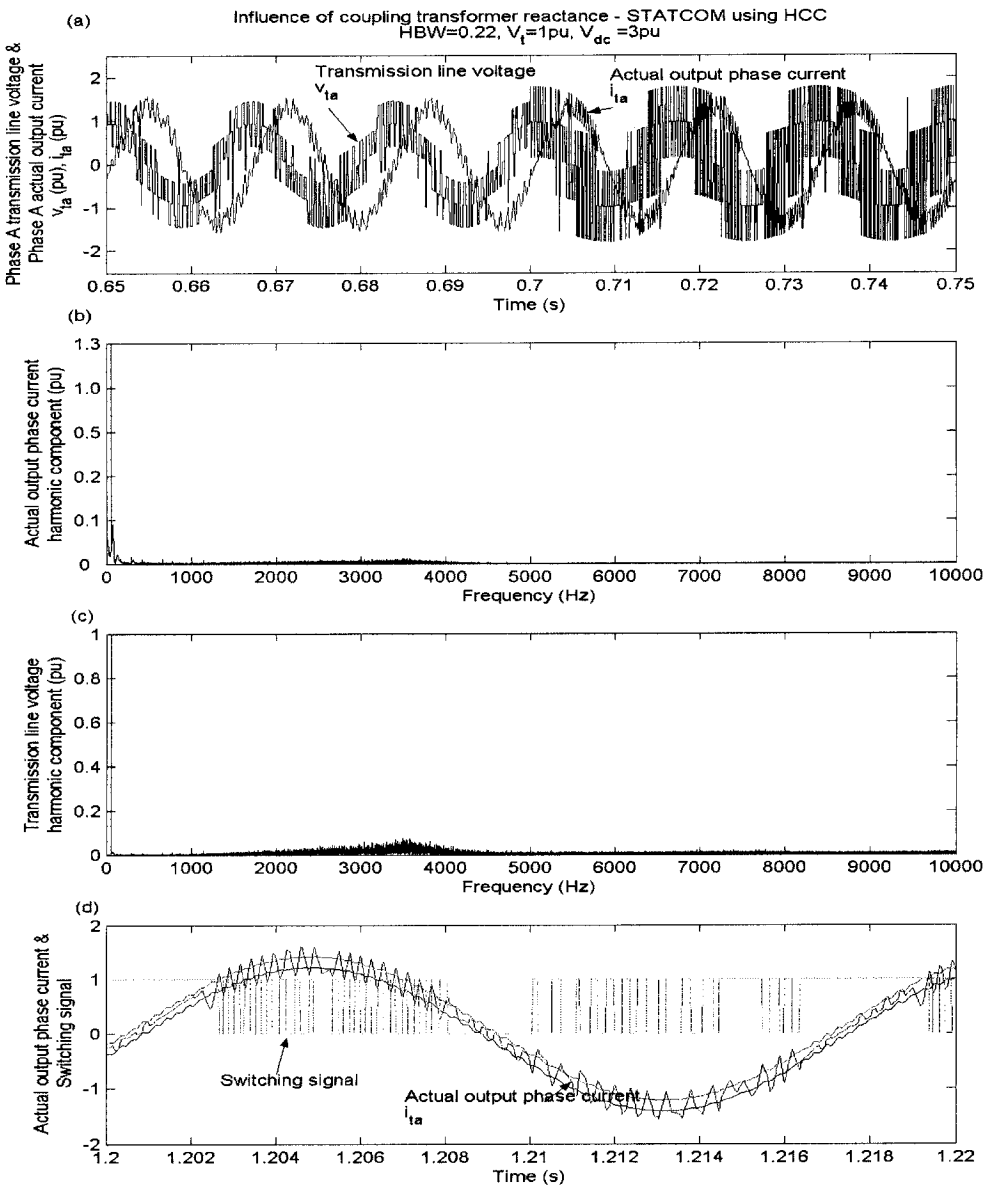

Figure 5. 10 Influence of coupling transformer reactance over HCC STATCOM output

5.4 Summary

In this chapter, the controller performance of STATCOM using PWM voltage control is compared with that of a STATCOM using HCC. As discussed in the simulation results comparison, HCC has faster response to small signal disturbance. The overshoots of HCC output are also lower than PWM voltage control.

Although the switching frequency is not related to the stability of the controllers, increasing the switching frequency can improve the waveform quality of the actual output phase current of STATCOMs operated in both control strategies, while causing a slightly increase THD% of transmission line voltage. When PWM switches the devices at a fixed frequency and the switching period is constant, HCC is operated at a changing frequency and the instantaneous frequency can be much higher than the average frequency.

High-pass filter is very effective in eliminating the harmonic components especially when the harmonic order is known and fixed. For HCC STATCOM output, high-pass filter is effective in eliminate the harmonic components distributed continuously along with the frequency axis, but may result in a rise of switching frequency.

Increasing the series-connected coupling transformer reactance is another way to minimize the harmonic components for STATCOMs with both control strategies. The rise of series-connected reactance also flattens the slope of the actual output phase current and therefore reduces the switching frequency of HCC. But the increase of reactance will result in more reactive power consumption on the transformer, therefore reducing the compensation capacity, and increasing the absorption capacity of STATCOM.

6. CONCLUSION AND FUTURE STUDIES

6.1 Conclusion

STATCOM is one of the most popular FACTS devices in high power electronics application. The ability of reactive power compensation and voltage regulation play a key role in the transmission system. The control method utilized for STATCOM is a major research topic.

This thesis presents two control strategies for STATCOM: PWM voltage control and HCC. Both of these control strategies are analyzed in the synchronous rotating reference frame for d-q decomposition to separate the active and reactive control loops. The classical and simple PI controllers are suitable for the controller designs. In the research work, the implementation of a 6-pulse 3-phase full bridge voltage source inverter is used to build STATCOM application for transmission system. The functions of the controllers in both strategies are verified by simulation in EMTP-RV software package. In order to compare the performance of the two control strategies, the identical topology of STATCOM and same power circuit are applied.

For STATCOM using PWM voltage control, the output voltage contains high harmonic components around the switching frequency and the multiples. The fixed switching frequency makes it easy to analyze and take steps to eliminate the harmonic components. The harmonic components can be counteracted by the phase displacement. This thesis describes the effect of high-pass filters and reactance of the coupling transformer, which do not change the topology of the STATCOM for the convenience of comparison.

Compared with STATCOM using PWM voltage control, STATCOM using HCC has a faster response and lower overshoots. The low-order harmonic components in the output

voltage are lower too. However, the voltage distortion of HCC STATCOM is not low enough to be ignored when the average switching frequency is kept the same as PWM STATCOM, and the constantly changed switching frequency brings difficulty in analyzing the harmonic components with an accurate mathematical model. This also makes multi-pulse topology and multi-level topology ineffective to HCC STATCOM. The application of a band filter undermines the cost advantage of HCC, while increases the switching frequency in the mean time.

Another drawback of HCC is the short instantaneous switching period even the average switching frequency is low. As described in Chapter 5, the shortest switching period can reach half or one third of the average switching period. The short switching period will increase the switching losses and the cost to eliminate the generated heat, which is disadvantageous to the high power semiconductor switches. Considering the low switching frequency of GTOs, the weakness of HCC is especially adverse.

Generally, HCC has advantages on control stability and response time. But the advantages are offset by the uncontrolled switching frequency and the difficulty in eliminating the harmonic components. Thus PWM voltage control is more acceptable in high power STATCOM application.

6.2 Future studies

The application of HCC in high power electronics is limited due to the ratings of switching devices and low performance. The weakness can be improved by the development of research in semi-conductors and future work in control schemes. Future studies on STATCOM using HCC are recommended as follows:

- Conduct the research in the performance of HCC when STATCOM is operated under unbalanced situation or fault.
- Study the relationship between switching frequency, voltage drop and actual output phase current in order to deduce more accurate mathematical model for current controlled STATCOM
- Conduct the research in fixed-frequency current control
- Study alternative techniques to eliminate the harmonic components in STATCOM output

REFERENCES

[1] B.M. Zhang, Q.F. Ding, "The development of FACTS and its control", *Advances in Power System Control, Operation and Management, APSCOM-97. Fourth International Conference,* Vol.1, Nov. 1997, pp: 48 – 53

[2] J.J. Paserba, "How FACTS controllers benefit AC transmission systems", *Power Engineering Society General Meeting, IEEE,* Vol.2, June 2004, pp:1257 - 1262

[3] A. Edris, "FACTS technology development: an update", *Power Engineering Review, IEEE*, Vol.20, Issue 3, March 2000, pp: 599 - 627

[4] L. Gyugyi, "Application characteristics of converter-based FACTS controllers", IEEE Conference on Power System Technology, Vol. 1, pp. 391 - 396, Dec. 2000.

[5] N.G. Hingorani and L. Gyugyi, *Understanding FACTS, Concepts and Technology of Flexible AC Transmission systems*, IEEE Press 2000

[6] N.G. Hingorani, "High power electronics and flexible AC transmission system", IEEE Power Engineering Review, Vol.8, No.7, pp.3-4, July 1988.

[7] IEEE FACTS Terms & Definitions Task Force of the FACTS Working Group of the DC and FACTS subcommittee, "Proposed terms and definitions for Flexible AC Transmission System (FACTS)", IEEE Trans. on Power Delivery, Vol. 12, No. 4, pp. 1848-1853, Oct. 1997.

[8] A.D. Rajapakse, A.M. Gole, and P.L. Wilson, "Electromagnetic transient's simulation models for accurate representation of switching losses and thermal performance in power electronic systems", IEEE Trans. on Power Delivery, Vol. 20, Issue 1, pp. 319 – 327, Jan 2005.

[9] A.D. Rajapakse, A.M. Gole, and P.L. Wilson, "Electromagnetic transient's simulation models for accurate representation of switching losses and thermal performance in power electronic systems", IEEE Trans. on Power Delivery, Vol. 20, Issue 1, pp. 319 – 327, Jan 2005.

[10] Sumi Yoshihiko, Harumoto Yoshinobu, Hasegawa T, "New Static Var Control Using Force-Commutated Inverters", *IEEE Trans. on Power Apparatus and Systems, 1981,* PAS-100(9); 4216-4224

[11] K. Matsuno, I. Iyoda, and Y. Oue, "An experience of FACTS developed 1980s and 1990s", *Transmission and Distribution Conference and Exhibition 2002: Asia Pacific, IEEE/PES,* Volume: 2, 6-10 Oct. 2002, 1378-1381 vol.2

[12] C. Schauder, M. Gemhardt, E. Staccy, T. Lemak, L. Gyugyi, T.W. Cease, and A. Edris, "Operation of ±100MVar TVA STATCON", *IEEE Trans. on Power Delivery,* Volume: 12 Issue: 4, Oct. 1997: 1805-1811

[13] E. Uzunovic, B. Fardanesh, L. Hopkins, "NYPA convertible static compensator (CSC) application phase I: STATCOM", *Transmission and Distribution Conference and Exhibition 2001:* Volume: 2, 28 Oct.-2 Nov. 2001, 1139-1143

[14] Azeddine Draou, Mustapha Benghanem, and Ali Tahri, "Multilevel Converters and VAR Compensation", *Power Electronics Handbook*, Academic Press, San Diego, CA, c2001, pp: 722 – 729

[15] A.W. Green and J.T. Boys, "Hysteresis Current-forced 3-phase voltage-sourced reversible rectifier", IEE Proceedings B, Vol.136, Issue: 3, May 1989

[16] D. Sutanto, L.A. Snider, and K.L. Mok, "EMTP simulation of a STATCOM using Hysteresis Current Control", Power Electronics and Drive Systems, Vol. 1, July 1999, pp: 531-535,

[17] C. Schauder, "Vector analysis and control of advanced static VAR compensators", IEEE Proceedings, Vol.140, No.4, July 1993.

[18] Ye Yang, M. Kazerani, and V.H. Quintana, "Modelling, Control and Implementation of 3-phase PWM Converters", *IEEE Trans. on Power Electronics,* Volume: 18, Issue: 3, May 2000, pp: 857-864

[19] Ye Yang, M. Kazerani, and V.H. Quintana, "A novel modeling and control method for 3-phase PWM converters", *Power Electronics Specialists Conference, 2001. PESC. 2001 IEEE 32nd Annual,* Volume: 1, pp: 102-107

[20] V. Blasko and I. Agirman, "Modeling and Control of 3-phase Regenerative AC-DC Converters", *Proceedings of the 40th IEEE Conference on Decision and Control,* Dec. 2001, Volume: 3, pp: 2235-2240

[21] V. Blasko and Kaura Vikram, "A New Mathematical Model and Control of A 3-phase AC-DC Voltage Source Converter", *IEEE Trans. on Power Electronics,* Volume: 12, Issue: 1, Jan. 1997, pp: 116-123

[22] G.C. Cho, G.H. Jung, N.S. Choi, and G.H. Cho, "Analysis and controller design of static Var compensator using three-level GTO inverter", *IEEE Trans. on Power Electronics,* Volume: 11, Issue: 1, Jan. 1996, pp: 57-65

[23] G.C. Cho, G.H. Jung, N.S. Choi, and G.H. Cho, "Control of Static Var Compensator (SVC) With DC Voltage Regulation and Fast Dynamics By Feedforward and Feedback Loop", *Power Electronics Specialists Conference, 1995. PESC '95 Record., 26th Annual IEEE,* Volume: 1, pp: 367-374

[24] Qingguang Yu, Pei Li, and Xiaorong Xie, "Overview of STATCOM Technologies", *Procedings of IEEE Conference on Electric Utility Deregulation, Restructuring and Power Technologies,* April 2004, Hong Kong.

[25] L.i Malesani and P. Tomasin, "PWM current Control Techniques of Voltage source Converters-a Survey", in Proc. IEEE Conference on Industrial Electronic, Control, and Instrumentation, Vol. 2, pp. 670-675, Nov 1993.

[26] J.T.Boys and A.W.Green, "Current-forced Single-phase Reversible Rectifier", IEE Proceedings, Vol.136, pp. 205-211, Sep.1989

[27] A. H. Norouzi and A. M. Sharaf, "Two control schemes to enhance the dynamic performance of the STATCOM and SSSC," IEEE Trans. on Power Delivery, Vol. 20, Issue 1, pp. 435 – 442, Jan 2005.

[28] Pranesh Rao, M.L. Crow, and Zhiping Yang, "STATCOM Control for Power System Voltage Control Applications", IEEE Trans. on Power Delivery, Vol. 16, No. 4, Oct 2000,

[29] J. K. Steinke, "Use of an LC filter to achieve a motor-friendly performance of the PWM voltage source inverter," IEEE Trans. on Energy Conversion, Vol. 14, No. 3, pp. 649-654, Sept.1999.

[30] L. Malesani, P. Mattavelli, and P. Tomasin, "Improved constant-frequency hysteresis current control of VSI inverters with simple feedforward bandwidth prediction", *Industry Applications, IEEE Trans.*, Vol. 33 , Sept.-Oct. 1997, pp. 1194 – 1202

[31] H. W. Van der Broeck, "Analytical calculation of the harmonic effects of single phase multilevel PWM inverters", *IEEE Conference on Industrial Electronics Society,* Vol.1, pp. 243 – 248, Nov. 2003.

Appendix A High-pass Filter Design for HCC STATCOM

A high-pass filter is a filter that passes high frequencies but attenuates (or reduces) frequencies lower than the cut-off frequency. As indicated in the harmonic Fourier spectrum in Figure 5.4 (b) and (c), the harmonic components are distributed between 1000Hz and 3000Hz. Therefore the high-pass filters at the two frequencies are designed.

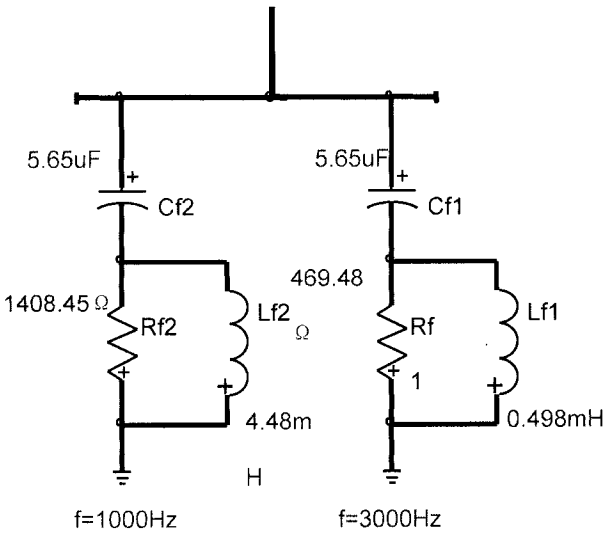

Figure A. 1 Electrical circuit of passive high-pass filter

The overall filter is designed to provide 20% of the rated reactive power of STATCOM. Therefore the parameter of filter is calculated as:

$$C = \frac{Q_C}{V^2 \omega_f} = 5.65\mu F$$

The cut-off frequency of the filter is determined by

$$f_c = \frac{1}{2\pi\sqrt{LC}} \tag{A-1}$$

The inductance of the filter is calculated as:

$$L = \frac{1}{C(2\pi f)^2} \tag{A-2}$$

The quality factor of the filter Q is calculated as:

$$Q = \frac{R}{\omega_C L} \tag{A-3}$$

The resistance and inductance for f_C = 1000Hz is calculated as:

$$R = 1408.45\Omega,\ L = 4.48mH$$

The resistance and inductance for f_C = 3000Hz is calculated as:

$$R = 469.48\Omega,\ L = 0498mH$$

Appendix B High-pass Filter Design for PWM STATCOM

A high-pass filter is also effective in eliminating the harmonic components in the output of PWM STATCOM. The design in Appendix A can also be applied. As indicated in the harmonic Fourier spectrum in Figure 5.3 (b), the harmonic components begins at 13th order frequency. Therefore the cut-off frequency of the high-pass filter is designed as 780Hz.

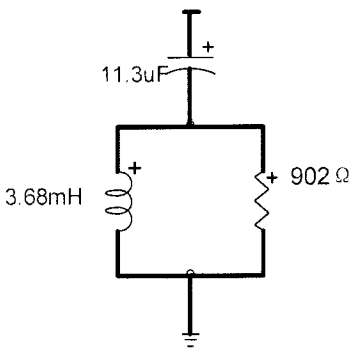

Figure B. 1 Electrical circuit of passive low-pass filter

The filter is designed to provide 20% of the rated reactive power of STATCOM. Therefore the parameter of filter is calculated as:

$$C = \frac{Q_C}{V^2 \omega_f} = 11.3\mu F$$

The cut-off frequency of the filter is determined by

$$f_c = \frac{1}{2\pi\sqrt{LC}} \tag{B-1}$$

The inductance of the filter is calculated as:

$$L = \frac{1}{C(2\pi f)^2} \tag{A-2}$$

The quality factor of the filter Q is calculated as:

$$Q = \frac{R}{\omega_C L} \tag{A-3}$$

The resistance and inductance for f_C = 780Hz is calculated as:

$$R = 902\Omega\,,\ L = 3.68mH$$

Appendix C Regulator Design for HCC STATCOM

d- control loop

The transfer function of the plant with unity feedback for the active power absorption is:

$$G(s) = \frac{1087}{1+2.9s}$$

The bode plot of plant is shown as:

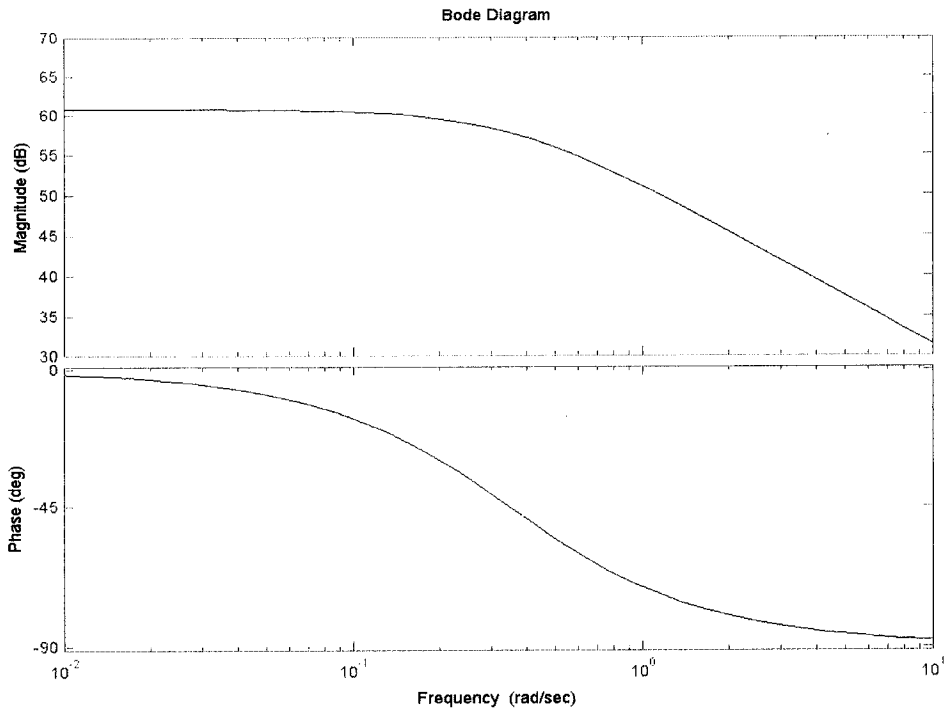

Figure C. 1Bode plot of d- control loop plant for HCC STATCOM

A type II PI controller is applied and expressed as:

$$G_C = \frac{k(1+s\tau)}{s\tau}\frac{1}{1+sT_P}$$

At the crossover frequency, $\omega_X = \frac{1}{\sqrt{\tau T_P}}$, and $\tau = A^2 T_P$

Considering the average switching frequency of VSI is around 900Hz, in order to achieve a fast settling time and keep the system stable, the design specifications for the controller are: 45°<PM<60° at the crossover frequency f_X = 180Hz. At the crossover frequency ω_X , $|G(s_X)|$ = 0.33, or -9.6 dB and $\phi(G(s_X))$ = -89.98°. Therefore, the controller has to introduce a lagging phase angle of θ_C =-45.02° and present a gain of 3.02 at the crossover frequency.

Factor A can be calculated from: $\theta_C = -90 + \tan^{-1} A - \tan^{-1}(1/A)$, By choosing A=3, We can get phase margin PM= 53°. Therefore, τ=0.00265, T_P =0.0003, and k=3.035.

Therefore, controller for plant ***G(s)*** is:

$$G_C = \frac{1145(1+0.00265s)}{s(1+0.0003s)}$$

The Bode plot of compensated system is:

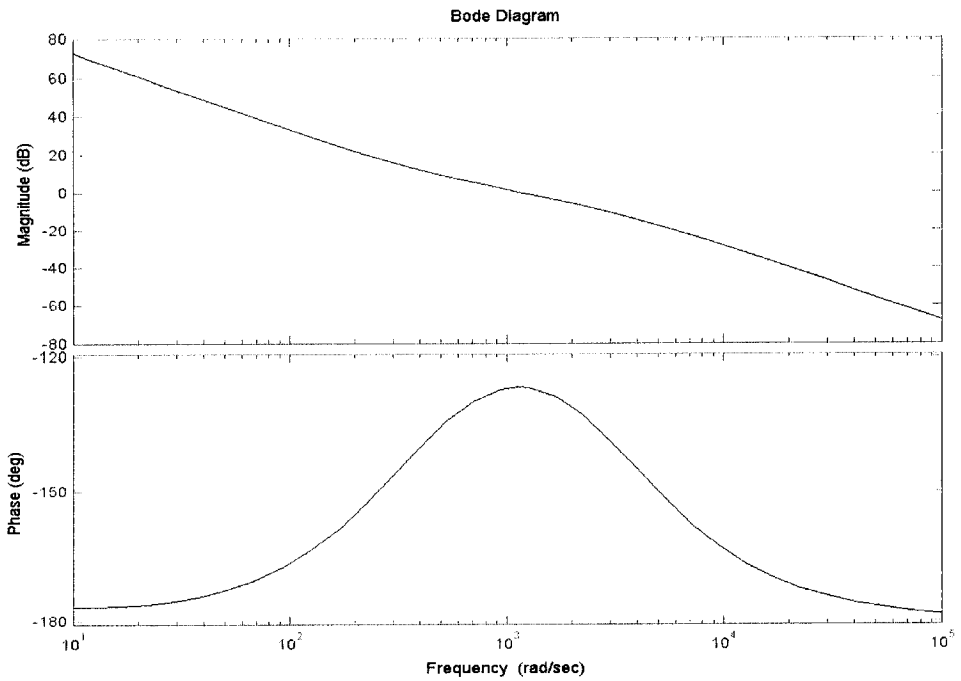

Figure C. 2 Bode plot of compensated d- control loop plant for HCC STATCOM

q- control loop

The transfer function of the plant with unity feedback for the reactive power compensation is:

$$G(s) = 0.176$$

The bode plot of plant is shown as:

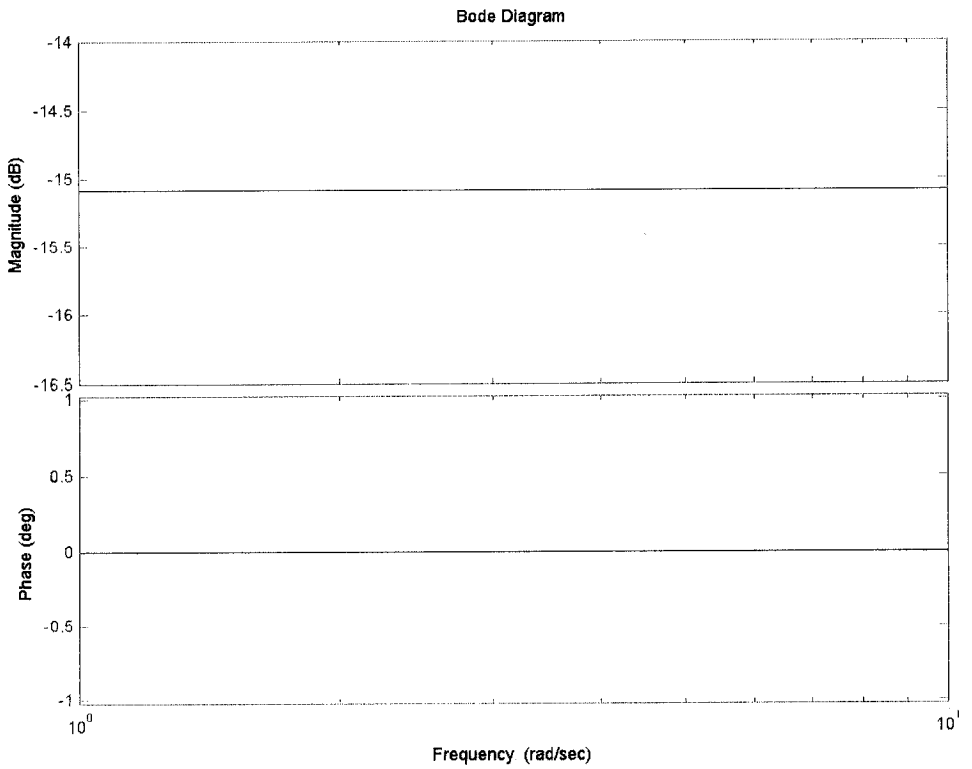

Figure C. 3 Bode plot of q- control loop plant for HCC STATCOM

A type II PI controller is applied and expressed as:

$$G_C = \frac{k(1+s\tau)}{s\tau}\frac{1}{1+sT_P}$$

At the crossover frequency, $\omega_X = \frac{1}{\sqrt{\tau T_P}}$, and $\tau = A^2 T_P$

Considering the average switching frequency of VSI is around 900Hz, in order to achieve a fast settling time and keep the system stable, the design specifications for the controller are: 45°<PM<60° at the crossover frequency $f_X = 180$Hz. At the crossover frequency ω_X, $|G(s_X)| = 0.176$, or -15.1 dB and $\phi(G(s_X)) = 0°$. Therefore, the controller has to introduce a lagging phase angle of θ_C =-135° and present a gain of 5.684 at the crossover frequency.

Factor A can be calculated from: $\theta_C = -90 + \tan^{-1} A - \tan^{-1}(1/A)$, By choosing A=0.5, We can get phase margin PM= 53°. Therefore, τ=0.000442, T_P =0.00177, and k=5.684. Therefore, controller for plant ***G(s)*** is:

$$G_C = \frac{12860(1+0.000442s)}{s(1+0.00117s)}$$

The Bode plot of compensated system is:

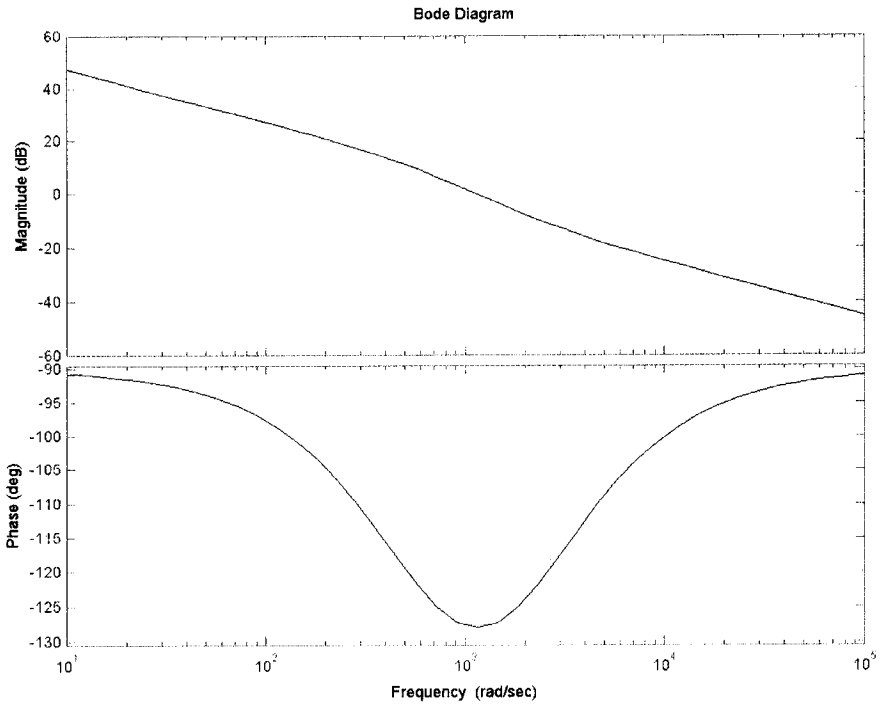

Figure C. 4 Bode plot of compensated q- control loop plant for HCC STATCOM

Appendix D Regulator Design for PWM STATCOM

d-control loop

The transfer function of the plant with unity feedback for the active power absorption is:

$$G(s) = \frac{1.4\times10^9}{s^3 + 0.173s^2 + 1.45\times10^5 s + 2465}$$

$$= \frac{1.4\times10^9}{(s+0.017)(s^2 + 0.156s + 1.45\times10^5)}$$

$$= G_m(s)\frac{1}{s+0.017}$$

The bode plot of G_m is shown as:

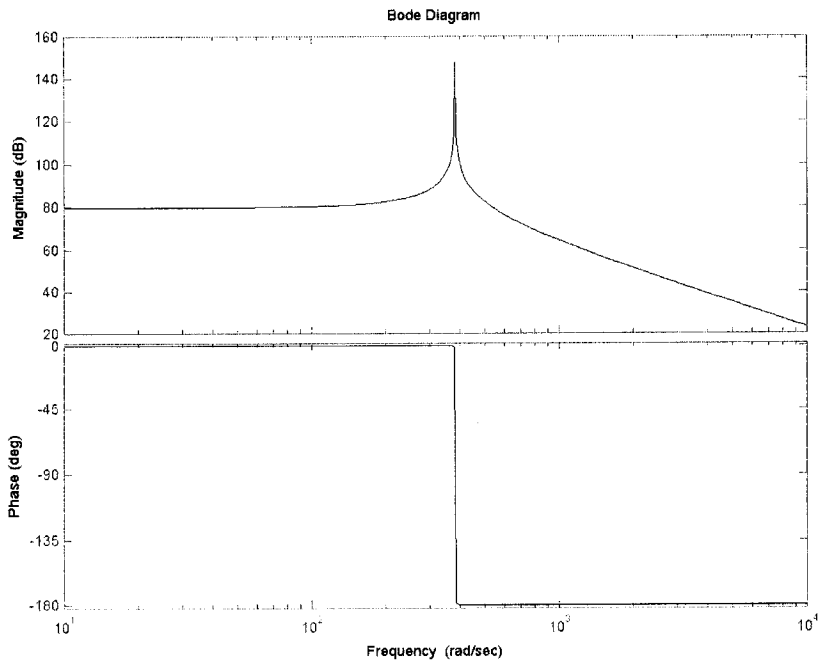

Figure D. 1 Bode plot of d- control loop plant for PWM STATCOM

Considering the average switching frequency of VSI is around 900Hz, in order to achieve a fast settling time and keep the system stable, the design specifications for the controller

are: 45°<PM<60° at the crossover frequency f_X = 180Hz. At the crossover frequency ω_X, $|G_m(s_X)| = 1234.4$, or 61.83 dB and $\phi(G(s_X))$ =-179.99°. A type III PI controller for $\boldsymbol{G_m}$ is applied and expressed as:

$$G_{Cm} = \frac{k(s+\omega_z)^2}{s(s+\omega_p)^2}$$

At the crossover frequency, $\omega_X{}^2 = \omega_z\omega_p$, and $\omega_p = A^2\omega_z$

Factor A can be calculated from: $\theta_C = -90 + 2\tan^{-1}A - 2\tan^{-1}(1/A)$, By choosing A=6, We can get phase margin PM= 52°. Therefore, ω_z = 188.5, ω_p = 6786, and k=33

Therefore, controller for plant ***G(s)*** is:

$$G_C = (s+0.017)G_{Cm} = \frac{33(s+0.017)(s+188.5)^2}{s(s+6786)^2}$$

The Bode plot of compensated system is:

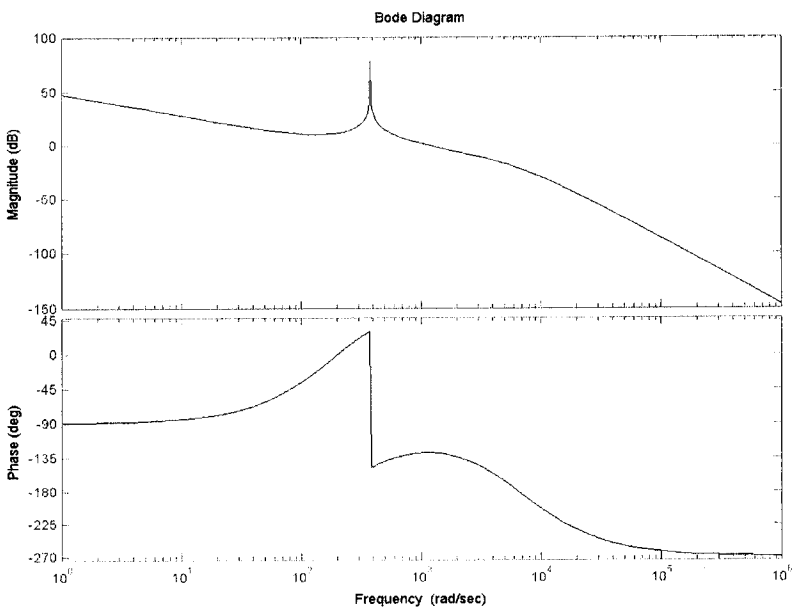

Figure D. 2 Bode plot of compensated d- control loop plant for PWM STATCOM

The transfer function of the plant with unity feedback for the reactive power compensation is:

$$G(s) = \frac{29.3s^2 + 5.1s}{0.026s^3 + 4.5 \times 10^{-3} s^2 + 3770s + 64}$$

$$= \frac{5.1s}{0.026\,s^3 + 4.5 \times 10^{-3} s^2 + 3770\,s + 64}(1 + 5.74\,s)$$

$$= (1 + 5.74s)G_m$$

The bode plot of $\boldsymbol{G_m}$ is shown as:

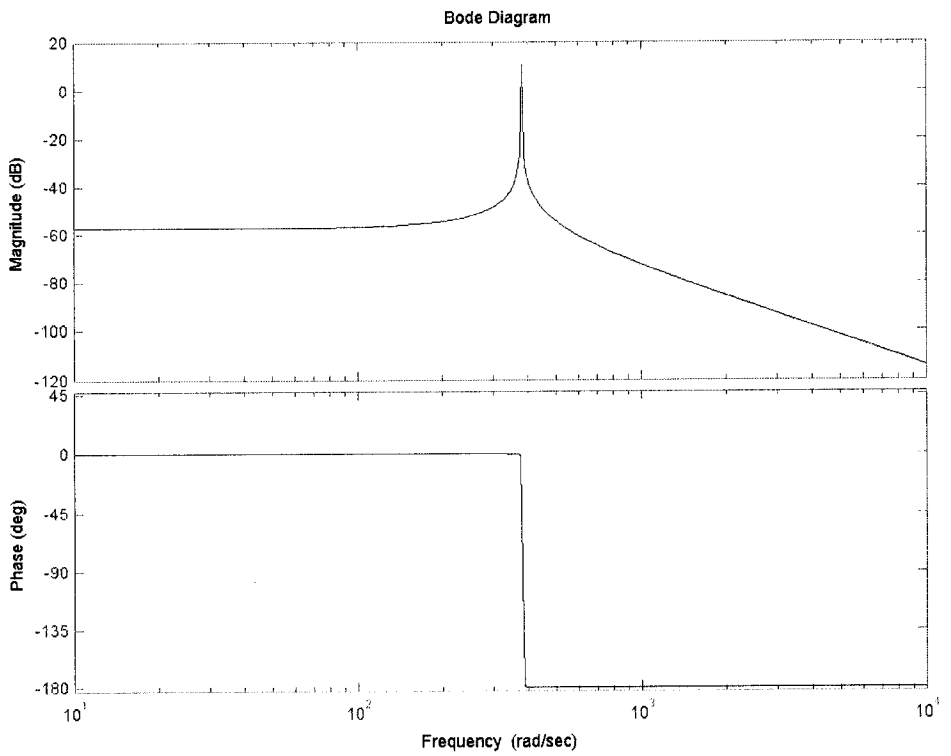

Figure D. 3 Bode plot of q- control loop plant for PWM STATCOM

Considering the average switching frequency of VSI is around 900Hz, in order to achieve a fast settling time and keep the system stable, the design specifications for the controller

are: 45°<PM<60° at the crossover frequency f_X = 180Hz. At the crossover frequency ω_X, $|G_m(s_X)| = 0.000174$, or -75.2 dB and $\phi(G_m(s_X)) = -179.99°$. A type III PI controller for $\boldsymbol{G_m}$ is applied and expressed as:

$$G_{Cm} = \frac{k(s+\omega_z)^2}{s(s+\omega_p)^2}$$

At the crossover frequency, $\omega_X{}^2 = \omega_z \omega_p$, and $\omega_p = A^2 \omega_z$

Factor A can be calculated from: $\theta_C = -90 + 2\tan^{-1} A - 2\tan^{-1}(1/A)$, By choosing A=6, We can get phase margin PM= 52°. Therefore, $\omega_z = 188.5$, $\omega_p = 6786$, and k=2.34x108

Therefore, controller for plant ***G(s)*** is:

$$G_C = (1+5.74s)G_{Cm} = \frac{1.34\times10^9 \times (s+0.174)(s+188.5)^2}{s(s+6786)^2}$$

The Bode plot of compensated system is:

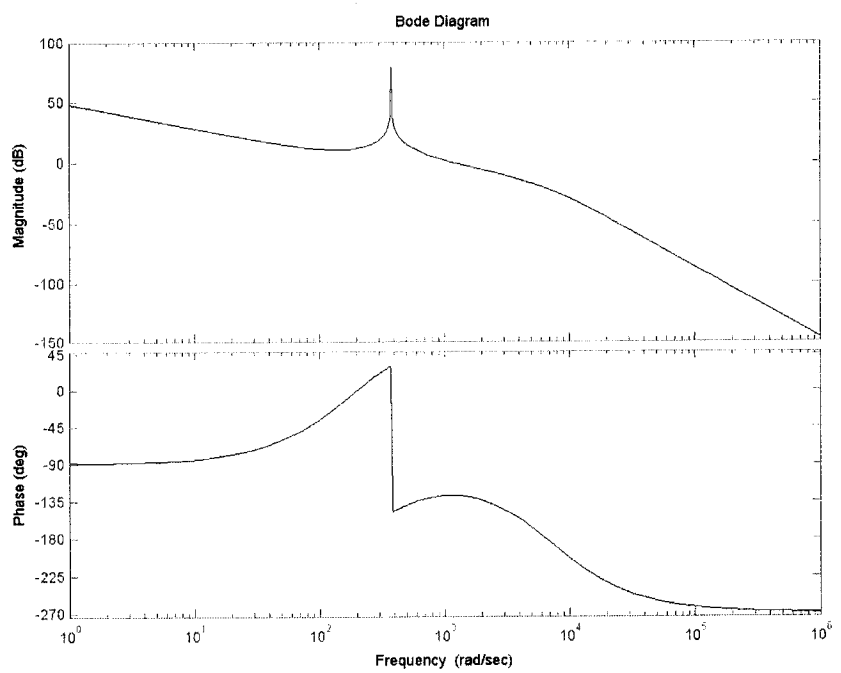

Figure D. 4 Bode plot of compensated q- control loop plant for PWM STATCOM